TIDAL CHANNEL MORPHOMETRY, FLOW, AND SEDIMENTATION IN A BACK-BARRIER SALT-MARSH: AVALON/STONE HARBOR, NEW JERSEY

By MARJORIE LEE ZEFF

A dissertation submitted to the

Graduate School-New Brunswick

Rutgers, The State University of New Jersey

in partial fulfillment of the requirements

for the degree of

Doctor of Philosophy

Graduate Program in Geological Sciences

Written under the direction of

Professor Gail M. Ashley

and approved by

Gail M. Ashley

Evelyn M. Maurmeyer

Norbert P. Psuty

Richard K. Olsson

John J. Flynn

New Brunswick, New Jersey

October, 1987

ABSTRACT OF THE DISSERTATION

Tidal Channel Morphometry, Flow, and Sedimentation
in a Back-Barrier Salt-Marsh:
Avalon/Stone Harbor, New Jersey

by MARJORIE LEE ZEFF, PhD.

Dissertation Director: Professor Gail M. Ashley

The tidal channels in a low-mesotidal back-barrier salt-marsh of southern New Jersey consist of i) large through-flowing (TF) channels which developed from flood tidal delta channels and connect the ocean with bays or channels to each other, and ii) smaller dead-end (DE) channels which evolved from ebb drainage patterns on the unvegetated portions of tidal delta islands and terminate on the marsh.

TF channels have at-a-station hydraulic geometries similar to other tidal marsh channels and DE channels have hydraulic geometries similar to rivers. The largest TF channel (160 m wide) had a measured mean spring v_{max} = 100 cm/sec, a mean neap v_{max} = 64 cm/sec, a spring Q_{max} = 700 m^3/sec, and neap Q_{max} = 500 m^3/sec. The smallest DE channel (1 m wide) had a mean neap v_{max} = 10 cm/sec and a neap Q_{max} < 1 m^3/sec.

DE channels have low w:d ratios (5-21) with high mud perimeters (averaging 79%) in contrast to TF channels with higher w:d ratios (34-129) and low mud perimeters (averaging 9%).

Three distinct environments are associated with the channels: i) a subtidal thalweg region, ii) an intertidal channel-margin flat (vegetated and unvegetated), and iii) a channel-margin marsh (levee and back-levee). Inter-channel sediment trends for each environment proceeding from large TF to small DE channels are: i) the fining of sediments from sands to silts and clays, ii) increasing total organic matter with increasing mud content, and iii) a change from predominantly physical to biological sedimentary structures. Intra-channel trends at channel cross-sections are: i) the fining of sediments with distance away from the thalweg region and ii) increasing total organic matter content from the thalweg region to the marsh.

The recognition of tidal channel facies and carbon-14 dating of vibracores indicate that the seaward margins of this marsh were occupied by flood tidal deltas 1300 years BP, aggraded to intertidal flats 800-1300 years BP, and were colonized by salt-marsh vegetation within the last 700 years.

ACKNOWLEDGMENTS

The author would like to express her appreciation to Dr. G. M. Ashley for her suggestions and comments throughout the course of this research, and her critical review and evaluation of the various forms of this manuscript.

I would also like to thank Drs. J. J. Flynn, E. M. Maurmeyer, R. K. Olsson, and N. P. Psuty for reviewing this dissertation and participating on my doctoral committee.

This work is the result, in part, of research sponsored by NOAA, Office of Sea Grant, Department of Commerce under Grant Nos. NA81AA-D-00065 and NA83AA-D-00034. This project was also supported by a grant provided by the New Jersey Department of Higher Education and administered by the New Jersey Marine Sciences Consortium, and the Department of Geological Sciences, Rutgers University, New Brunswick, New Jersey.

I would particularly like to thank R. Grizzle for his invaluable assistance in the field; A. Bliss for building and fixing laboratory and field equipment; H. Dudar both for her help when using the facilities of the Center for Coastal and Environmental Studies at Rutgers and in the field; and M. Ferland for arranging helicopter flights over the study area by the U. S. Army.

My appreciation is equally extended to K. Ashley, A. Brower, B. Ekwurzel, M. Kaeding, P. Radomsky, and P.

Schuster for field work; R. Dimmick for computer bail-outs; and D. Rhoads for providing X-ray equipment.

Finally, I would like to thank my parents for their unyielding encouragement, and my husband, Barry Kipnis, without whose loving understanding, patience, enthusiasm, and support I would not have had so much fun finishing this to the very end.

TABLE OF CONTENTS

TABLE OF CONTENTS (cont.)

LIST OF TABLES

LIST OF FIGURES

INTRODUCTION

And the sea lends large, as the marsh: lo, out of his plenty
the sea
Pours fast: full soon the time of the flood-tide must be:
Look how the grace of the sea doth go
About and about through the intricate channels that flow
Here and there,
Everywhere,
Till his waters have flooded the uttermost creeks and the
low-lying lanes,
And the marsh is meshed with a million veins,
That like as with rosy and silvery essences flow
In the rose-and-silver evening glow.
Farewell, my lord Sun!
The creeks overflow: a thousand rivulets run
'Twixt the roots of the sod; the blades of the marsh-grass
stir;
Passeth a hurrying sound of wings that westward whirr;
Passeth, and all is still; and the currents cease to run;
And the sea and the marsh are one.

from The Marshes of Glynn
Sidney Lanier (1878)

Purpose of Study

Salt-marshes are intertidal flats covered with salt tolerant plants (halophytes). They have a wide global distribution (Chapman, 1960) and are incised with intricate tidal channel drainage networks. The objective of this study has been to uniquely investigate the tidal channel drainage system of southern New Jersey by the integration of three interrelated aspects of many channels: i) geomorphology/morphometry, ii) modern processes, and iii) depositional facies. Specific objectives have been to: i) develop a model of tidal channel sedimentation in a low-mesotidal back-barrier salt-marsh of southern New Jersey, ii) describe the sedimentary facies associated with the channels of this marsh, and iii) determine the role of tidal channels in the evolution of this region during the Holocene rise in sea-level. The primary hypothesis to be tested is that differences in flow characteristics amoung tidal channels of various orders are reflected in sediment transport characteristics and tidal channel depositional facies.

Previous Investigations

In the United States the sedimentary processes of tidal channels have been investigated in tidal marshes of Georgia (Land and Hoyt, 1966; Edwards and Frey, 1977; Letzsch and Frey, 1980a and b), South Carolina (Settlemyre and Gardner, 1977; Barwis, 1978; Duc, 1981; Ward, 1981), Delaware (Kraft and Margules, 1971; Elliot, 1972; Allen, 1977), New Jersey (Garofalo, 1980; Ashley and Zeff, 1985a and b, 1986, 1987a and b), California (Pestrong, 1965, 1972; Warme, 1971), Virginia (Myrick and Leopold, 1963; Boon, 1973, 1975) and Massachusetts (Daboll, 1969; Redfield, 1972). In Europe investigations have been conducted in England (Evans, 1965; Bayliss-Smith et al., 1979; Pethick, 1980; Healey et al., 1981), the Netherlands and Germany (Dankers et al., 1984), and Denmark (Jakobsen, 1962).

The marshes they traverse range from back-barrier marshes infilling lagoons to those fringing open coasts and drowned river valleys or occupying the swales between beach ridges. The channels themselves range from drowned fluvial reaches to interior marsh channels, and they span all size dimensions and tidal ranges.

Previous studies of tidal marsh channels have been limited in scope. For instance, Pestrong (1965), in characterizing the at-a-station hydraulic geometry of marsh channels, restricted his measurements to a single channel cross-section within the complex system. Sedimentologic studies usually focus on one aspect of a single tidal channel. Barwis (1978), for example, was concerned with point bar geometry and deposits of one channel in two South Carolina marshes and Ward (1981) investigated suspended sediment transport at one cross-section of one of Barwis' channels.

Models of barrier coast evolution that have incorporated the role of salt-marsh tidal channels are derived from the study of systems unlike southern New Jersey. Kraft et al. (1979) and Kayan and Kraft (1979) discuss the evolution of marshes fringing a drowned river estuary (Delaware Bay) and tidal channels that originated as tributaries to the ancestral Delaware River. Tye (1984) recognized deposits of salt-marsh tidal channels in South Carolina that are relict ebb tidal delta channels abandoned by inlet migration and preserved by swash bar welding onto the barrier. The origin and role of other channel types within the marsh, however, are not considered.

The most comprehensive series of back-barrier salt-marsh studies to date have been done in Georgia (Howard and Frey, 1985; Frey and Howard, 1986). They provide a good descriptive understanding of the wide sedimentary variation of the marsh and channels in the Georgia back-barrier region, however, the geomorphic and process analyses of tidal drainage patterns undertaken by Wadsworth (1980) are not incorporated into the overall framework of the evolutionary history of the environment.

Ashley and Zeff (1985a) proposed a salt-marsh tidal channel classification that has been confirmed by the empirical data of this study. They found that channels of the salt-marshes of southern New Jersey can be subdivided as: i) through-flowing (TF) and ii) dead-end (DE). The through-flowing channels are larger and connect the ocean with a lagoon/bay or connect two channels with each other. Dead-end systems are comprised of discrete branching networks of smaller channels that feed into TF channels via a trunk channel and terminate on the marsh at their distal ends (Figure 1).

Area of Study

The coastline of New Jersey lies on the Atlantic Coastal Plain, marking the boundary of the emergent Outer New Jersey Coastal Plain province and the submergent continental shelf portion. The New Jersey Coastal Plain consists of a southeast dipping, seaward thickening wedge of unconsolidated and partly consolidated Cretaceous to Quaternary sediments lying unconformably upon a

Figure 1. Salt-marsh tidal channel classification of Ashley and Zeff (1985a): OBTF (ocean-to-bay through-flowing channels); CCTF (channel-to-channel through-flowing channels); DE (dead-ending channel networks).

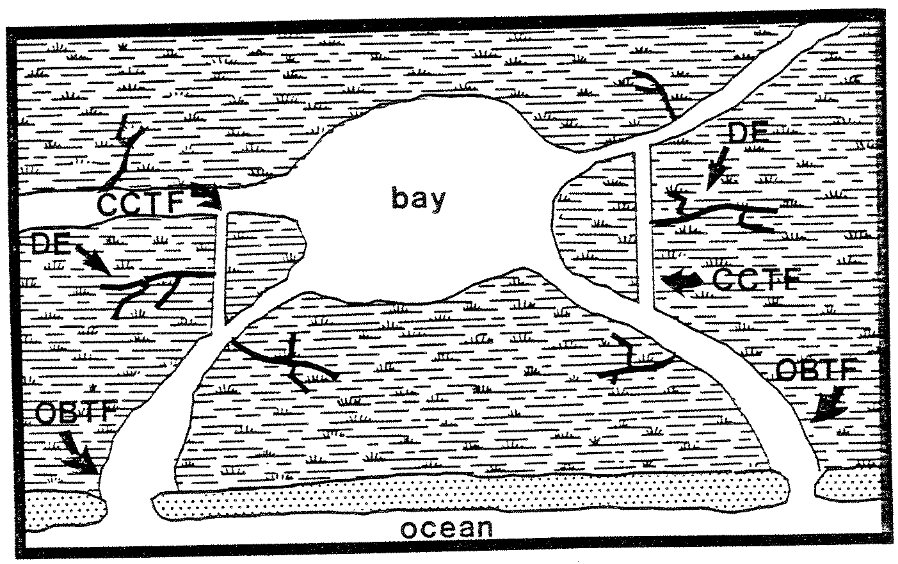
bay
CCTF
DE
DE
CCTF
OBTF
OBTF
ocean

Precambrian(?), early Paleozoic, and Triassic basement (Owens and Sohl, 1969).

The geomorphic configuration of the Recent sediments comprising the modern New Jersey shoreline is similar to other barrier island coasts along the Atlantic margin of the U. S. (Fisher, 1967; Hayden and Dolan, 1979; Kochel et al., 1985). Their characteristic features are: i) a mainland coast or eroding headland with attached barriers, ii) a long, continuous barrier island chain with few inlets backed by lagoons fringed with marshes that become, with distance from the headland, a iii) short, discontinuous barrier island chain with more frequent inlets backed by a more extensive marsh.

The area of study of this investigation consists of the marshes located landward of a barrier island of the Cape May Peninsula bordered by Townsends Inlet on the north and Hereford Inlet on the south (Figure 2). This island, occupied by the towns of Avalon and Stone Harbor, is approximately 13 km long and 0.5-1 km wide. The back-barrier region, about 45 km^2 in area, consists of intertidal salt-marshes and flats, 2 shallow lagoons (Great Sound, 6 km^2 and Jenkins Sound, 2 km^2), and tidal channels (ranging approximately 1 meter wide and a few centimeters deep to over 150 meters wide and 5-8 meters deep).

Tides are semidiurnal. The mean tidal range at Townsends Inlet is 1.16 meters and the spring tidal range

Figure 2. General study area. Detailed morphometric analyses were conducted within the dashed area. Area within box is enlarged in Figure 3. Scale = 1 km.

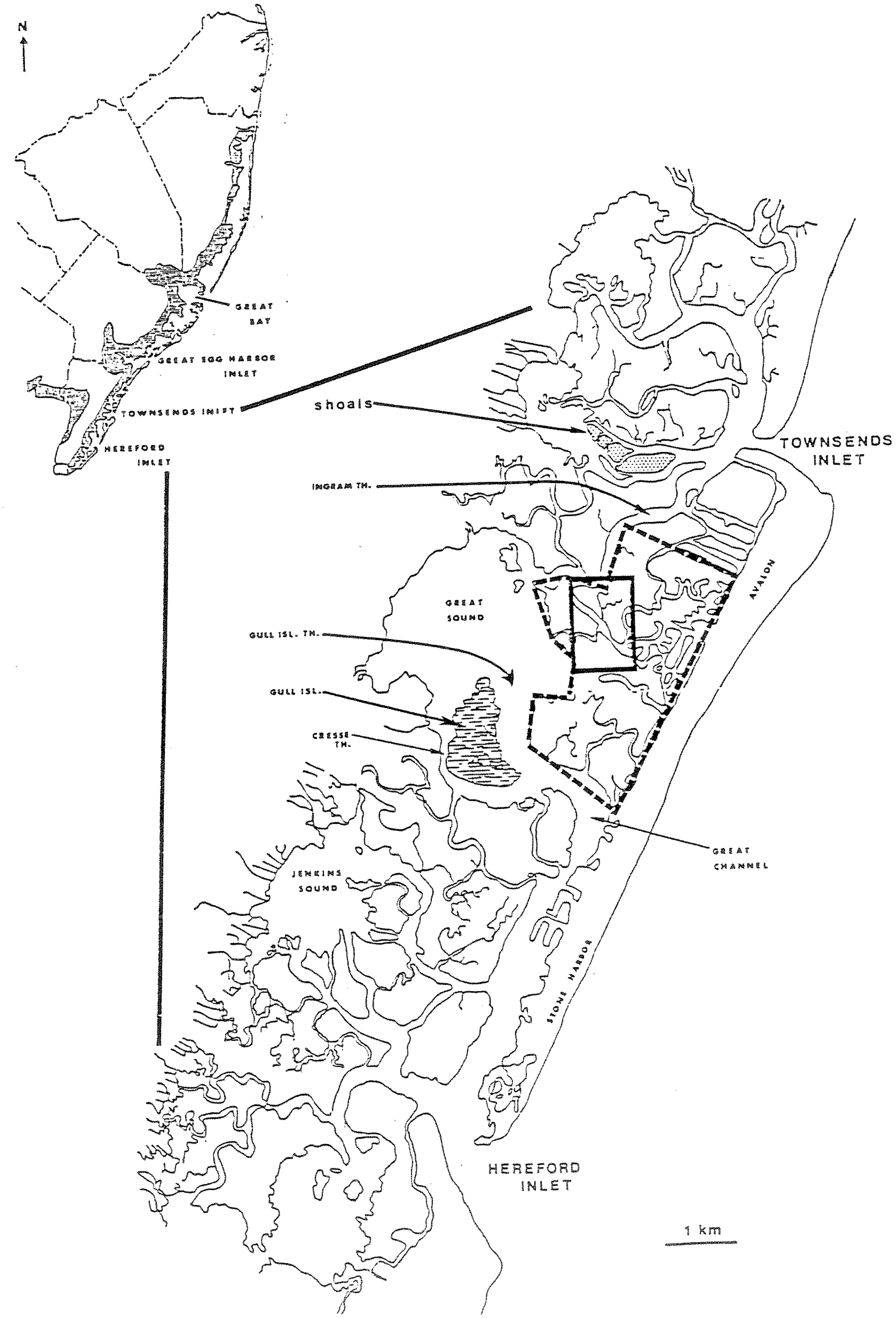
N
GREAT BAY
GREAT EGG HARBOR INLET
TOWNSENDS INLET
HEREFORD INLET
shoals
TOWNSENDS INLET
INGRAM TH.
GREAT SOUND
AVALON
GULL ISL. TH.
GULL ISL.
CRESSE TH.
GREAT CHANNEL
JENKINS SOUND
STONE HARBOR
HEREFORD INLET
1 km

is 1.40 meters. Hereford Inlet, on the other hand, has a mean tidal range of 1.25 meters and a spring tidal range of 1.52 meters (U. S. Dept. of Commerce, 1986). The tidal prism through Townsends Inlet is 15.7 X 10^6 m^3, and 33.7 X 10^6 m^3 through Hereford Inlet (Jarrett, 1976).

The Great Sound area is affected by winds similar to those reported by the National Weather Service at Atlantic City, 45 km to the north (R. Grizzle, pers. comm.). Long-term (1923-1952) records show 30-35 km/hr northeast winds and 20-30 km/hr south and west-northwest winds to predominate. Wind generated waves (0.3-0.5 m height) resuspend bottom sediments of the Sound (Ashley and Grizzle, in prep.).

There is little or no freshwater input to the Avalon/Stone Harbor system by surface runoff and the nearest river is 37 km north of the study area (Kran, 1975). Salinities measured in Great Sound show typical values ranging 25-33 ppt with noticeable reductions to 20-24 ppt after heavy rainfall (Royer, 1980; Ashley and Grizzle, in prep.).

Peak flow velocities in the channels are unequal with peak mean flood velocities exceeding peak mean ebb velocities under both spring and neap tidal conditions. Measured fair-weather peak mean flood current velocities reached approximately 97 cm/s in the largest channel (Ingram Thorofare) at spring tide and 64 cm/sec at neap tide. Maximum mean current velocities measured in the smallest channels at neap tide are 7-12 cm/sec.

Maximum mean velocities in Great Sound range >40 cm/sec to <10 cm/sec (Ashley and Grizzle, 1987).

Maximum discharges reach about 700 m^3/sec in Ingram at spring tide and 475 m^3/sec at neap, and less than 1 m^3/sec in the smallest channels at neap.

Potential sources of fine-grained inorganic sediment entering the back-barrier regions of the Cape May Peninsula through tidal inlets are the inner continental shelf, beaches, and Delaware Bay (Kelley, 1983). Storms may transport shelf clays landward to Stone Harbor as washover fans (Meza and Paola, 1977).

Suspended sediment in the study area consists of individual silt and sand grains, organic-mineral aggregates, and fecal pellets (Carson et al., 1987). Single grains dominate in channels when flow velocities exceed 30 cm/sec. The organic-mineral aggregates dominate at lower velocities and in Great Sound, and fecal pellets consistantly represent less than 30% of the suspended load.

The total suspended sediment load concentrations of the tidal channels under fair-weather conditions range from 15 mg/l in the large ocean-to-bay TF channels to 30 mg/l in the channel-to-channel through-flowers and 30-35 mg/l in the small DE channels (Ashley and Zeff, 1987b). Values of 400 mg/l were measured in Ingram Thorofare during Hurricane Gloria.

In Great Sound, near-bottom suspended sediment concentrations range 10-50 mg/l (Ashley and Grizzle, 1987). Stirring by wind generated waves produce concentrations over 300 mg/l.

Coarser sediment also enter the system through tidal inlets as indicated by flood tidal deltas. Erosion of the salt-marsh and the production of macro- and microfaunal shell debris and organic detritus (plant remains and pellets) within the back-barrier system itself contributes to the total sediment supply.

Coastal New Jersey has been undergoing a rise in sea-level associated with receding late-Wisconsinan glaciers since before 7000 years BP at a rate that markedly declined 2000-2500 years BP from approximately 2-3 mm/yr to about 1 mm/yr (Ferland, 1985; Psuty, 1986). Over the past century Atlantic City has recorded a rise in sea-level at a rate of about 4 mm/year (Hicks et al., 1983). Maximum rates of accumulation in Great Sound range 1-5 mm/yr based on Pb-210 profiles (Thorbjarnarson et al., 1985).

The area of study for morphometric analysis consisted of a wide expanse of back-barrier marsh outlined in Figure 2. Sites where hydraulic geometries were determined and locations where surface and vibracores were taken are shown in Figure 3. Average channel dimensions of six cross-sections are given in Table 1. Long Reach is known to have been dredged.

Figure 3. Channel sample sites located within the boxed area of Figure 2. Sediment samples were analyzed for the 12 cross-sections shown. Hydraulic geometry and w:d calculations were made at 6: IT-A, LR-B, RC-A, OC, RGN, and AQ. Note the wide variety of channel dimensions, the near perpendicular junction angle of DE systems and TF channels (white arrows), and salt pan (black arrow). Vibracore sites are numbered 2, 3, 4, and 5 (SM-2, SM-3, SM-4, and SM-5). Abbreviations are: Ingram Thorofare (IT), Long Reach (LR), Old Turtle Reach (OT), Gravens Thorofare (GR), Redfield Creek (RC), Oarlock Creek (OC), Regnes Creek (RGN), and African Queen (AQ). Scale = 100 m.

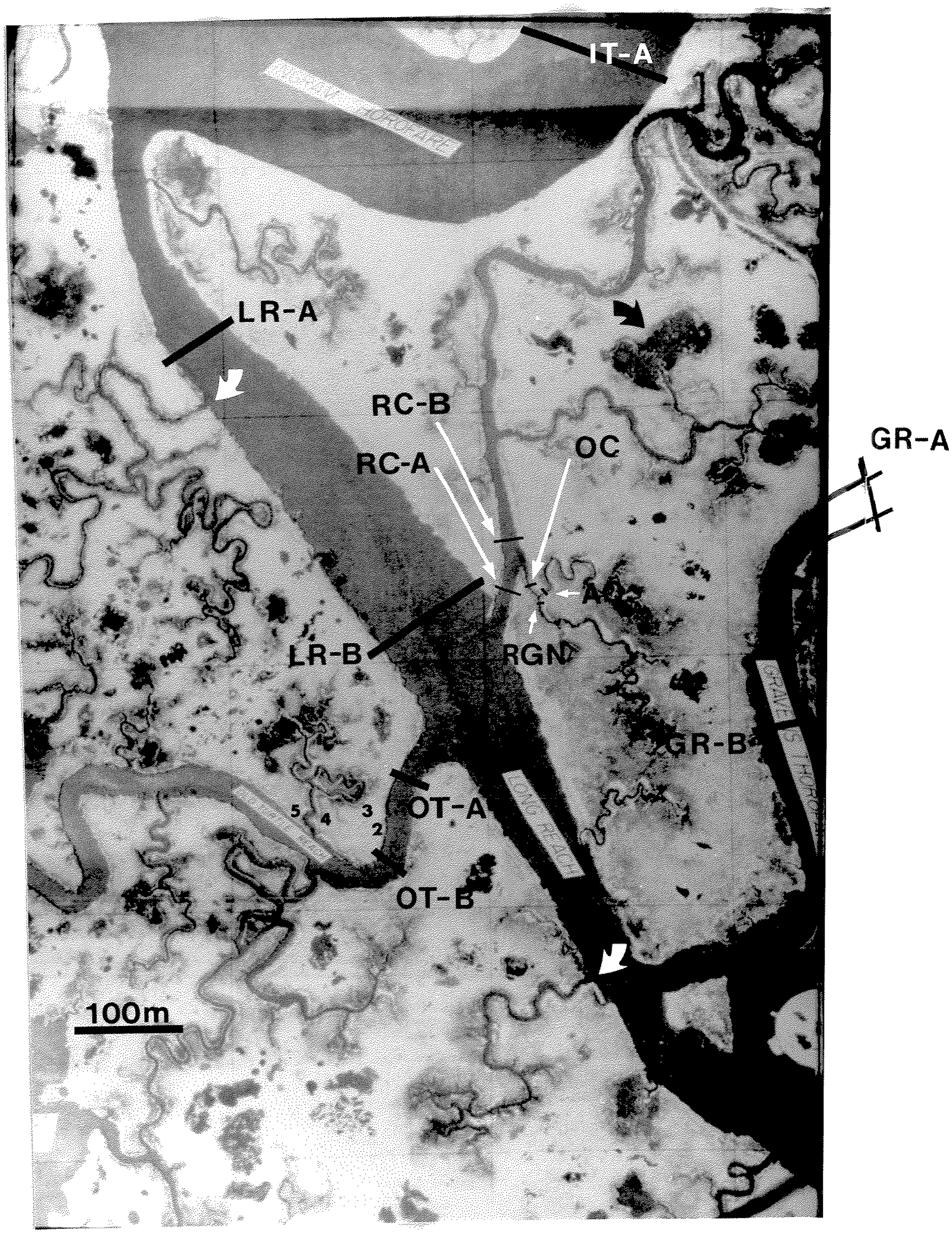
IT-A
LR-A
RC-B
RC-A
OC
GR-A
AC
LR-B
RGN
GR-B
OT-A
5
4
3
2
OT-B
100m

TABLE 1

AVERAGE CHANNEL DIMENSIONS (meters)

channel	w	d
IT-A	159.63	4.66
LR-B	104.11	0.81
RC-A	20.96	1.02
OC	5.00	0.39
RGN	3.27	0.23
A2	1.27	0.27

METHODOLOGY

Morphometric Analyses

Horton (1945) developed numerical methods of morphometric analysis of fluvial drainage patterns that have been widely adapted by subsequent workers. With some modification similar methods have been applied to tidal channel networks (Myrick and Leopold, 1963; Pestrong, 1965; Wadsworth, 1980). The morphometric parameters used to characterize the channels of this study are listed in Table 2.

Traces of the channel networks were made from 1:2400 aerial photomaps provided by the New Jersey Department of Environmental Protection. The smallest channels that dead-end on the marsh interior are included in these base maps. Added detail was gained from color aerial slides taken by the author on several helicopter flights over the study area.

The Strahler (1952) modification of Horton's (1945) system of channel ordering was used to place a total of 1039 channel segments into a hierarchical scheme (Figure 4a). All unbranched (dead-end) segments are considered 1st-order. Tracing the channel form in the ebb direction, the joining of two 1st-order reaches produces a 2nd-order segment; the junction of two 2nd-order segments forms one of the 3rd-order, etc. The bifurcation of a channel to two segments was counted as two in number. If these two

TABLE 2

MORPHOMETRIC PARAMETERS OF THIS STUDY

order (u)

number of segments (N)

bifurcation ratio (R_b) = N_u/N_{u+1}

sinuous channel length = L_{sin}

straight channel length = L_{str}

sinuosity ratio (R_s) = L_{sin}/L_{str}

junction angle

average width-depth ratio (w:d)

total channel length (L_t)

drainage area (A_t)

drainage density (D_d) = (L_t/A_t)

subsection cross-sectional area = A_i

mean subsection velocity = v_i

discharge (Q) = $\Sigma A_i v_i$

hydraulic geometry:

width = aQ^b

depth = cQ^f

velocity = kQ^m

Figure 4. Morphometric Measurements.

A) The Strahler (1952) method was used to place segments in a system of orders (see text).

B) The bifurcation of a channel into 2 segments was counted as 2 in number (N=2). If these segments rejoined, the entire form was counted as 1 (N=1).

C) Channel lengths and junction angles (α) were measured along channel axes after Lubowe (1964) (see text).

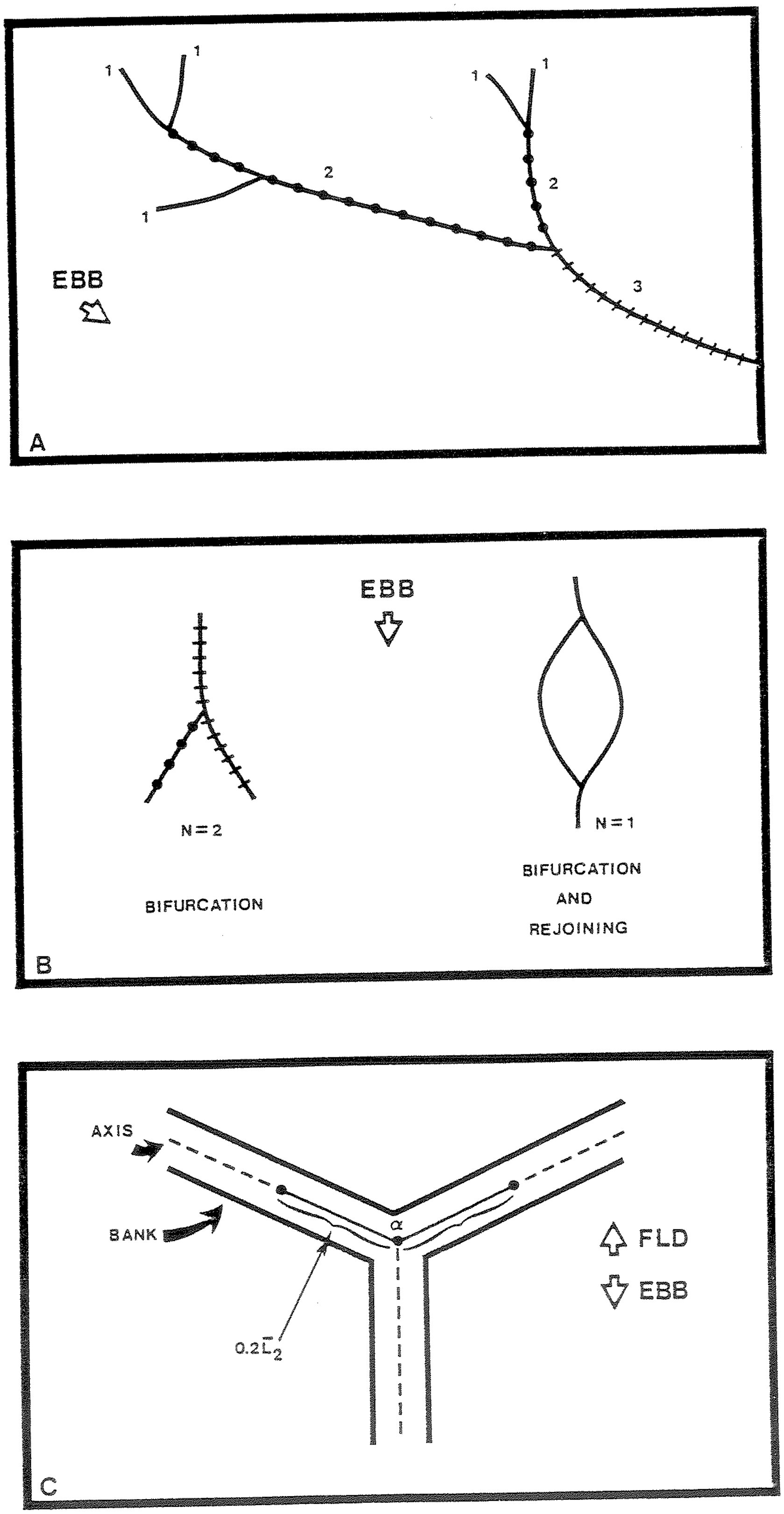
1
1
1
1
2
2
1
3
EBB
A
EBB
N=2
BIFURCATION
N=1
BIFURCATION
AND
REJOINING
B
AXIS
BANK
α
FLD
EBB
0.2$\bar{L}_2$
C

segments rejoined to form a circle, the entire form was considered as one continuous segment (Figure 4b).

All channel lengths and junction angles were measured along channel axes (Figure 4c). Junction angle values are calculated after Lubowe (1964) whereby fluvial junction angles are defined as those formed by the ends of channel segments extending from the point of junction to an upstream (flood direction in this study) point a distance equal to 0.2 of the average length of the 2nd-order channels.

A series of IBM-PC Basic programs used in conjunction with a GTCO DIGI-PAD digitizer were developed by the author to accurately measure channel segment lengths, widths, and cross-sectional areas, drainage areas, and junction angles from base maps and drawings (Appendix 1). The parameters R_b(bifurcation ratio), D_d(drainage density), and R_s(sinuosity) are derived values. Horton's Laws of Drainage Composition were determined through regression analysis performed on a TI-55II calculator.

Changes in channel width, depth, and flow velocity that accompanied changes in discharge at channel cross-sections (at-a-station hydraulic geometry) were measured at six channel sites during part of a tidal cycle (Figure 3). Water surface widths (w) were measured with scaled rope and from depth-sounding profiles obtained with a Raytheon Model DE-719B Survey Fathometer. Each cross-section (A) was subdivided into subsections, the areas of which (A_i) were determined by a digitizing routine developed by the author (Appendix 1). Mean flow velocities of each subsection (v_i) were collected 0.4-0.5d (d=depth) above the bottom and averaged over three minutes (1 minute at Redfield Creek on 10-24-84) with a Marsh McBirney Model 201 Portable Water Current Meter. Discharge (Q) values at any point in time were then calculated as $Q = \Sigma A_i v_i$. Final determinations of the coefficients and exponents of the hydraulic geometry equations ($w=aQ^b$, $d=cQ^f$, $v=kQ^m$) were calculated by regression analysis with a TI-55II calculator using known values of w,d,v, and Q where v (mean velocity) = Q/A and d (mean depth) = A/w after Leopold and Maddock (1953).

Bedforms were recorded with the Raytheon fathometer.

Modern Sediments

Seventy-eight surface samples and short cores were collected from 12 channel transects, the marsh, and lagoon (Figure 3). Marsh samples were collected by cutting through dense *Spartina alterniflora* root systems and lifting out the bounded mass. Channel and lagoon samples consisted mostly of the top 3-5 cm of short cores (4.5 cm in diameter X 20-25 cm long). Grabs were used for some flats, the thalweg sample at GR-A was recovered from an anchor, and the thalweg sample of IT-A was collected with a Helley-Smith bedload sampler. Upon return to the laboratory samples were immediately placed in a cold-room until processing for grain-size, total organic matter

(TOM), sedimentary structures, and foraminiferal content. Grain-Size: Sand:silt:clay ratios were determined by dry sieving and pipette techniques after removal of organic matter. Organic matter was oxidized by adding 30% hydrogen peroxide to the samples. The organic-free sediments were then wet-sieved with a 63um sieve to separate sands and muds. The sands were oven-dried and weighed. Medium:fine:very fine sand ratios for sand fractions (1-18 grams) were determined using an ATM Model L3P Sonic Sifter with 3-inch diameter sieves. Smaller samples were visually examined for the modal size class. Ingram Thorofare thalweg samples were analyzed for only sand with a Ro-Tap Model B Sieve Shaker with 8-inch diameter sieves.

The sonic sifter was chosen over the Ro-Tap for several reasons. Firstly, the sonic sifter requires only small sample sizes (less than 20 grams) while 30-70 grams of sand are needed for the Ro-Tap. Secondly, 3-inch sieve diameters are preferred over the standard 8-inch diameter sieve when analyzing small amounts of sands recovered from modern marine cores (McManus, 1965).

In order to substantiate this decision Dudar and Zeff conducted an experiment to compare the two techniques (Appendix 2). Five medium sands from the Ingram Thorofare thalweg region analyzed by Zeff with the Ro-Tap (RT) were re-analyzed in replicate (2-6 times) by Dudar with the sonic sifter (SS). Sonic sifter results are reproducible at the 1/4 phi level, yet there can be sizable discrepancies between the Ro-Tap and sonic sifter at the medium/coarse sand boundary. Significantly, however, there is little discrepancy at 1 phi intervals. Similarly, the data reported by Wolcott (1978) shows no difference between the sonic sifter and Ro-Tap at 1 phi intervals when the mean weight per cents of three estuarine sands (four replicates each) are rounded to the nearest per cent. The variance was largest for both methods at 3 and 4 phi (fine and very fine sand). Considering the high reproducibility of the sonic sifter, the small sample sizes, and the excellent correlation of the two methods at 1 phi intervals, the author feels the sonic sifter was preferable for this study.

0.67 grams of Na-oxalate (to produce a 0.01N solution in 1L of water) was added to the mud to act as a dispersant during pipetting. Proper pipette withdrawal times were after Folk (1974).

Several samples were analyzed in duplicate (Table 3). All give very good to excellent reproducibility with the exception of RGN-SMt. RGN-SMt was a marsh sample affected by binding of vegetation roots.

The $CaCO_3$ content of sands was determined by weighing before and after dissolution with dilute HCl.

Organic Matter: The total organic matter (TOM) content of sediments were determined by loss-on-ignition. A review of the literature (Gross, 1971; Byers et al., 1978; Duc,

TABLE 3

DUPLICATE MEASUREMENTS*

sample	sd:st:cy	m:f:vf sand (or mode)	type
IT-A-LWF	92:04:04	t:40:59	unveg. flat
	92:04:04	t:33:66	
SM-3	75:17:08	10:72:18	core
(358-360)	74:18:08	12:71:17	
SM-3	11:48:41	vf	core
(315-316)	13:47:40	vf	
RGN-SMt	15:39:46	vf	levee marsh
	23:53:24	vf	
		%TOM	
RC-B-WF	21:52:27	10	unveg. flat
		11	

* (sd=sand;st=silt;cy=clay;m=medium;f=fine;vf=very fine;t=trace)

1981; Stumpf, 1933) revealed accepted heating values ranging 450° -550° C for 1-4 hours. The procedures adopted for this study were as follows: Damp sediments were placed in porcelain crucibles and oven-dried for 3 hours at 100° C then for 12 hours at 90° C. The dry samples were cooled to room temperature in a desiccator and weighed. They were then heated to approximately 485° C for about 4 hours in a Lindberg Moldatherm Box Furnace. Samples were again cooled to room temperature in a desiccator and reweighed. The weight loss is a measure of the TOM content present and is calculated as:

$$\%TOM = \frac{\text{(dry weight)} - \text{(post-ignition weight)}}{\text{dry weight}} \times 100$$

Duplicate measurements were made (Table 3).

Sedimentary Structures: Sedimentary structures were examined by X-ray radiography. Box cores (3 cm thick) and short tube cores (4.5 cm diameter) were X-rayed with a Kramex PX-20N Deluxe Portable X-Ray Unit. Kodak Industrex AA Ready Pack negative film was used. Exposures ranged 10-60 seconds at 10 MA and 80 KVP. Negative development followed the recommended procedures for manual processing found in Kodak Products for Industrial Radiography (1984, p. 18). Positive prints followed standard printing procedures.

Foraminifera

Samples untreated with hydrogen peroxide were wet-sieved with a 63um screen to extract the sand fraction. This sand was placed in water and decanted to remove fine organic matter. Forams were concentrated through flotation in perchlorotetraethylene. The identifications of picked specimens are according to Todd and Low (1981).

Holocene Sedimentary Sequence (Stratigraphy)

Four vibracores 4-5 meters long were recovered from the marsh using a custom-built unit belonging to the New Jersey Marine Sciences Consortium. Six meter length aluminum irrigation pipes (7.6 cm in diameter) easily penetrated the marsh.

The cores were split in half in the laboratory by cutting the sides with a table saw and drawing through a metal guitar string. Cores were logged and photographed within a few days of opening. Half was left undisturbed for archival purposes, the other subsampled for sediment analysis.

Core logs noted color, grain-size, structures, plant and shell remains, and the nature of unit contacts. Subsamples were taken for grain-size and X-ray analysis following the same procedures outlined for modern sediments. Samples for X-ray radiography were obtained by sliding a half-section of a clear, plastic soda bottle under the sediment and lifting out.

Three subsamples from core SM-5 (peat, *Crassotrea* *virginica*, *Mercenaria mercenaria*) were radiocarbon dated by Beta Analytic Inc., Coral Gables, Florida. The shells were pretreated by acid etching of the outer layers. The peat was picked free of roots and treated with acid to remove carbonates. Dates were calculated using a 5568 year half-life. 95% of the activity of the NBS oxalic acid was the modern standard. Years BP are radiocarbon years before 1950 and errors represent one standard deviation.

RESULTS

Morphometric Analyses

The morphometric measurements used to characterize the tidal channels of this study are summarized in Tables 4-7 and Figures 5-15. Results are summarized below.

Order and R_b: Channel segment order is logarithmically related to the number of segments (Figure 5). This relationship is described by the Law of "stream" numbers (Horton, 1945).

The bifurcation ratio (R_b) is defined as the ratio of the number of streams of a particular order to the number of streams of the next highest order (Horton, 1945) and is expressed as the slope of the line connecting individual points. R_b values range 2.2-4.5 in this system (Table 4).

Length and R_s: Sinuosity (R_s) is a measure of the degree to which channels deviate from perfectly straight paths. Pestrong (1965) defines R_s in tidal networks as the ratio

TABLE 4

SUMMARY OF MORPHOMETRIC DATA*

ORDER	#	R_b	TOTAL L(m) sin	TOTAL L(m) str	MEAN L(m) sin	MEAN L(m) str	R_s
1	783		26,827	18,114	34	23	1.5
		4.1					
2	191		23,580	12,910	123	68	1.8
		3.9					
3	49		18,955	10,711	387	219	1.8
		4.5					
4	11		10,446	6170	950	561	1.7
		2.2					
5	5		7208	5305	1442	1061	1.4

TOTAL SIN LENGTH (m) = 87,016
TOTAL STR LENGTH (m) = 53,210
DRAINAGE AREA (square km) = 7.19

SIN DRAINAGE DENSITY $\frac{\text{(total sin length)}}{\text{(area X 1000)}} = 12.1\ km/km^2$

STR DRAINAGE DENSITY $\frac{\text{(total str length)}}{\text{(area X 1000)}} = 7.4\ km/km^2$

*abbreviations: m (meters); sin (sinuous); str (straight); L (length); km (kilometers)

TABLE 5

MEAN JUNCTION ANGLES
degrees(n)
n = number of angles measured

order

order		1	2	3	4	5
	1	89(184)				
	2	104(186)	110(40)			
	3	102(108)	110(46)	113(8)		
	4	92(31)	97(38)	102(10)	101(3)	
	5	98(6)	105(7)	74(7)	87(3)	---(0)

TABLE 6

WIDTH:DEPTH RATIOS

CHANNEL	WEIGHTED MEAN* % MUD	w:d	ORDER	TYPE
IT-A	4	34	5	TF
LR-B	14	129	5	TF
RC-A	39	21	4	DE
OC	87	13	3	DE
RGN	95	14	3	DE
AQ	94	5	2	DE

*after Schumm (1960)

TABLE 7

HYDRAULIC GEOMETRY SUMMARY

CHANNEL	STAGE	b	f	m	
Ingram Thoro	ebb	-0.01	-0.51	1.50	
Long Reach	ebb	-0.01	-0.03	1.02	GRP 1 (TF/DE)
Redfield Creek	flood	0.15	-0.01	0.85	GRP 1 (TF/DE)
	ebb	0.05	-0.11	1.05	GRP 1 (TF/DE)
	comb	0.09	-0.07	0.97	GRP 1 (TF/DE)
	ebb	0.11	0.16	0.74	
Oarlock Creek	flood	0.14	0.26	0.61	GRP 2 (DE)
African Queen	flood	0.22	0.62	0.17	GRP 3 (DE)
Regnes Creek	flood	0.17	0.49	0.33	GRP 3 (DE)

Pestrong (1965)	flood	0.10	0.27	0.68	
Myrick & Leopold (1963) (VA)	flood	0.04	0.18	0.78	tidal marsh
Myrick & Leopold (1963) (DE)		0.08	0.14	0.78	tidal marsh
Gilbert (1917)		0.14	0.08	0.78	tidal marsh
Boon (1973)				0.91*	
average rivers (Leopold & Maddock, 1953)		0.26	0.40	0.34	

*derived from figure 22a

Figure 5. Log (number of segments) vs order is plotted for this and previous studies. The slope of each line represents R_b (bifurcation ratio).

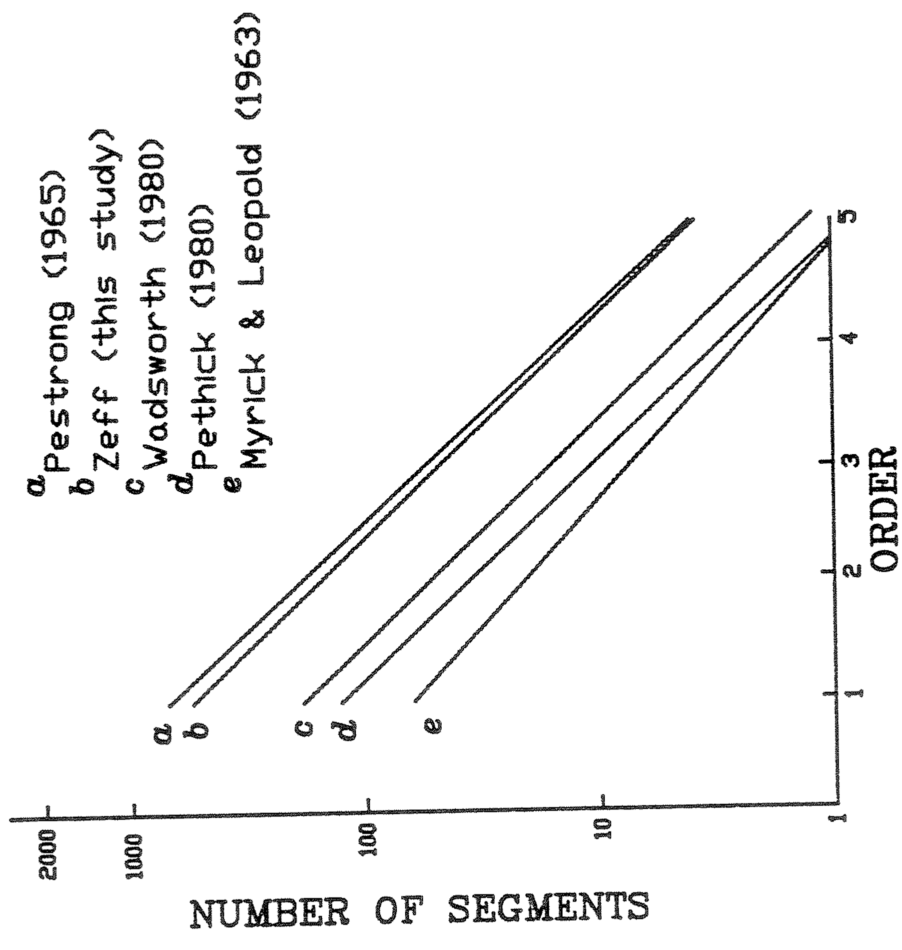
a Pestrong (1965)
b Zeff (this study)
c Wadsworth (1980)
d Pethick (1980)
e Myrick & Leopold (1963)
a
b
c
d
e
NUMBER OF SEGMENTS
2000
1000
100
10
1
1
2
3
4
5
ORDER

Figure 5

Figure 6. Log (sinuous mean length) vs order is plotted for this and previous studies.

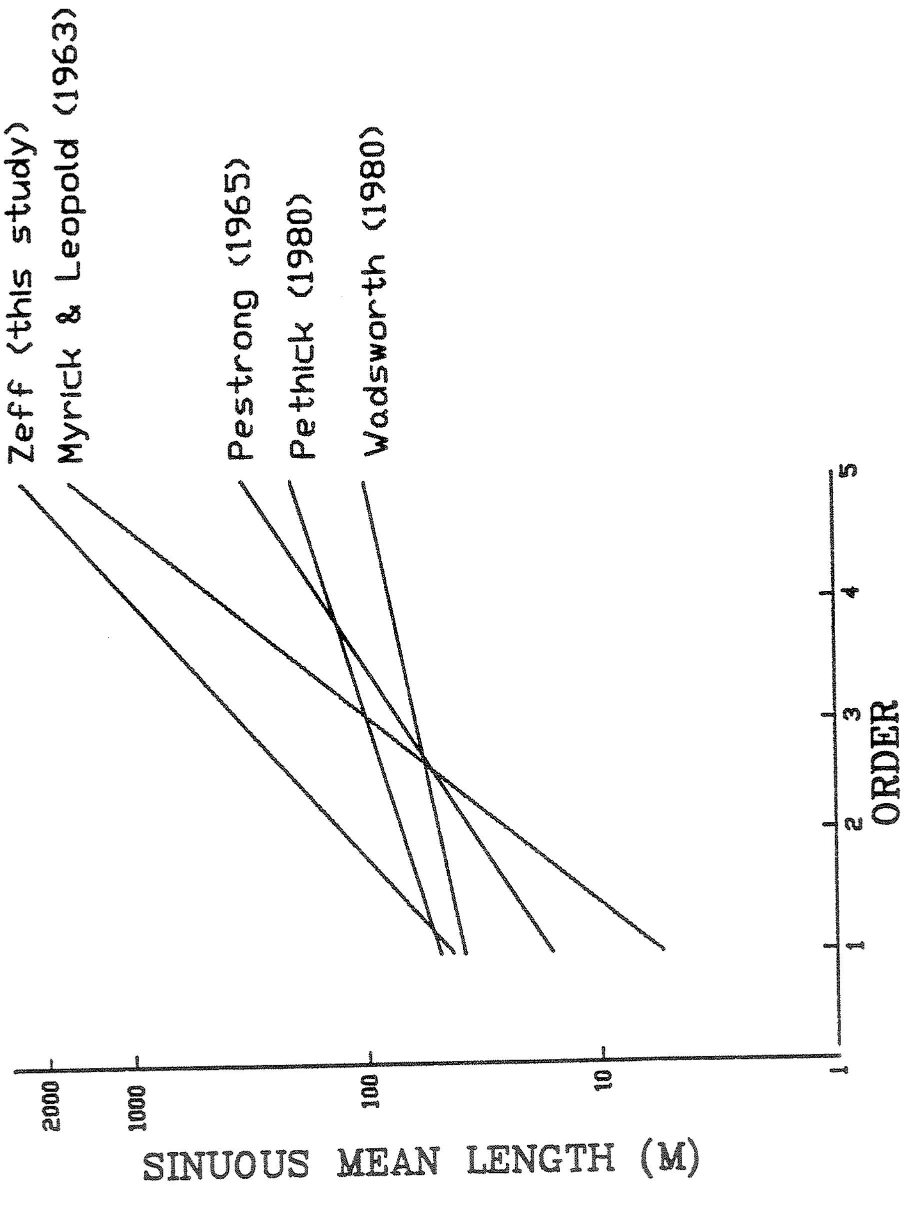
Zeff (this study)
Myrick & Leopold (1963)
Pestrong (1965)
Pethick (1980)
Wadsworth (1980)
SINUOUS MEAN LENGTH (M)
2000
1000
100
10
1
1
2
3
4
5
ORDER

Figure 6

Figure 7. Log (cumulative sinuous mean length) vs order is plotted for this and previous studies.

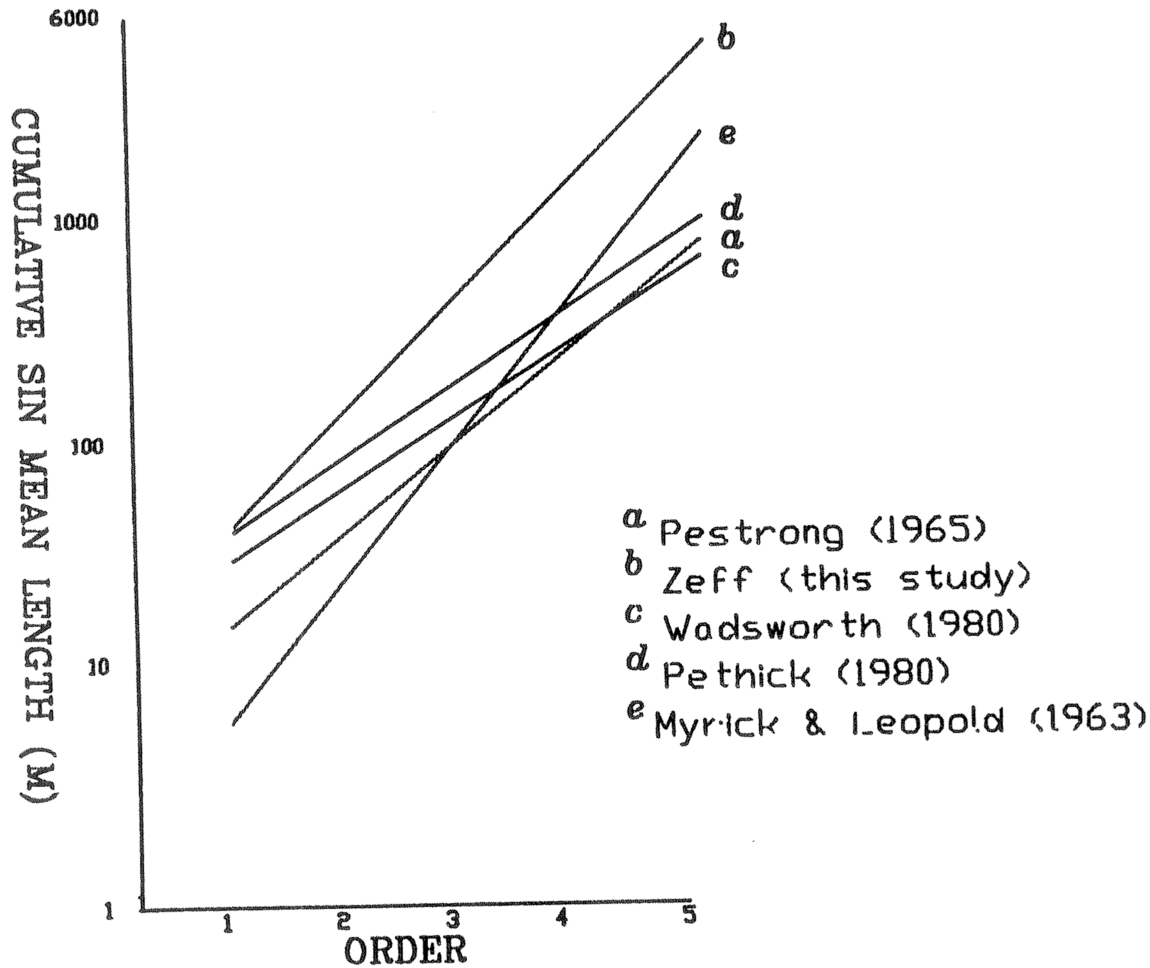
CUMULATIVE SIN MEAN LENGTH (M)
6000
1000
100
10
1
1
2
3
4
5
ORDER
b
e
d
a
c
a Pestrong (1965)
b Zeff (this study)
c Wadsworth (1980)
d Pethick (1980)
e Myrick & Leopold (1963)

Figure 7

Figure 8. Six channel profiles drawn to scale.

lw=landward, sw=seaward, e=east, w=west, n=north, s=south

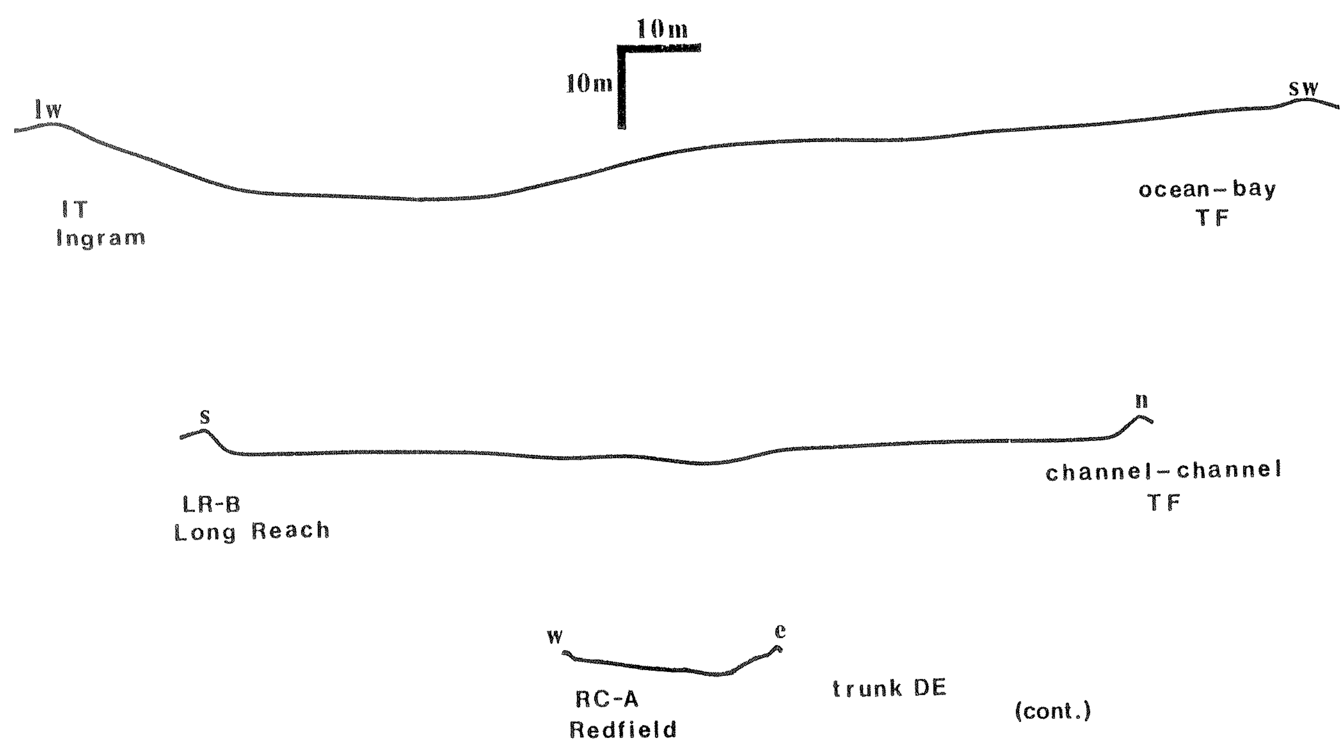
10m
10m
lw
sw
IT
Ingram
ocean–bay
TF
s
n
LR-B
Long Reach
channel–channel
TF
w
e
RC-A
Redfield
trunk DE
(cont.)

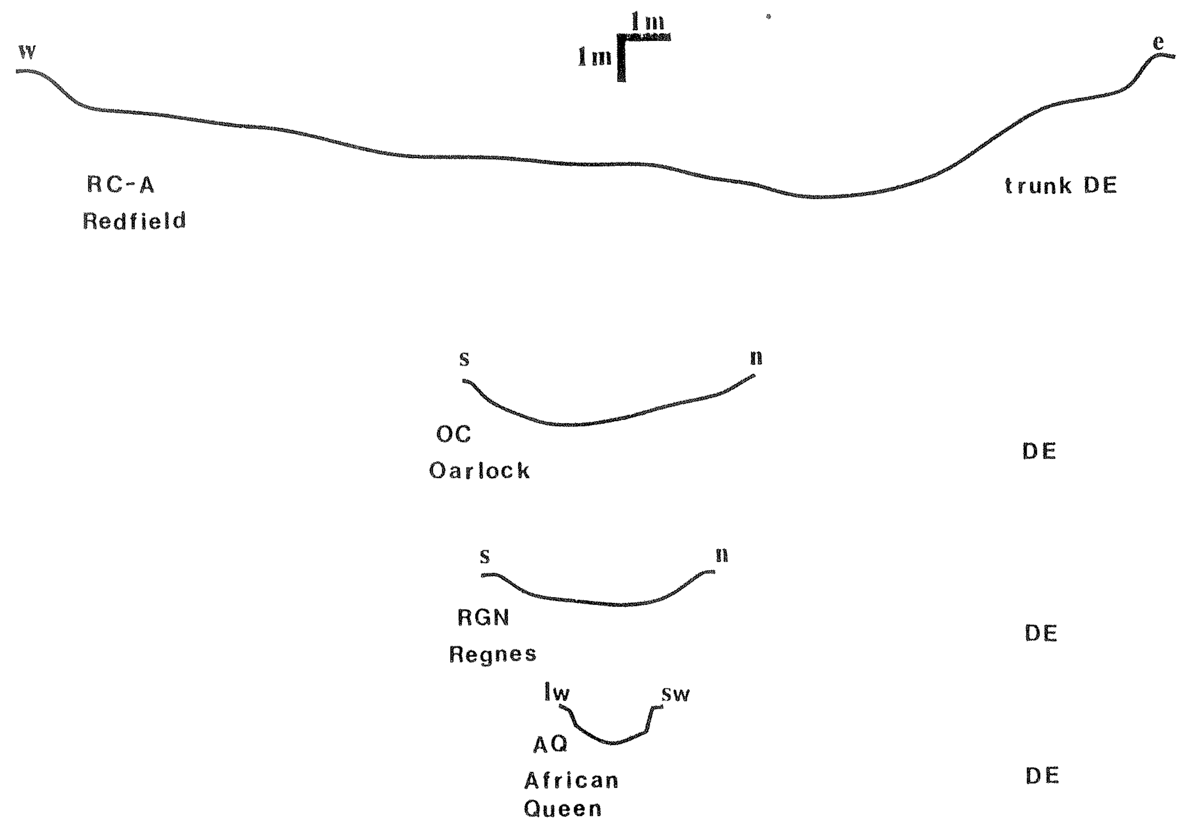

1m
1m
w
e
RC-A
Redfield
trunk DE
s
n
OC
Oarlock
DE
s
n
RGN
Regnes
DE
lw
sw
AQ
African
Queen
DE

Figures 9-15. At-a-station hydraulic geometry relationships for six channel cross-sections.

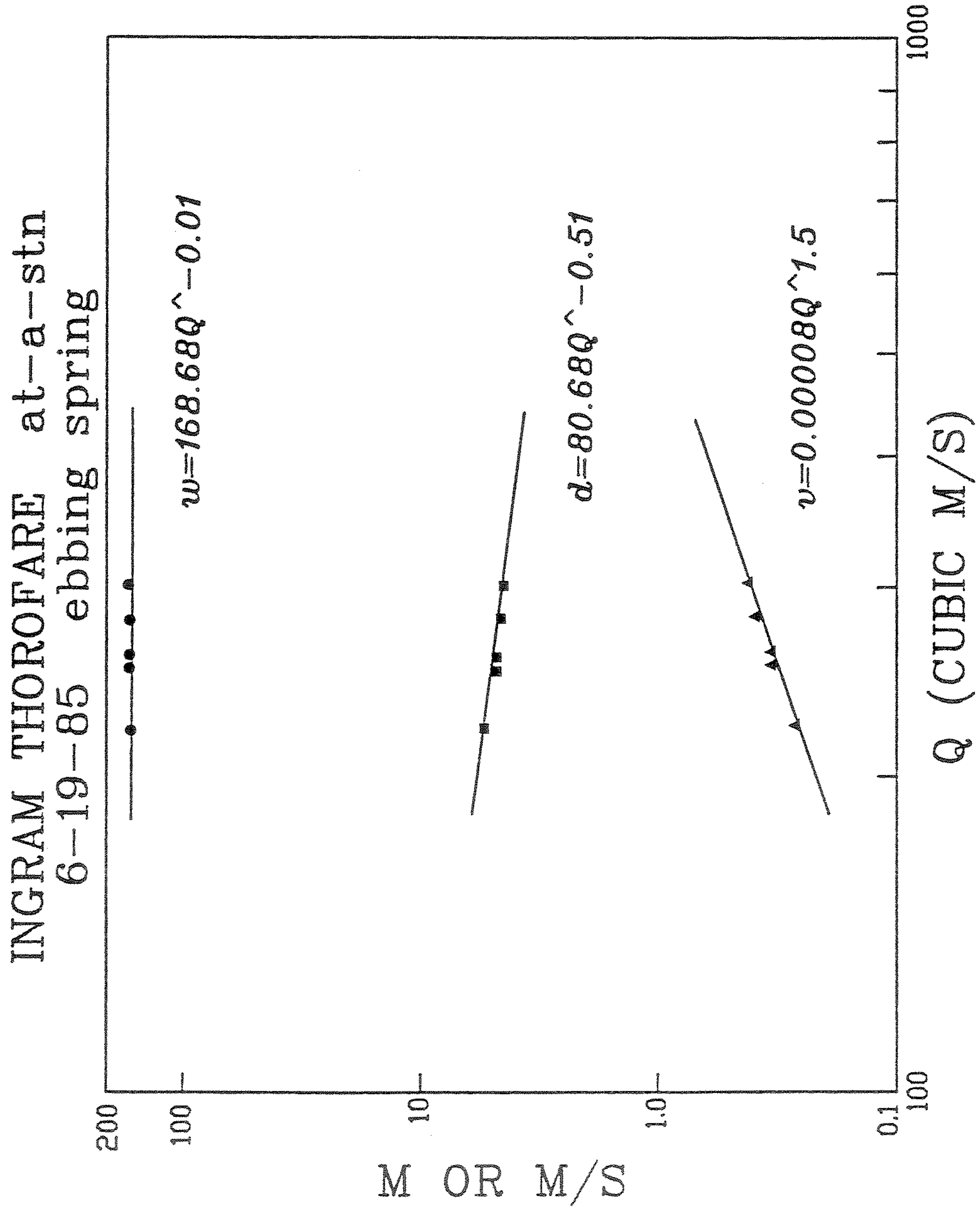
INGRAM THOROFARE at—a—stn
6—19—85 ebbing spring
w=168.68Q^—0.01
d=80.68Q^—0.51
v=0.000008Q^1.5
M OR M/S
200
100
10
1.0
0.1
100
1000
Q (CUBIC M/S)

Figure 9

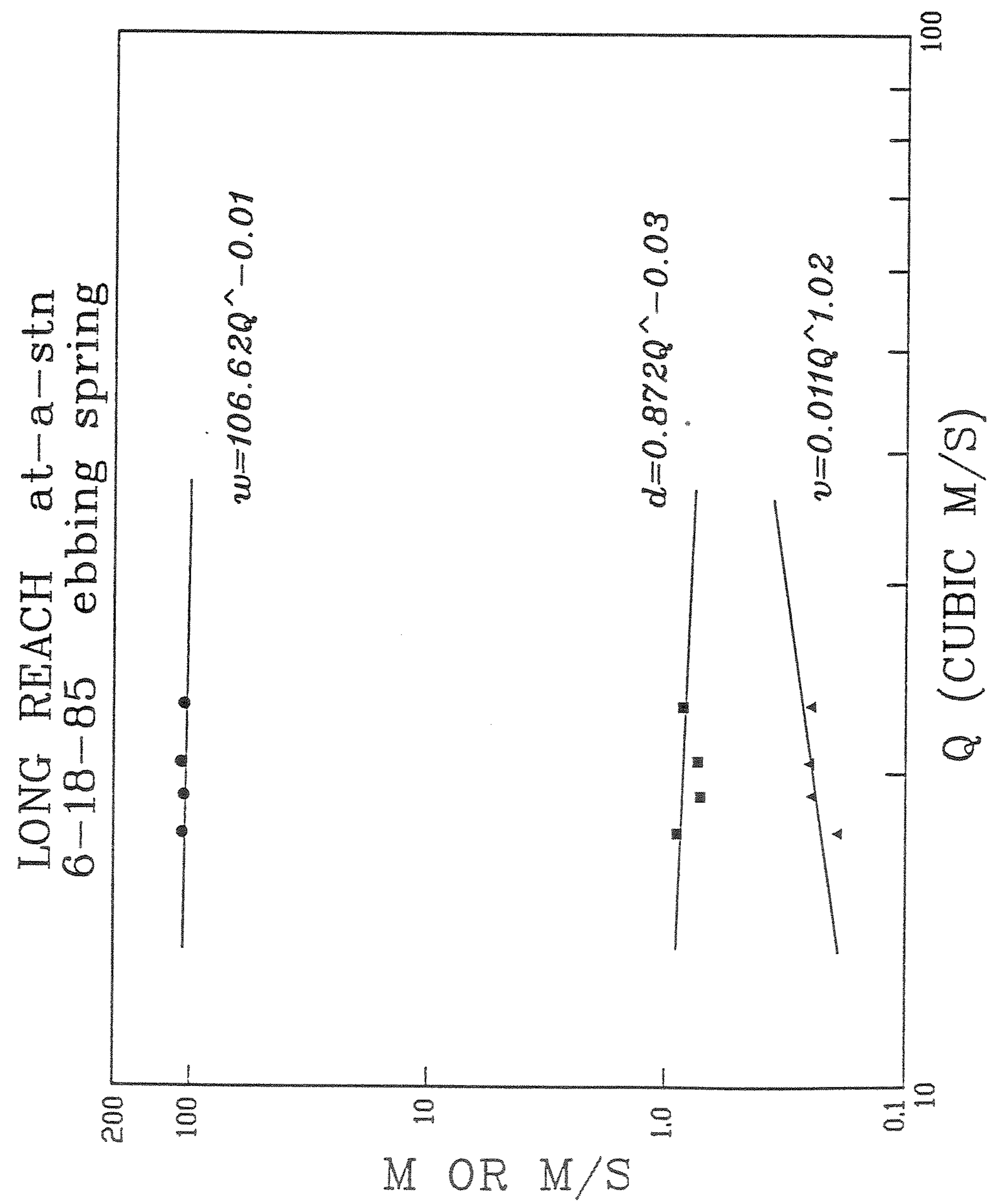
LONG REACH at-a-stn
6-18-85 ebbing spring
w=106.62Q^-0.01
d=0.872Q^-0.03
v=0.011Q^1.02
200
100
10
1.0
0.1
M OR M/S
10
100
Q (CUBIC M/S)

Figure 10

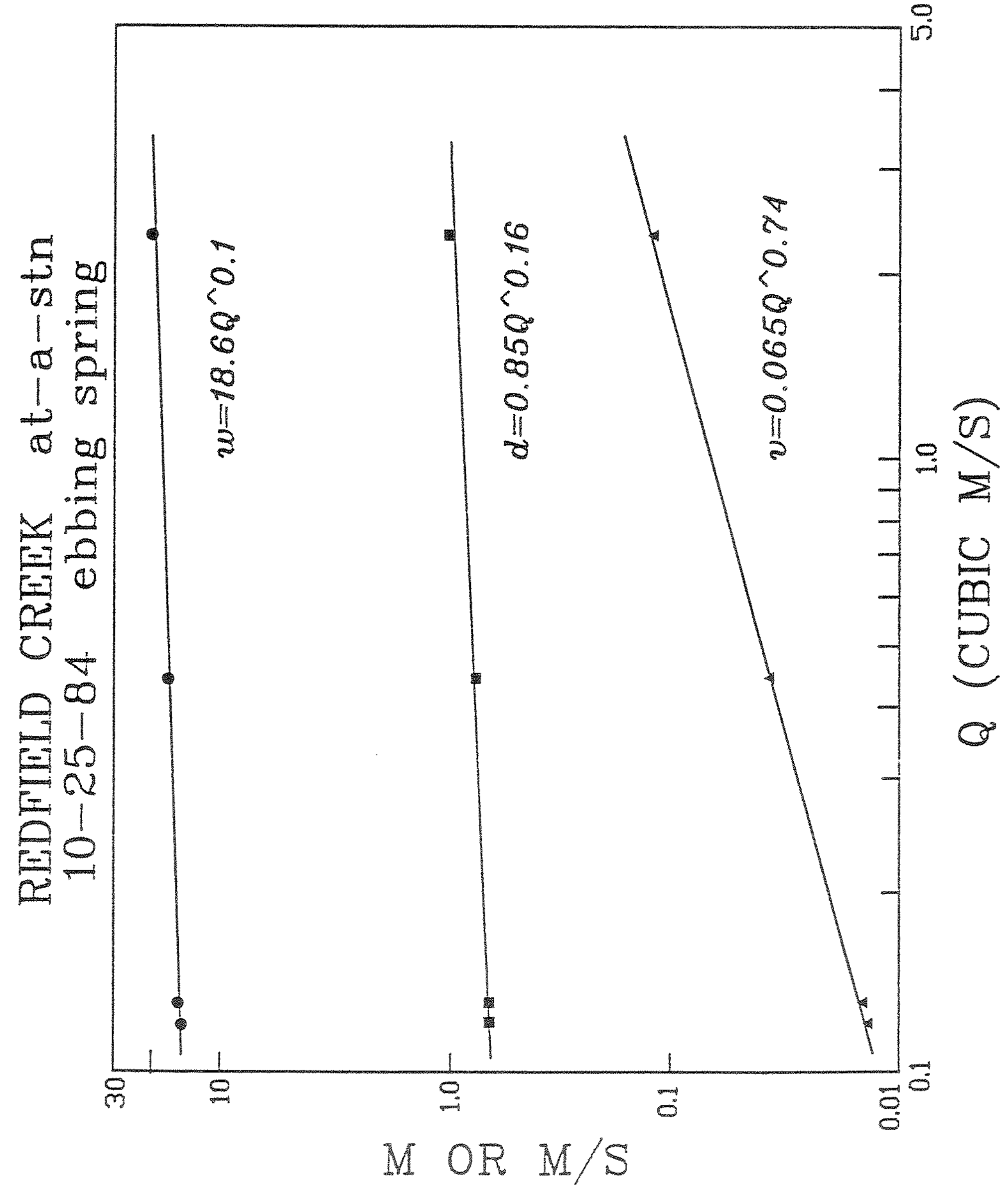

REDFIELD CREEK at-a-stn
10-25-84 ebbing spring
w=18.6Q^0.1
d=0.85Q^0.16
v=0.065Q^0.74
M OR M/S
30
10
1.0
0.1
0.01
0.1
1.0
5.0
Q (CUBIC M/S)

Figure 11

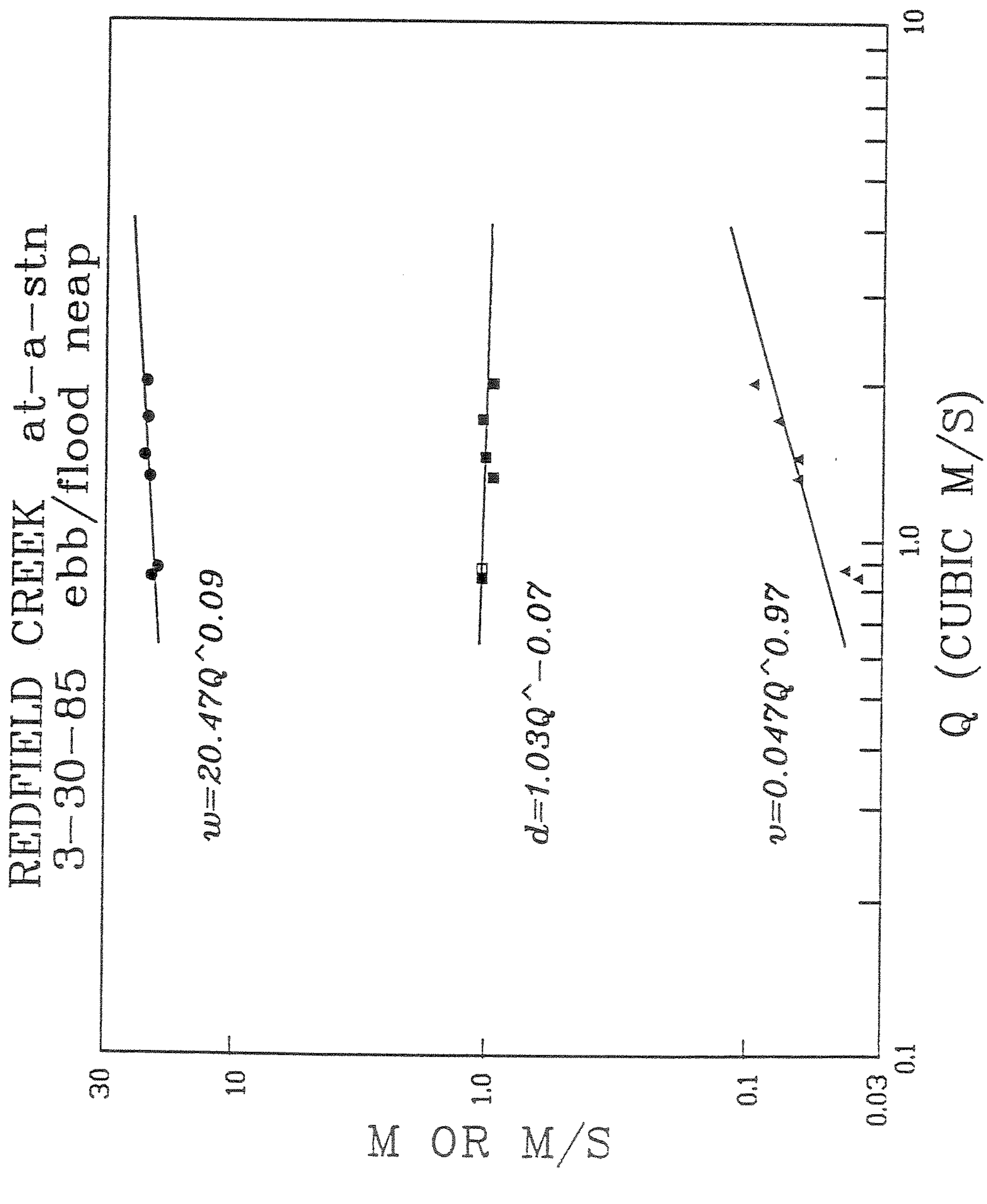
REDFIELD CREEK at-a-stn
3-30-85 ebb/flood neap
w=20.47Q^0.09
d=1.03Q^-0.07
v=0.047Q^0.97
M OR M/S
30
10
1.0
0.1
0.03
0.1
1.0
10
Q (CUBIC M/S)

Figure 12

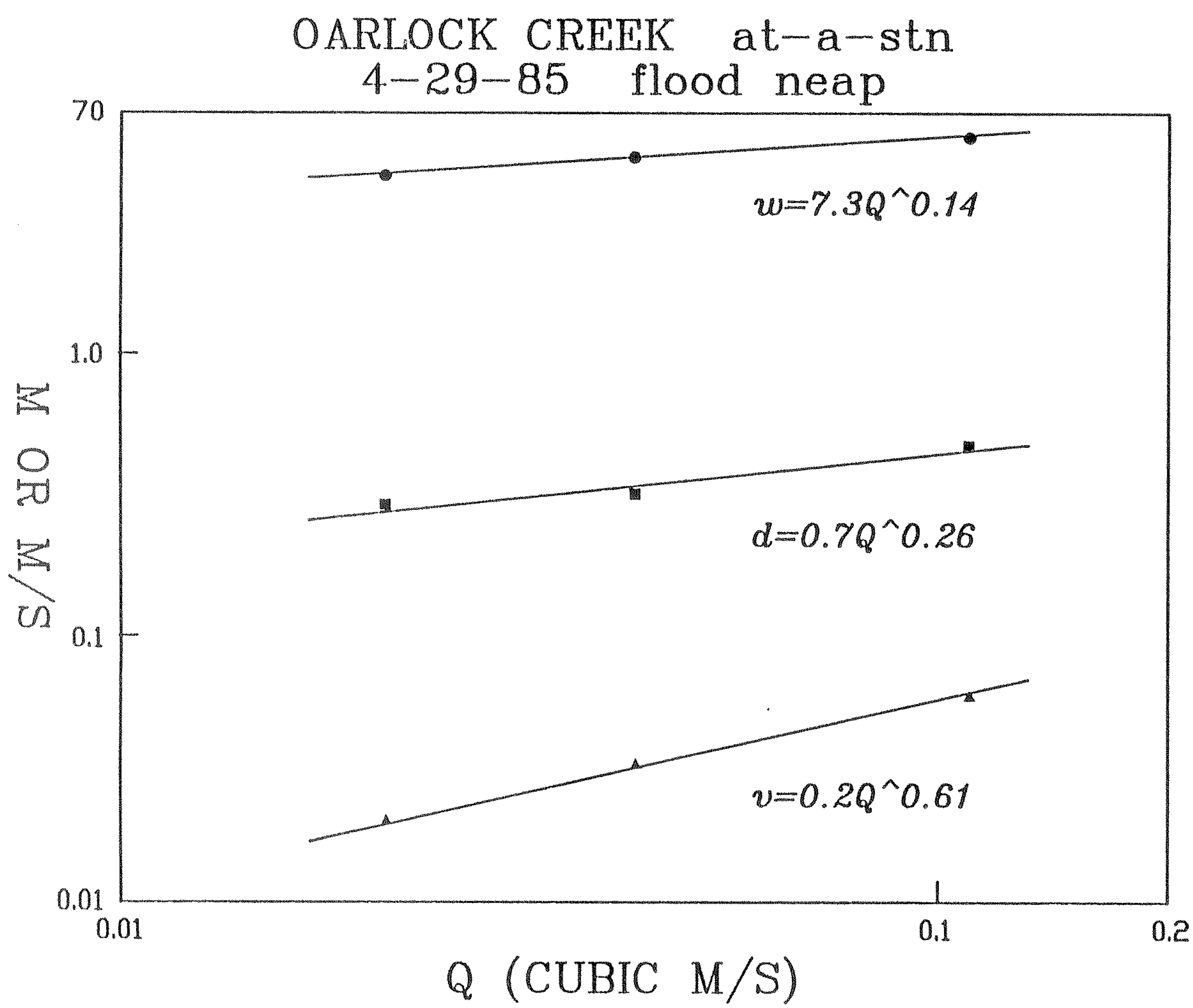
OARLOCK CREEK at-a-stn
4-29-85 flood neap
70
1.0
0.1
0.01
M OR M/S
0.01
0.1
0.2
Q (CUBIC M/S)
w=7.3Q^0.14
d=0.7Q^0.26
v=0.2Q^0.61

Figure 13

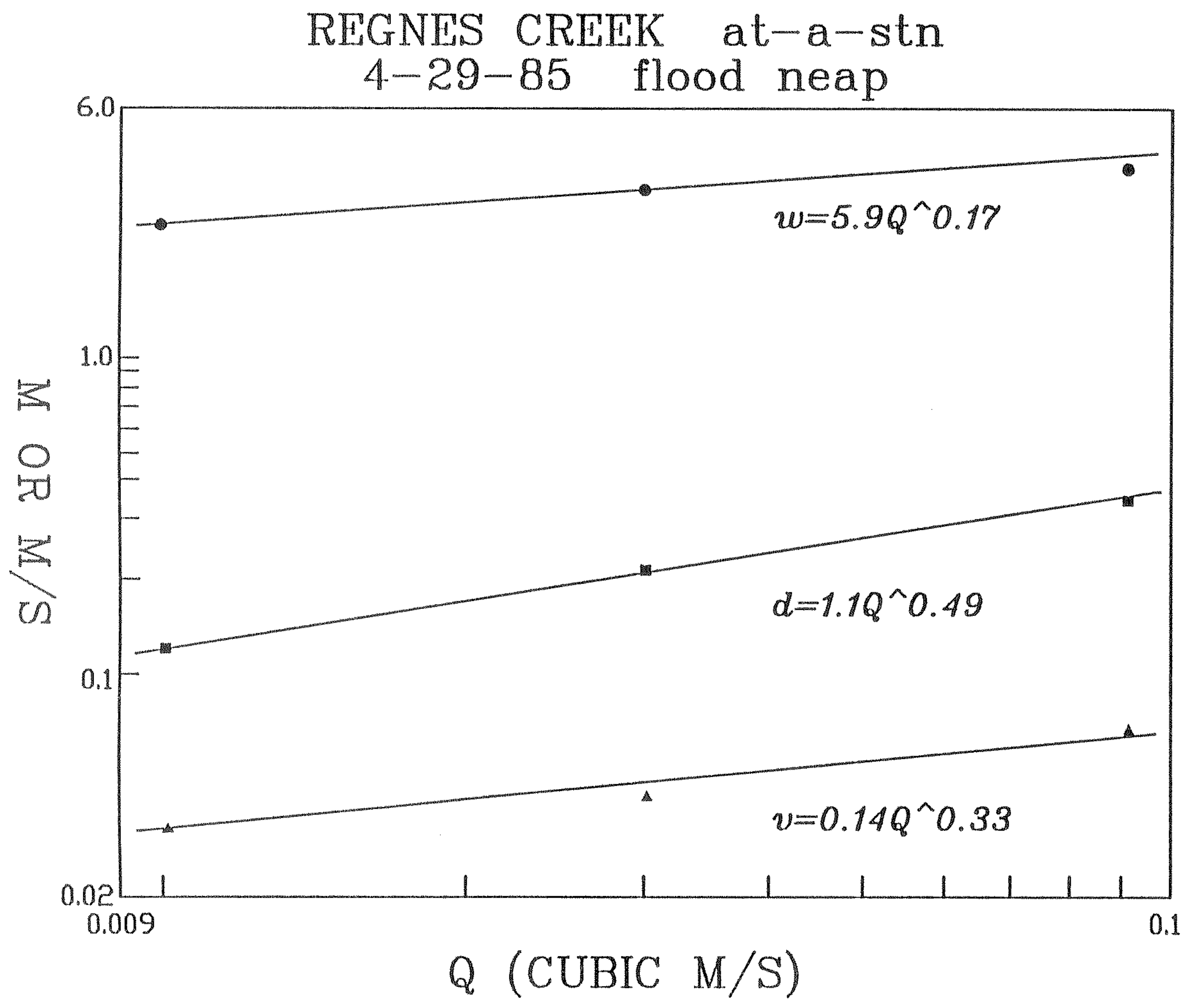
REGNES CREEK at—a—stn
4—29—85 flood neap
w=5.9Q^0.17
d=1.1Q^0.49
v=0.14Q^0.33
M OR M/S
6.0
1.0
0.1
0.02
0.009
0.1
Q (CUBIC M/S)

Figure 14

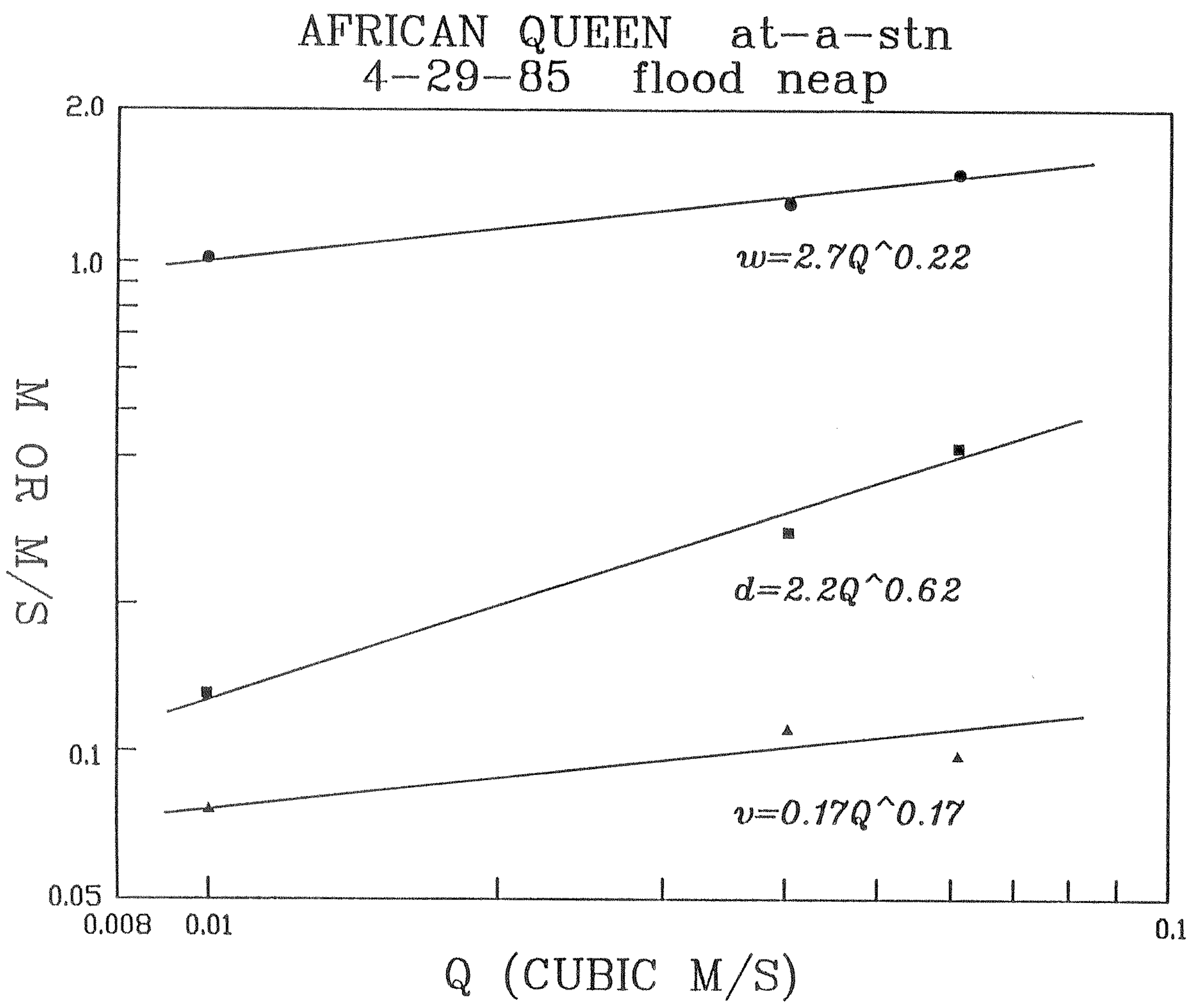
AFRICAN QUEEN at-a-stn
4-29-85 flood neap
2.0
1.0
0.1
0.05
M OR M/S
w=2.7Q^0.22
d=2.2Q^0.62
v=0.17Q^0.17
0.008
0.01
0.1
Q (CUBIC M/S)

Figure 15

between channel segment axial length (sinuous length) and the straight line distance between the ends of the segment (straight length). On average, the highest and lowest order channels are least sinuous (Table 4). Mid-order channel paths can be quite tortuous in planform. Channel length is logarithmically related to channel order (Figures 6 and 7) and described by Horton (1945) as the Law of "stream" lengths.

Junction Angles: Mean junction angles of channel confluences are given in Table 5. There are fewer junctures with high order channels than among the low orders (n). There is considerable scatter of data as is indicated by the standard deviation values which range 18° to 54°.

Drainage Area and Density: The drainage area considered here (Figure 2) is 7.2 km^2 with a drainage density (average length of channels per unit area) (Horton, 1945) of 12.1 (sinuous) and 7.4 (straight) km/km^2 (Table 4).

Width:Depth Ratios: Width:depth ratios based on the average of width and depth measurements determined according to Leopold and Maddock (1953) are presented in Table 6. There is a general trend in shape change with relatively wide and shallow higher order TF channels in contrast to relatively narrow and deeper lower order DE channels. This trend can be seen in the channel profiles drawn to scale in Figure 8. Values vary 5-34 with a high 129 in Long Reach.

Hydraulic Geometry: Leopold and Maddock (1953) established a series of empirical functions describing the changes in stream channel width (w), depth (d), and velocity (v) as discharge (Q) varies at a given river cross-section (at-a-station measurements). These relationships define a fluvial channel's "hydraulic geometry" and are given as follows:

$$w = aQ^b$$
$$d = cQ^f$$
$$v = kQ^m$$

where a,c, and k are site specific coefficients, Q = wdv ack = 1.0, and b+f+m = 1.0. The exponent values of these relations describe how the shape of a channel adjusts to changing flow conditions. Different values of b, f, and m would indicate w, d, and v increasing with Q at different rates.

The at-a-station hydraulic geometry equations for six channels are given in Table 7 and Figures 9-15. The channels fall into three distinct groups on the basis of exponent values.

Modern Sediments

Three distinct environments are associated with the channel cross-sections of this salt-marsh: i) a subtidal thalweg region, ii) an intertidal channel-margin flat, and iii) a channel-margin marsh. Schematic representations of these environments and their subenvironments at each channel cross-section are shown with grain-size data in

Figures 16-27. Grain-size, TOM, and sedimentary structure data are summarized in Tables 8-10.

Thalweg Region: Channels have single and double thalweg regions. Double thalwegs occur at confluences and along the channel-to-channel TF channels of Long Reach and Gravens Thorofare.

This environment is the coarsest at each cross-section and there is a fining trend from large, through-flowing, high order channels to smaller, dead-ending, interior channels (Table 8). Medium sand predominates at IT-A, fine or very fine sand in Gravens Thorofare, and very fine sand in Long Reach and Redfield Creek. Old Turtle Reach thalwegs are sandy silts, and low order channels Oarlock, African Queen, and Regnes are muds with much less sand.

Calcareous debris does not constitute a significant portion of thalweg sediments. Shell fragments make up Ingram's gravel fraction (<3% of total) but drastically diminish to <2% of the modal medium sand fraction. An occasional gravel-sized shell fragment has been encountered at other sample sites. More notable and significant are field observations of shallow creeks with thalwegs littered with whole bivalve shells, articulated and disarticulated.

The TOM content of thalweg sediments increases from large, through-flowers to small, DE channels and correlates with grain-size. TOM is 4% in the coarsest

Figures 16-27. Schematic channel cross-sections indicating the subenvironments present. Sand:silt:clay ratios are given with medium:fine:very fine sand ratios or modal sand size in parentheses, with the exception of the thalweg region of IT-A (Figure 16, *) showing very coarse:coarse: medium sand ratio.

LW=landward, SW=seaward, E=east, W=west, N=north, S=south

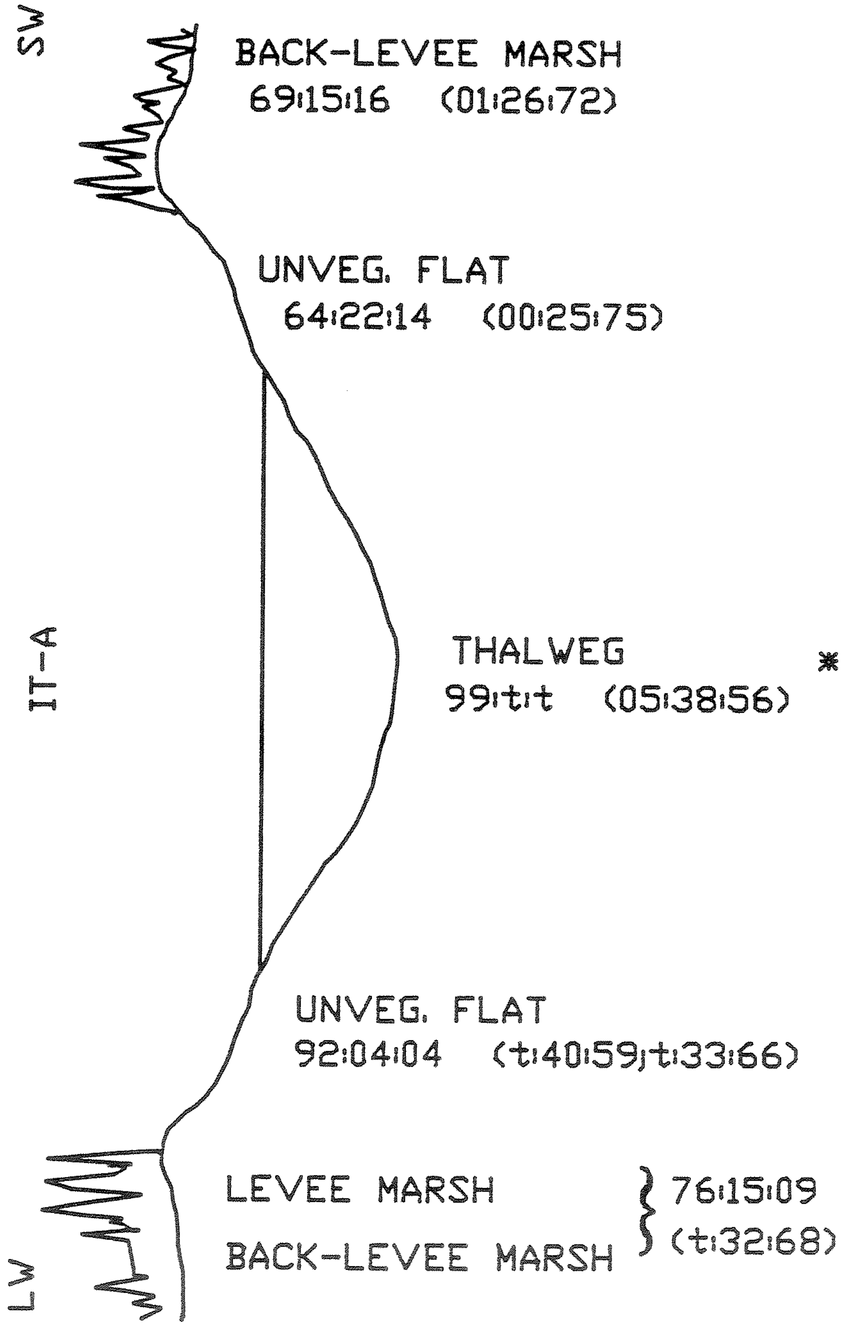
SW
BACK-LEVEE MARSH
69:15:16 (01:26:72)
UNVEG. FLAT
64:22:14 (00:25:75)
IT-A
THALWEG
99:t:t (05:38:56)
*
UNVEG. FLAT
92:04:04 (t:40:59;t:33:66)
LEVEE MARSH
BACK-LEVEE MARSH
76:15:09
(t:32:68)
LW

Figure 16

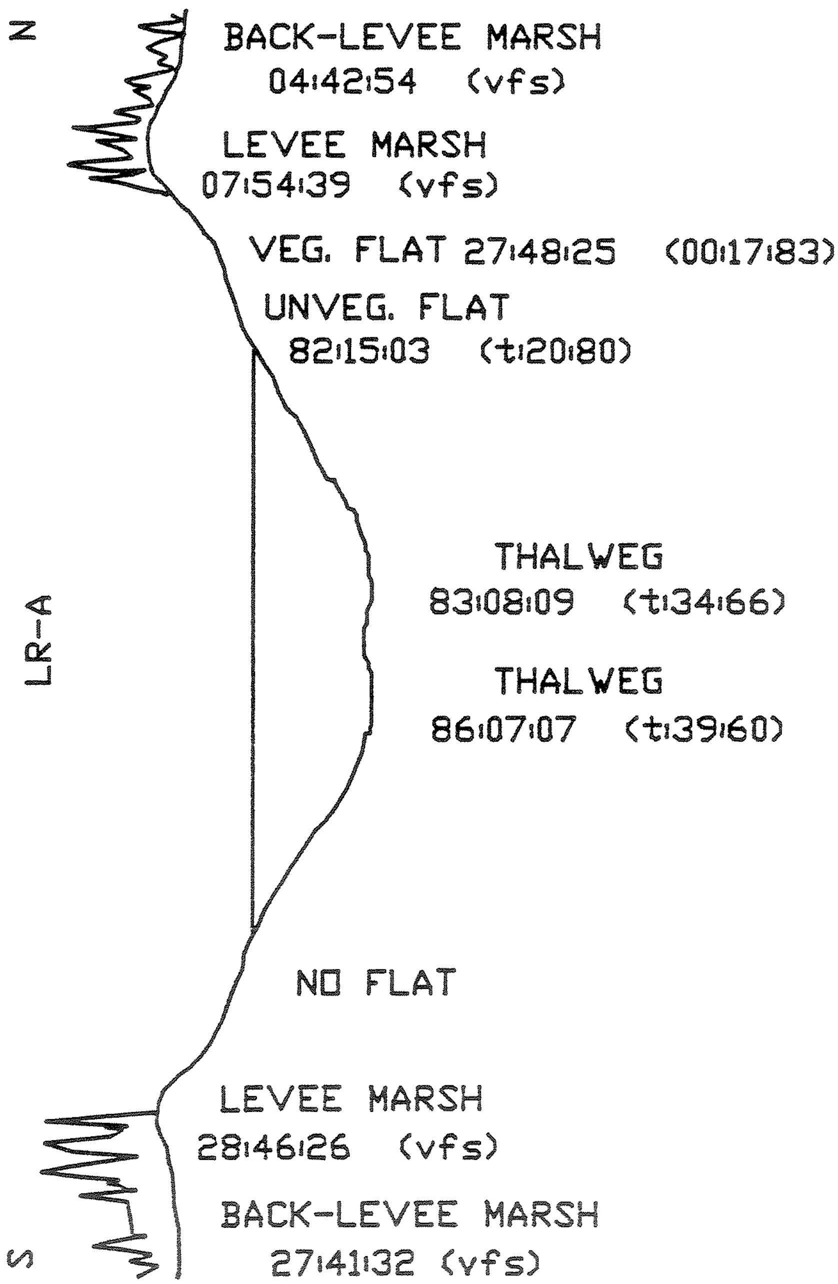
N
BACK-LEVEE MARSH
04:42:54 (vfs)
LEVEE MARSH
07:54:39 (vfs)
VEG. FLAT 27:48:25 (00:17:83)
UNVEG. FLAT
82:15:03 (t:20:80)
LR-A
THALWEG
83:08:09 (t:34:66)
THALWEG
86:07:07 (t:39:60)
NO FLAT
LEVEE MARSH
28:46:26 (vfs)
BACK-LEVEE MARSH
27:41:32 (vfs)
S

Figure 17

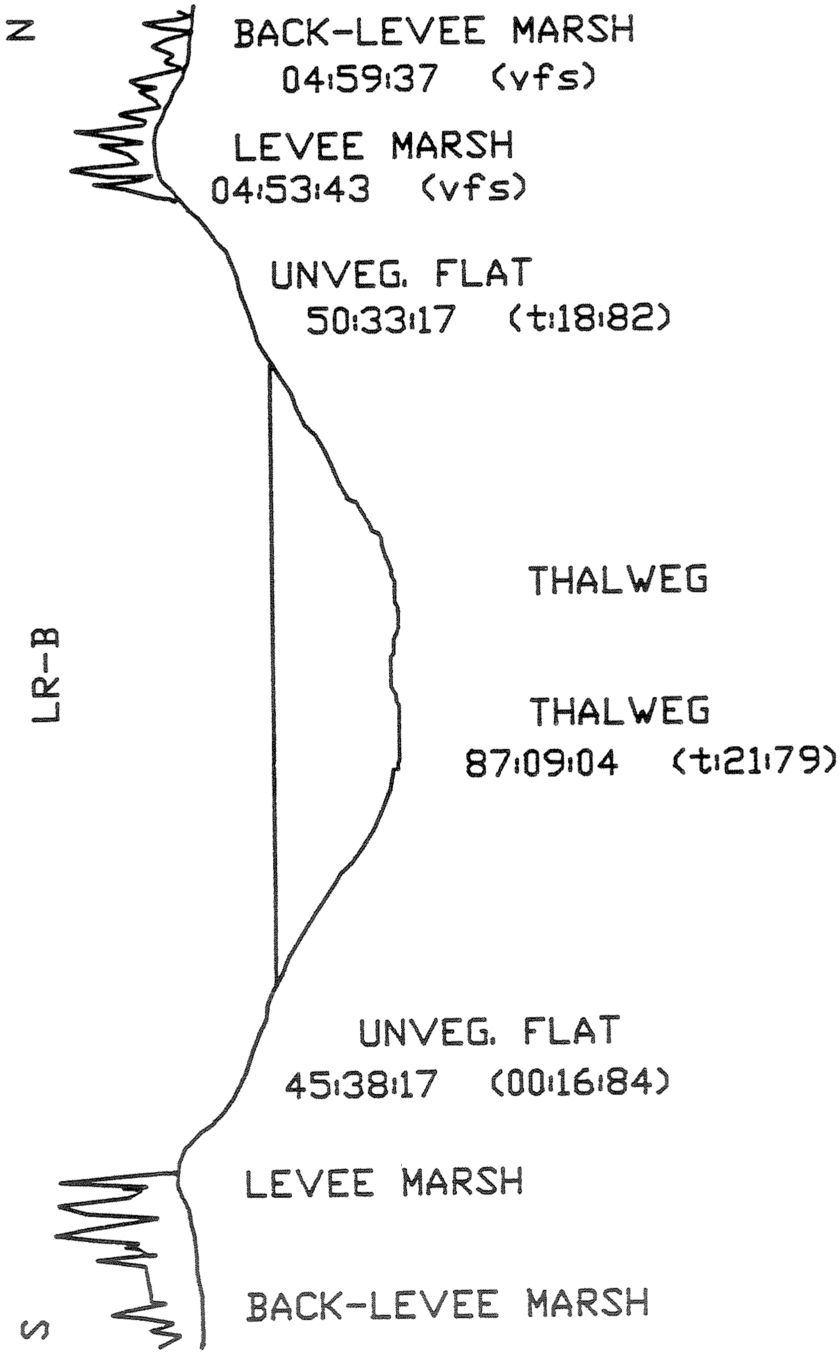
N
BACK-LEVEE MARSH
04:59:37 (vfs)
LEVEE MARSH
04:53:43 (vfs)
UNVEG. FLAT
50:33:17 (t:18:82)
THALWEG
LR-B
THALWEG
87:09:04 (t:21:79)
UNVEG. FLAT
45:38:17 (00:16:84)
LEVEE MARSH
BACK-LEVEE MARSH
S

Figure 18

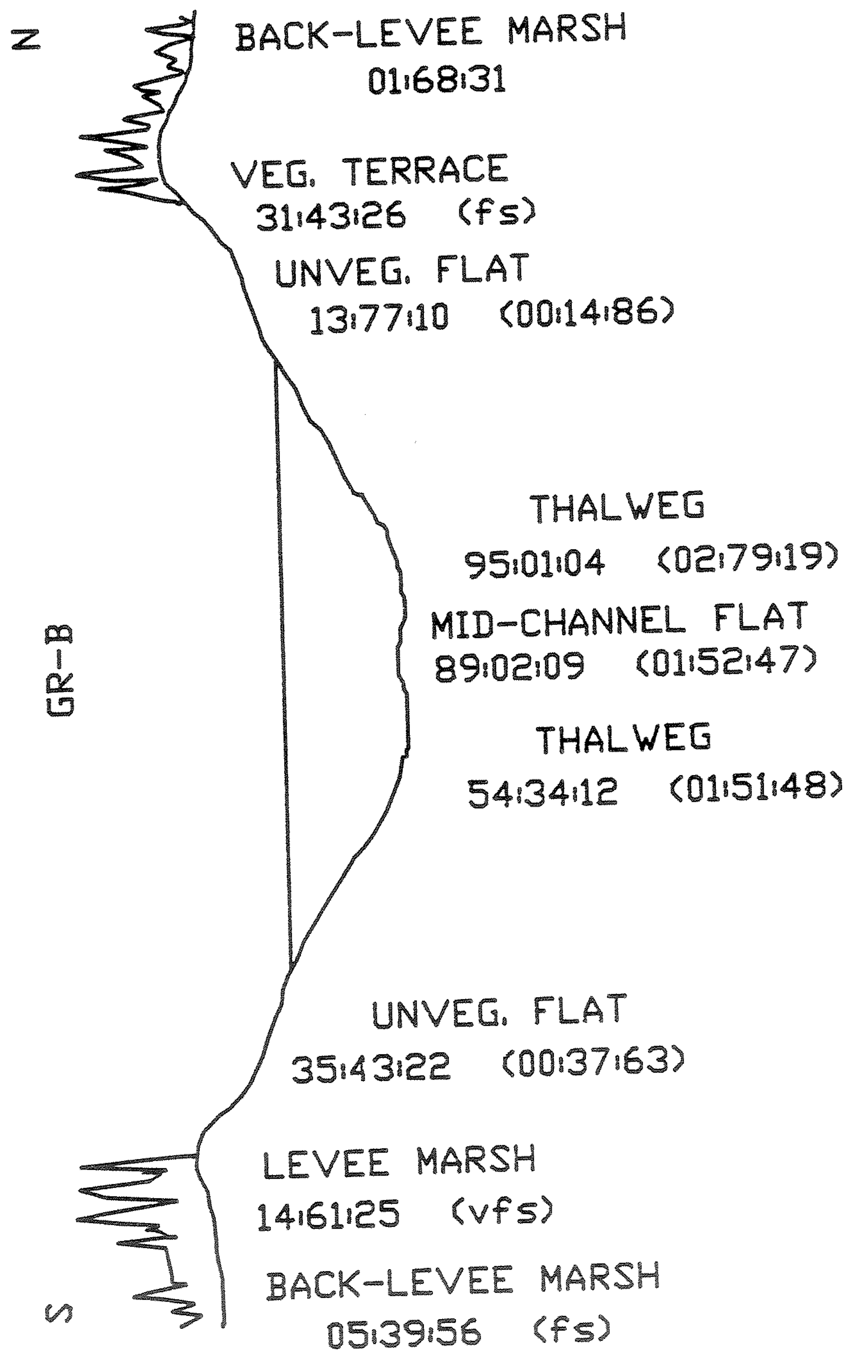
N
BACK-LEVEE MARSH
01:68:31
VEG. TERRACE
31:43:26 (fs)
UNVEG. FLAT
13:77:10 (00:14:86)
THALWEG
95:01:04 (02:79:19)
MID-CHANNEL FLAT
89:02:09 (01:52:47)
THALWEG
54:34:12 (01:51:48)
GR-B
UNVEG. FLAT
35:43:22 (00:37:63)
LEVEE MARSH
14:61:25 (vfs)
BACK-LEVEE MARSH
05:39:56 (fs)
S

Figure 19

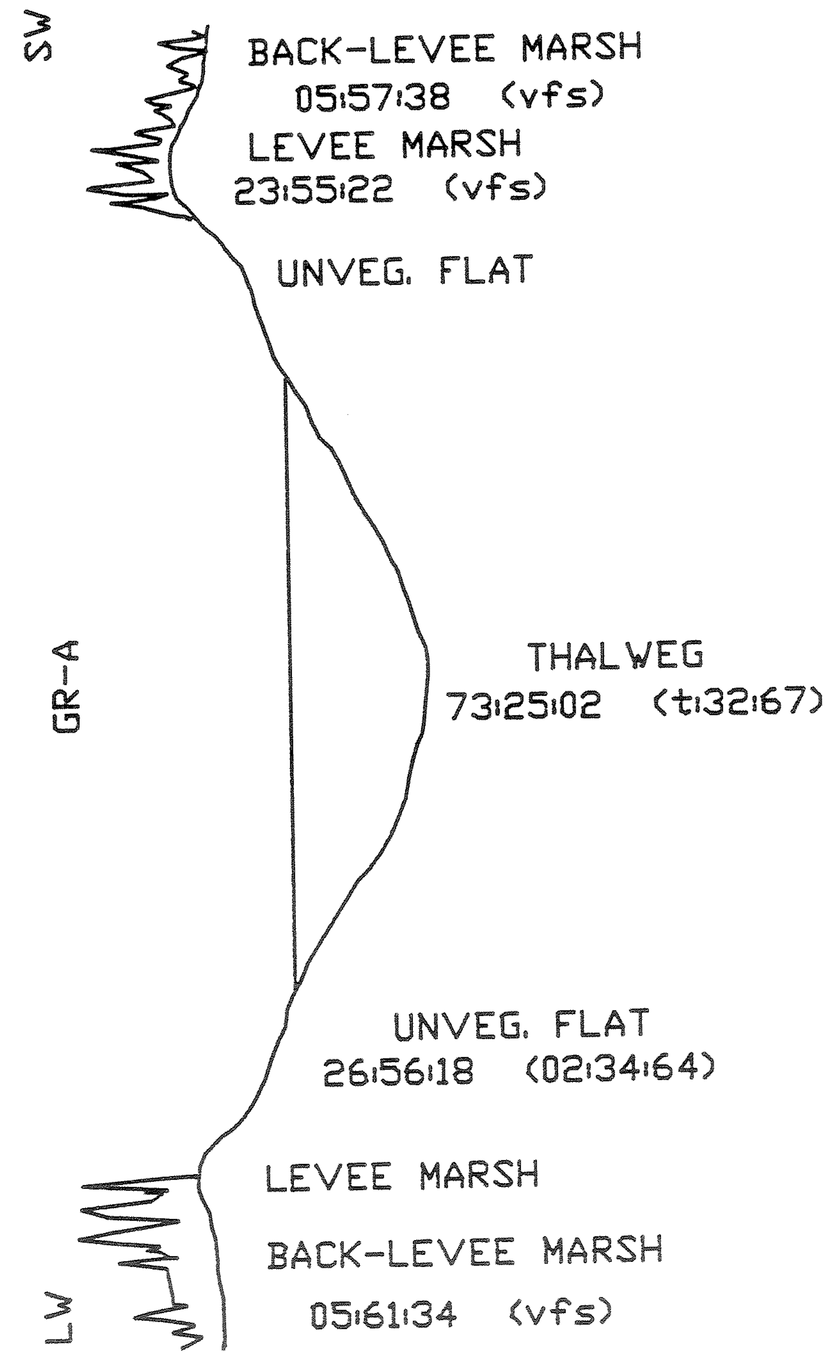
SW
BACK-LEVEE MARSH
05:57:38 (vfs)
LEVEE MARSH
23:55:22 (vfs)
UNVEG. FLAT
GR-A
THALWEG
73:25:02 (t:32:67)
UNVEG. FLAT
26:56:18 (02:34:64)
LEVEE MARSH
BACK-LEVEE MARSH
LW
05:61:34 (vfs)

Figure 20

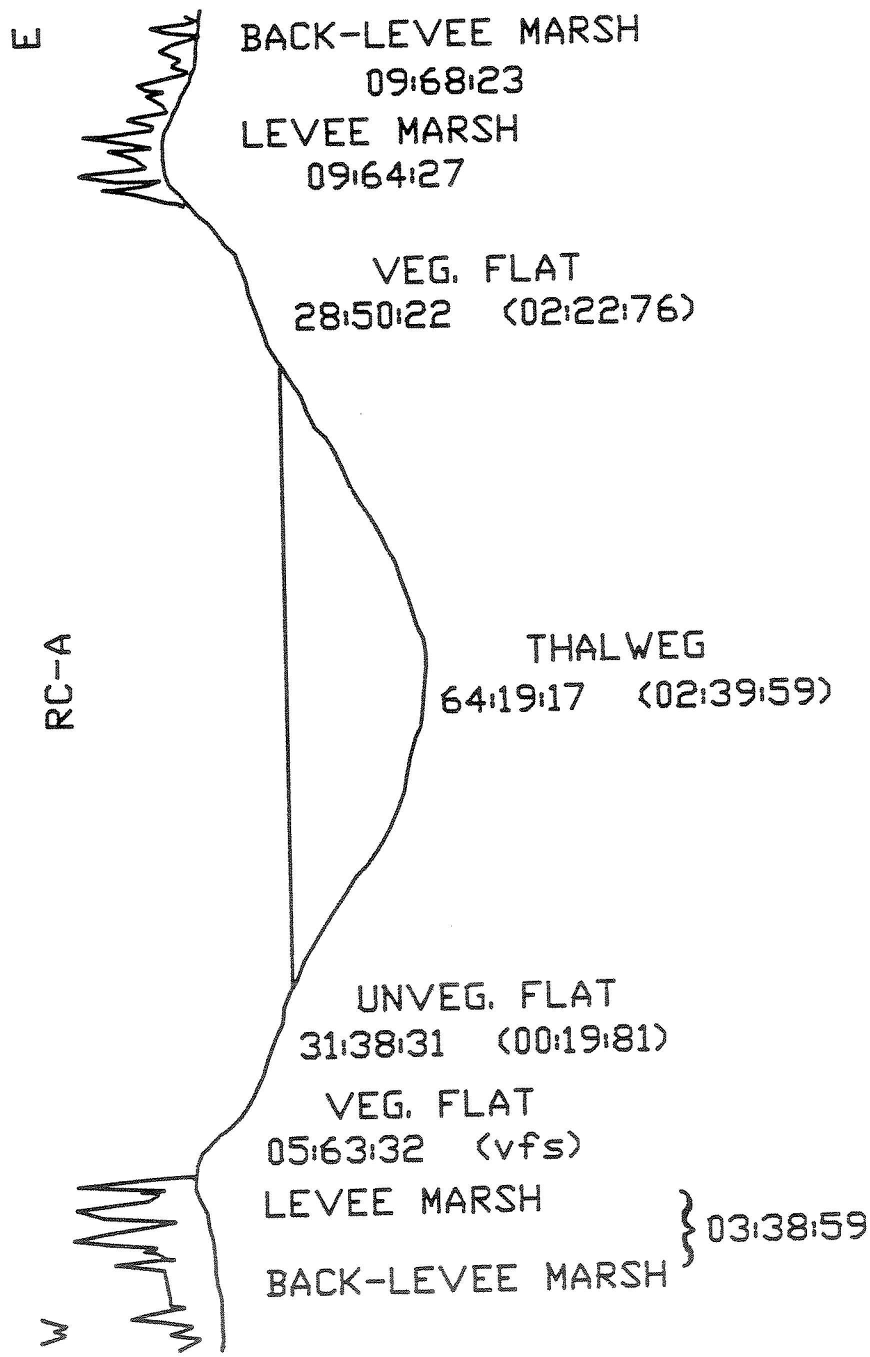
E
BACK-LEVEE MARSH
09:68:23
LEVEE MARSH
09:64:27
VEG. FLAT
28:50:22 (02:22:76)
RC-A
THALWEG
64:19:17 (02:39:59)
UNVEG. FLAT
31:38:31 (00:19:81)
VEG. FLAT
05:63:32 (vfs)
LEVEE MARSH
BACK-LEVEE MARSH
03:38:59
W

Figure 21

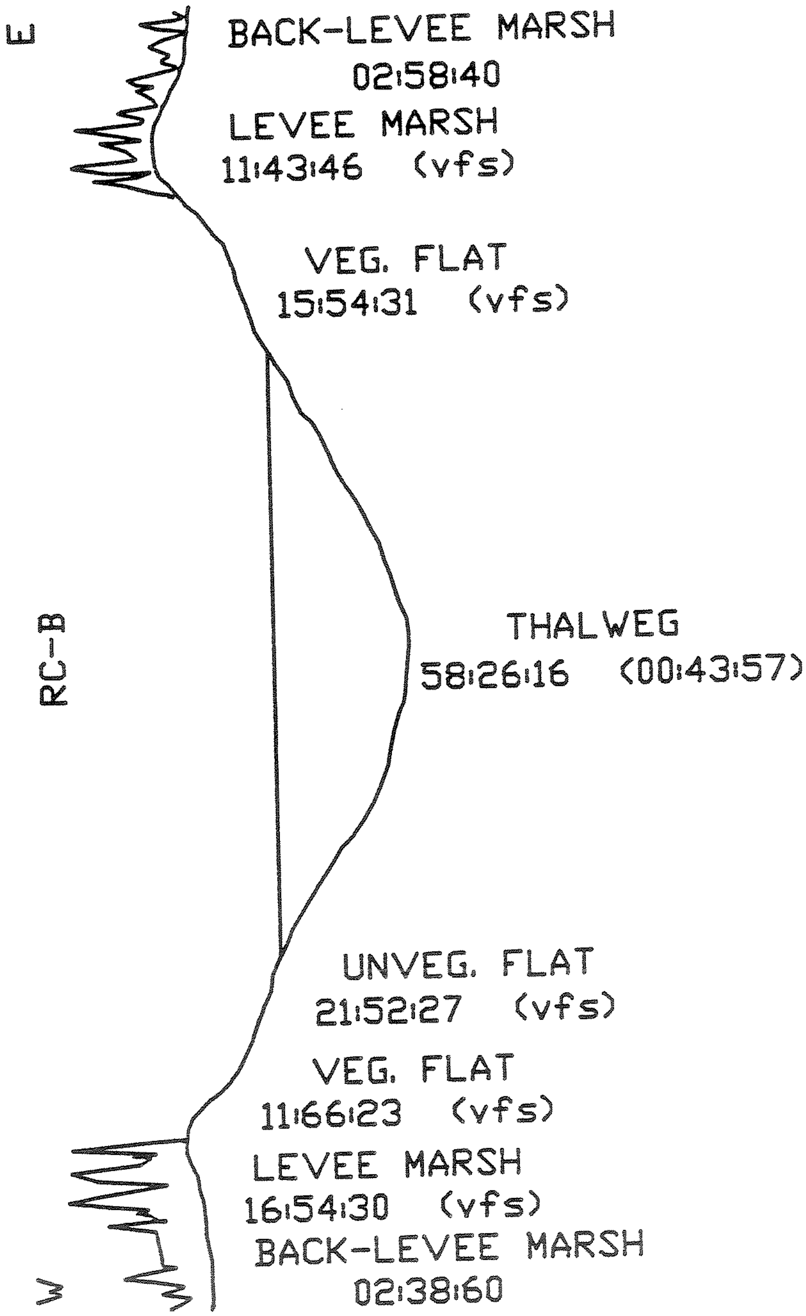
E
BACK-LEVEE MARSH
02:58:40
LEVEE MARSH
11:43:46 (vfs)
VEG. FLAT
15:54:31 (vfs)
RC-B
THALWEG
58:26:16 (00:43:57)
UNVEG. FLAT
21:52:27 (vfs)
VEG. FLAT
11:66:23 (vfs)
LEVEE MARSH
16:54:30 (vfs)
BACK-LEVEE MARSH
02:38:60
W

Figure 22

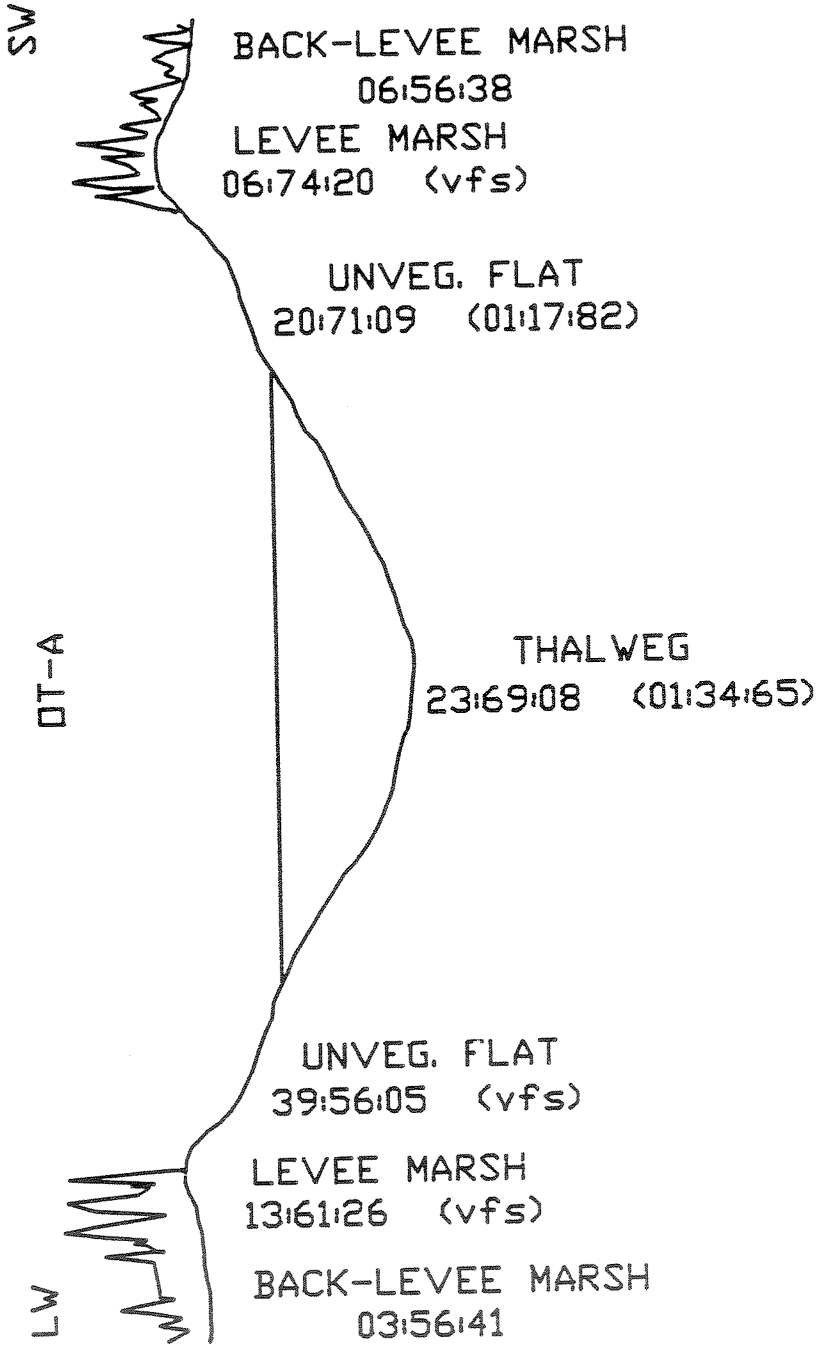
SW
BACK-LEVEE MARSH
06:56:38
LEVEE MARSH
06:74:20 (vfs)
UNVEG. FLAT
20:71:09 (01:17:82)
DT-A
THALWEG
23:69:08 (01:34:65)
UNVEG. FLAT
39:56:05 (vfs)
LEVEE MARSH
13:61:26 (vfs)
BACK-LEVEE MARSH
03:56:41
LW

Figure 23

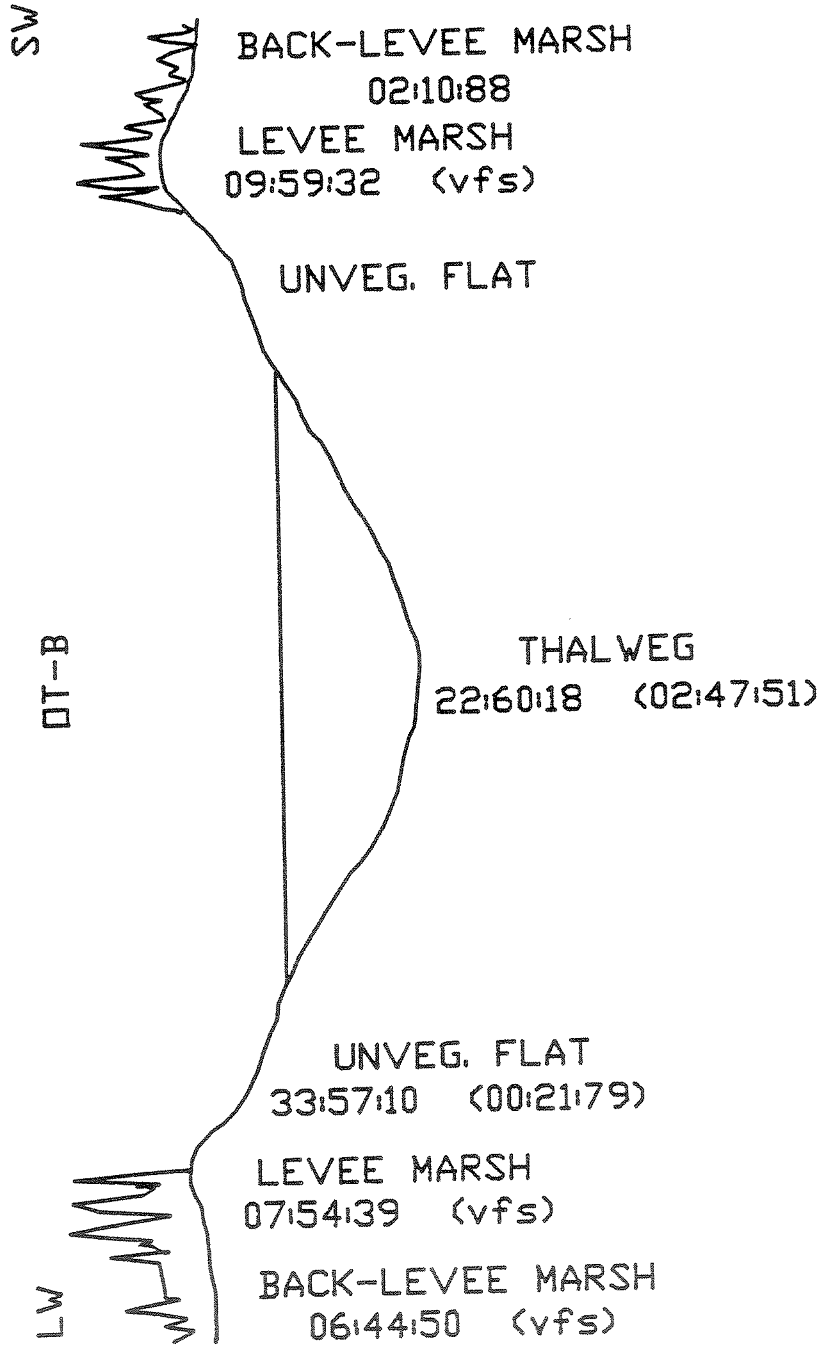
SW
BACK-LEVEE MARSH
02:10:88
LEVEE MARSH
09:59:32 (vfs)
UNVEG. FLAT
DT-B
THALWEG
22:60:18 (02:47:51)
UNVEG. FLAT
33:57:10 (00:21:79)
LEVEE MARSH
07:54:39 (vfs)
BACK-LEVEE MARSH
06:44:50 (vfs)
LW

Figure 24

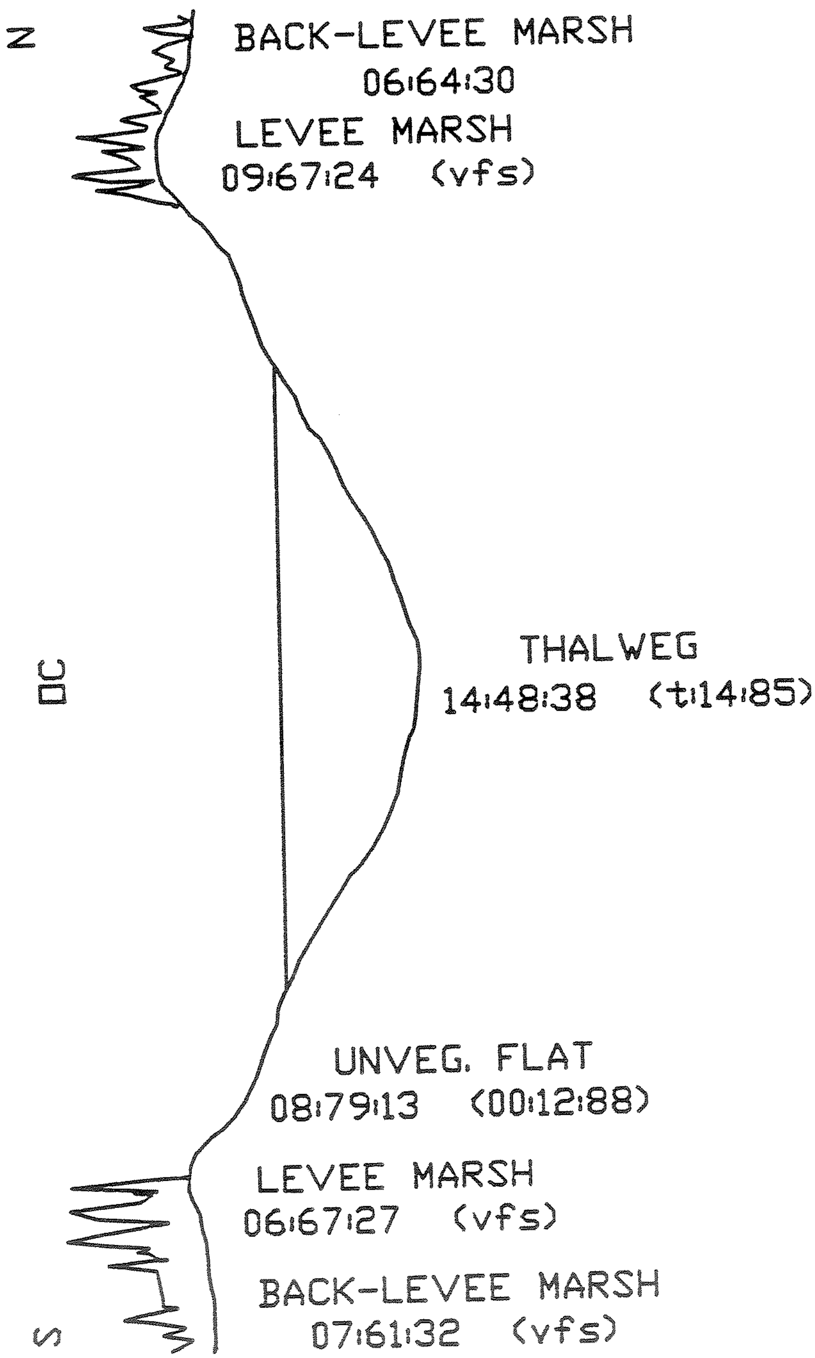
N
BACK-LEVEE MARSH
06:64:30
LEVEE MARSH
09:67:24 (vfs)
DC
THALWEG
14:48:38 (t:14:85)
UNVEG. FLAT
08:79:13 (00:12:88)
LEVEE MARSH
06:67:27 (vfs)
BACK-LEVEE MARSH
07:61:32 (vfs)
S

Figure 25

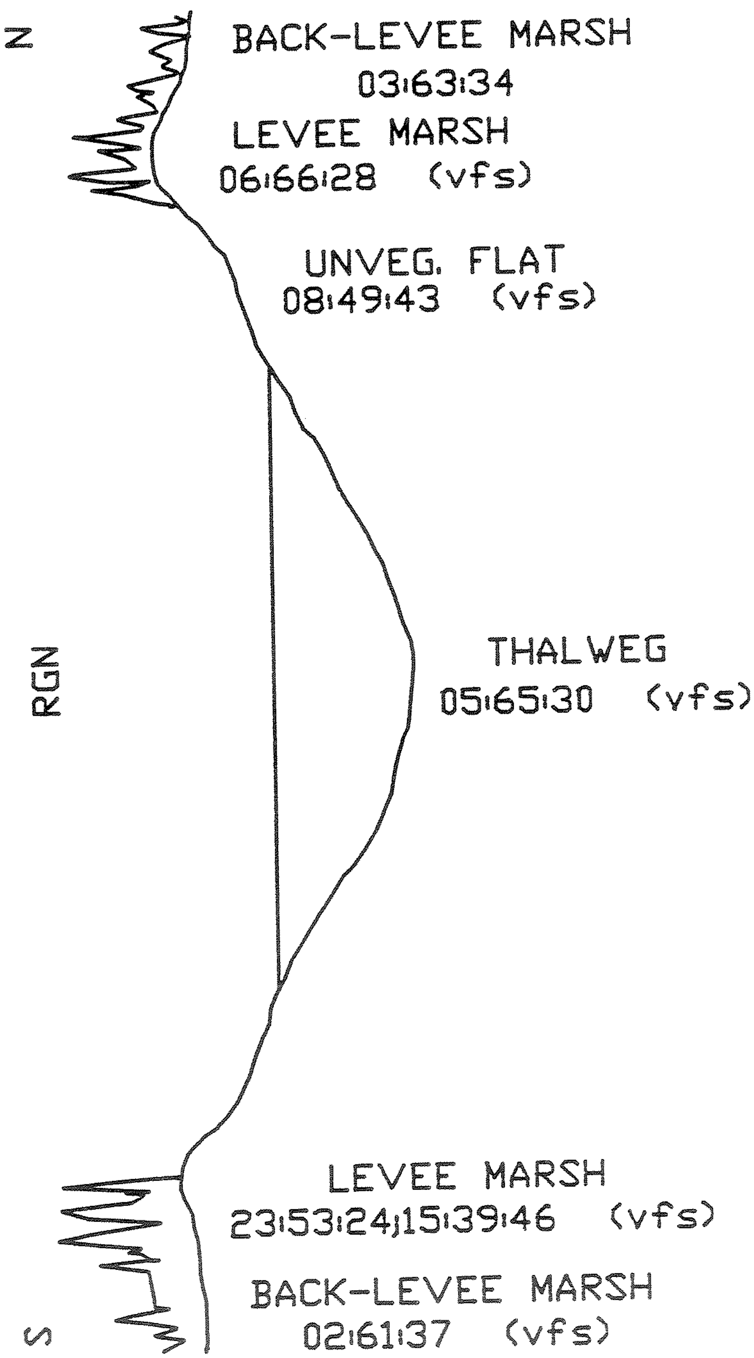
N
BACK-LEVEE MARSH
03:63:34
LEVEE MARSH
06:66:28 (vfs)
UNVEG. FLAT
08:49:43 (vfs)
RGN
THALWEG
05:65:30 (vfs)
LEVEE MARSH
23:53:24;15:39:46 (vfs)
BACK-LEVEE MARSH
02:61:37 (vfs)
S

Figure 26

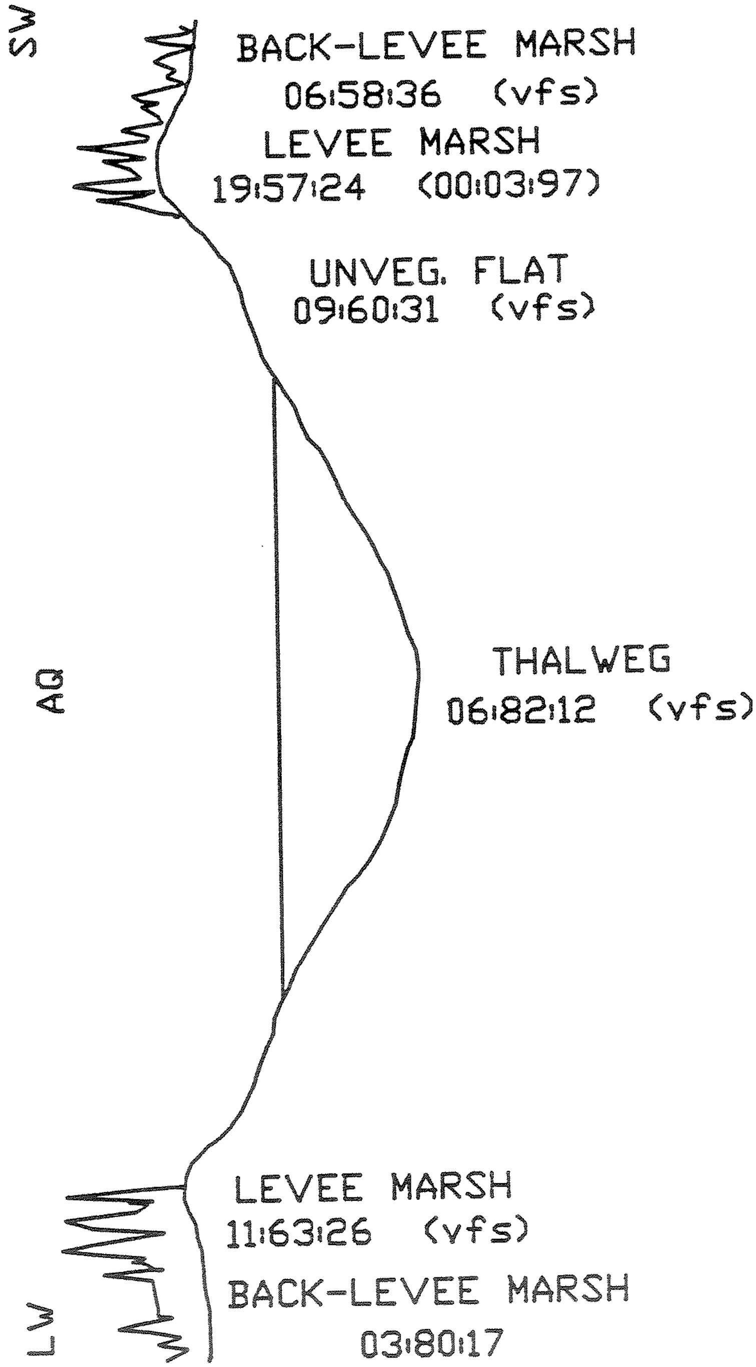
SW
BACK-LEVEE MARSH
06:58:36 (vfs)
LEVEE MARSH
19:57:24 (00:03:97)
UNVEG. FLAT
09:60:31 (vfs)
AQ
THALWEG
06:82:12 (vfs)
LEVEE MARSH
11:63:26 (vfs)
BACK-LEVEE MARSH
03:80:17
LW

Figure 27

TABLE 8

GRAIN-SIZE DATA*

	sd:st:cy	m:fs:vfs (or mode)
LAGOON		
GS-2	78:14:08	t:22:77
T-2	18:32:50	vfs
THALWEG REGION		
IT-A	99:t:t	05:38:56 (vc:c:m)*
LR-A south	86:07:07	t:39:60
LR-A north	83:08:09	t:34:66
LR-B south	87:09:04	t:21:79
GR-B south	54:34:12	01:51:48
GR-B north	95:01:04	02:79:19
GR-A	73:25:02	t:32:67
RC-A	64:19:17	02:39:59
RC-B	58:26:16	00:43:57
OT-A	23:69:08	01:34:65
OT-B	22:60:18	02:47:51
OC	14:48:38	t:14:85
AQ	06:82:12	vfs
RGN	05:65:30	vfs
UNVEGETATED FLAT		
IT-A sw	64:22:14	00:25:75
IT-A lw	92:04:04	t:40:59
	92:04:04	t:33:66
LR-A north	82:15:03	t:20:80
LR-B south	45:38:17	00:16:84
LR-B north	50:33:17	t:18:82
GR-B south	35:43:22	00:37:63
GR-B mid	89:02:09	01:52:47
GR-B north	13:77:10	00:14:86
GR-A lw	26:56:18	02:34:64
RC-A west	31:38:31	00:19:81
RC-B west	21:52:27	vfs
OT-A sw	20:71:09	01:17:82
OT-A lw	39:56:05	vfs
OT-B lw	33:57:10	00:21:79
OC south	08:79:13	00:12:88
AQ	09:60:31	vfs
RGN	08:49:43	vfs

TABLE 8 (cont.)

	sd:st:cy	m:fs:vfs (or mode)
VEGETATED FLAT		
LR-A north	27:48:25	00:17:83
RC-A west	05:63:32	vfs
RC-A east	28:50:22	02:22:76
RC-B west	11:66:23	vfs
RC-B east	15:54:31	vfs
VEGETATED TERRACE		
GR-B north	31:43:26	fs
LEVEE MARSH		
LR-A south	28:46:26	vfs
LR-A north	07:54:39	vfs
LR-B north	04:53:43	vfs
GR-B south	14:61:25	vfs
GR-A sw	23:55:22	vfs
RC-A east	09:64:27	---
** RC-A west	03:38:59	---
RC-B west	16:54:30	vfs
RC-B east	11:43:46	vfs
OT-A sw	06:74:20	vfs
OT-A lw	13:61:26	vfs
OT-B sw	09:59:32	vfs
OT-B lw	07:54:39	vfs
OC south	06:67:27	vfs
OC north	09:67:24	vfs
AQ sw	19:57:24	00:03:97
AQ lw	11:63:26	vfs
RGN south	23:53:24	vfs
	15:39:46	vfs
RGN north	06:66:28	vfs

(cont.)

TABLE 8 (cont.)

	sd:st:cy	m:fs:vfs (or mode)
BACK-LEVEE MARSH		
IT-A sw	69:15:16	01:26:72
IT-A lw	76:15:09	t:32:68
LR-A south	27:41:32	vfs
LR-A north	04:42:54	vfs
LR-B north	04:59:37	vfs
GR-B south	05:39:56	fs
GR-B north	01:68:31	too little
GR-A sw	05:57:38	vfs
GR-A lw	05:61:34	vfs
** RC-A west	03:38:59	---
RC-A east	09:68:23	too little
RC-B west	02:38:60	too little
RC-B east	02:58:40	too little
OT-A sw	06:56:38	too little
OT-A lw	03:56:41	too little
OT-B sw	02:10:88	too little
OT-B lw	06:44:50	vfs
OC south	07:61:32	vfs
OC north	06:64:30	too little
AQ sw	06:58:36	vfs
AQ lw	03:80:17	too little
RGN south	02:61:37	vfs
RGN north	03:63:34	too little

*(abbreviations: sd=sand;st=silt;cy=clay;vc=very coarse sand;c=coarse sand;m=medium sand;fs=fine sand;vfs=very fine sand;t=trace;sw=seaward;lw=landward)

**location between levee and back-levee marsh

TABLE 9

ORGANIC CONTENT

ENVIRONMENT		SAND:SILT:CLAY	%TOM
IT:	flat	92:04:04	1
	marsh	76:15:09	5
LR:	thalweg	87:09:04	4
	flat	50:33:17	7
	marsh	04:59:37	24
RC:	thalweg	58:26:16	9
	flat	21:52:27	10
	marsh	02:38:60	22
RGN:	thalweg	05:65:30	10
	flat	08:49:43	13
	marsh	03:63:34	16

TABLE 10

SEDIMENTARY STRUCTURES

	sd:st:cy*	structures
THALWEG REGION		
LR-B north	83:08:09	stratification
LR-B south	87:09:04	stratification
GR-B north	95:01:04	distinct burrows and stratification
GR-B south	54:34:12	distinct burrows and mottled
RC-A	64:19:17	distinct burrows and mottled
RC-B	58:26:16	mottled (and burrowed?)
OT-A	23:69:08	mottled (and burrowed?)
OC	14:48:38	mottled
AQ	06:82:12	homogeneous
RGN	05:65:30	mottled
UNVEGETATED FLAT		
IT-A lw	92:04:04	stratification
LR-A north	82:15:03	stratification
LR-B south	45:38:17	mottled
LR-B north	50:33:17	stratification
GR-B mid	89:02:09	distinct burrows
RC/@LR west	silt	stratification, slump feature, mottled
RC/@LR east	silt	distinct burrows and mottled
RC-A west	31:38:31	distinct burrows
OT-A sw	20:71:09	homogeneous
OT-A lw	39:56:05	distinct burrows
OC south	08:79:13	distinct burrows
AQ	09:60:31	distinct burrows
RGN	08:49:43	distinct burrows

*abbreviations follow Table 8

sediment (LR-B) and increases to 10% in the finest (RGN) (Table 9).

Sedimentary structures also show a correlation with grain-size, and hence, show a trend in their distribution. Sandy thalweg areas have stratification features intact while increasing proportions of silt and clay favor the presence of invertebrate burrowers that destroy stratification through bioturbation, producing a mottled texture (Table 10; Figure 28a and b).

Bedforms are only produced in the higher energy medium sands of Ingram Thorofare (Ashley and Zeff, 1985b). They are flood-oriented with 15-30 meter spacing and a 0.5-1.5 meter height.

Channel-Margin Flats: Intertidal flats border channel margins. This environment displays the greatest degree of variability in sediment texture (Table 8). Flats are alternately covered and uncovered with each tidal cycle and may be unvegetated or sparsely vegetated. Vegetated areas are nearest the marsh and are covered with the tall form of *S. alterniflora*. Unvegetated flats are usually heavily covered with fiddler crab burrows, snail tracks and trails, and/or algae of various forms. Flats at a cross-section usually occur at one side only.

At a cross-section, flats are finer grained than thalweg sediments. Where vegetated and unvegetated flats are adjacent, the vegetated flats are finer grained, *e.g.* LR-A (Figure 17). This is apparent either in the

Figure 28. X-radiographs (positives) of cores. Scale at top equals 1 cm. Upper surface marks the sediment/water interface.

A) Sands of south thalweg of LR-B display clear stratification with whole gastropod shell at depth.

B) The muddier thalweg of RC-A is mottled with a distinct U-shaped burrow within the upper 7 cm.

C) The flat mud of LR-B is generally mottled with some stratification preserved at the top of the core. Gastropods and a pelecypod valve are seen at depth. The hatched area of the upper 2 cm is a wire mesh used in coring.

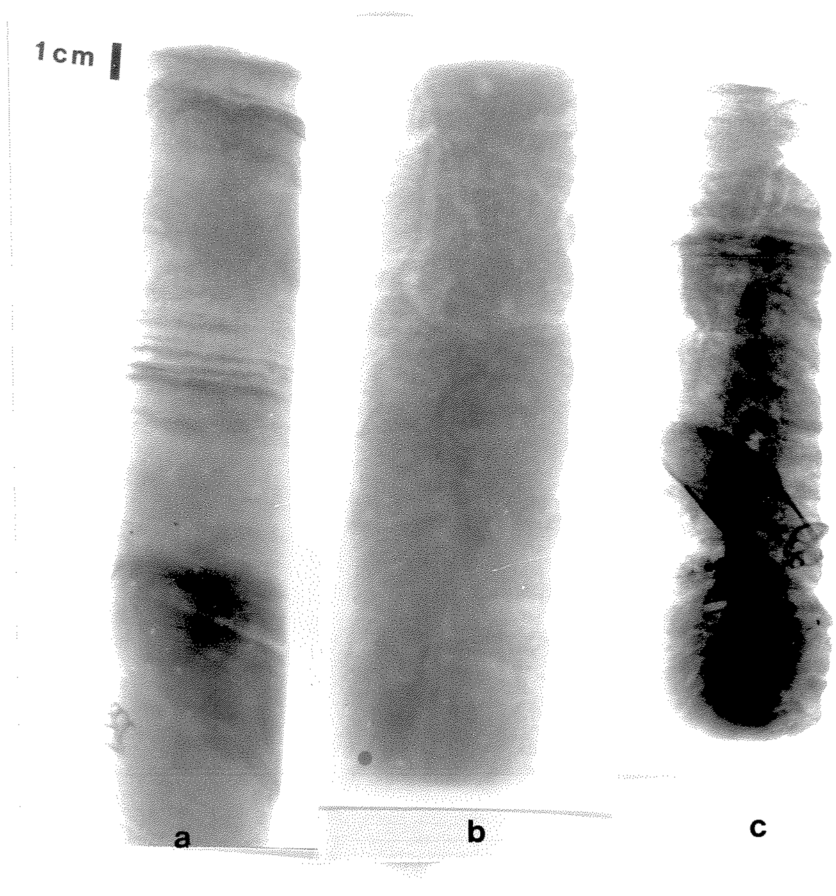
1 cm
a
b
c

proportion of sand:mud or in the proportion of medium:fine:very fine sand if sand content remains the same. In African Queen and Regnes, the smallest channels of this study, flats are finer grained than thalwegs as measured by an increase in clay content (Figures 26 and 27). As with the thalweg deposits, there is a general fining of flat deposits from the larger, higher order, TF channels to the smaller, lower order, DE channels.

The TOM content of intertidal flats follows the same general trend as that found in thalweg samples. A low of 1% is found at IT-A, the coarsest, and a high of 13% in RGN flats, the finest (Table 9). .

Sedimentary structures also display similar trends in flats as those identified in the thalweg region. Coarse, sand flats preserve stratification features while muddier flats are burrowed and mottled by bioturbation (Table 10; Figure 28c). A slump feature was noted in a partly stratified and mottled box core in Redfield Creek.

Calcareous material is not an important constituent as only occasional fragments are present.

<u>Channel-Margin Marsh</u>: Approximately 1-2 meters above the channel-margin flat is the marsh surface. Sometimes a terrace is positioned at a level mid-way between the flat and marsh surface. This terrace may represent healed slump blocks (G. M. Ashley, pers. comm.). They are often covered with the tall form of <u>S. alterniflora</u>. The marsh immediately adjacent to the channel is slightly elevated

above the more interior marsh and covered with <u>S. alterniflora</u> tall form. This is the levee marsh. Channels are quite discernible at a distance by following the distribution of <u>S. alterniflora</u> tall form along the levee. Beyond the levee marsh is the back-levee marsh which is covered with the short and medium forms of <u>S. alterniflora</u>. <u>Salicornia</u> <u>sp.</u> is present, but rare.

The marsh at one channel-margin is inundated before the other indicating that the elevation of the levee marsh on either side of a channel cross-section differs.

At times there are sparsely vegetated to barren areas of marsh bordering the channels. These areas may be set back from the channel margin. Evidence of fiddler crab burrows are often encountered here. Sediments of the marsh, with the exception of these localized strips, are intricately bound with plant root systems. Roots are so dense that coring by hand is futile. Vertically exposed freshly collapsed bank margins reveal the stratified nature of the marsh although the dense root system obscures and destroys sedimentary structures at the surface.

Levee marsh areas are coarser than juxtaposed back-levee marshes as sand:mud or silt:clay indicate (Table 8). Channel-margin marshes without distinct, adjacent flats are sandier than the marsh at the opposite bank with a flat, <u>e.g.</u> LR-A (Figure 17).

Levee marshes can be quite sandy. With the exception of IT-A and LR-A (south), however, all back-levee marshes have <10% sand, often <5%.

The TOM content of marsh samples ranged 16-24% for the muddy back-levee samples to 5% in the sandy marsh of Ingram Thorofare (Table 9).

Foraminifera

Within the small area represented in this study there is a variety of different environments with similar physical sedimentary characteristics. In order to establish the potential value of forams as a tool in discriminating sand and mud facies as lagoon, intertidal flat, or subtidal thalweg region, representative samples of each were examined for foram content (Table 11). An exhaustive foram investigation was not undertaken. The intent was only to evaluate future uses of forams in facies analysis of salt-marsh back-barrier environments.

All identifications were made according to Todd and Low (1981). Four benthonic genera predominate: Elphidium, Trochammina, Textularia, and Miliammina. Elphidium, the only calcareous form, is restricted to the two lagoon sites. The remainder are agglutinate forms.

Holocene Sedimentary Sequence (Stratigraphy)

Four units are recognized in the four vibracores (SM-2, SM-3, SM-4, SM-5) recovered from the marsh. They are: i) an upper organic silt, ii) an interbedded silt/fine to very fine sand, iii) a medium to fine sand, and iv) a lower mud (Figures 29-32).

TABLE 11

FORAMINIFERAL CONTENT

sample	env.	sand:mud	specimens	species*
GS-2	intertidal flat (lagoon)	78:22	2	E. incertum
			1	T. inflata
			1	M. fusca
T-2	subtidal lagoon	18:82	11	E. incertum E. clavatum
			5	T. inflata
			1	T. earlandi
LR-B north	intertidal flat (channel)	50:50	21	T. inflata/ macrescens T. squamata/ T. ochracea
			13	T. earlandi
			1	M. fusca
			1	Reophax(?) sp.
LR-A north	intertidal flat (channel)	82:18	13	T. inflata/ macrescens T. squamata/ T. ochracea
			4	T. earlandi
LR-B south	intertidal flat (channel)	45:55	13	T. inflata/ macrescens T. squamata/ T. ochracea
			9	T. earlandi
			2	M. fusca
RC-B west	intertidal flat (channel)	21:79	18	T. inflata/ macrescens T. squamata/ T. ochracea
			1	T. earlandi
			3	M. fusca
GR-A	thalweg region	73:27	14	T. inflata/ macrescens T. squamata/ T. ochracea

* species = Elphidium incertum, clavatum; Trochammina inflata, macrescens, squamata, ochracea; Textularia earlandi; Miliammina fusca; Reophax(?)

Figures 29-32. Core logs and interpretation of facies of vibracores SM-2, SM-3, SM-4, and SM-5. Sections subsampled for grain-size and X-rays are indicated and described at right. Unit contacts are gradual (dashed line) or sharp (solid line). Per cent compaction given at top is compaction due to coring.

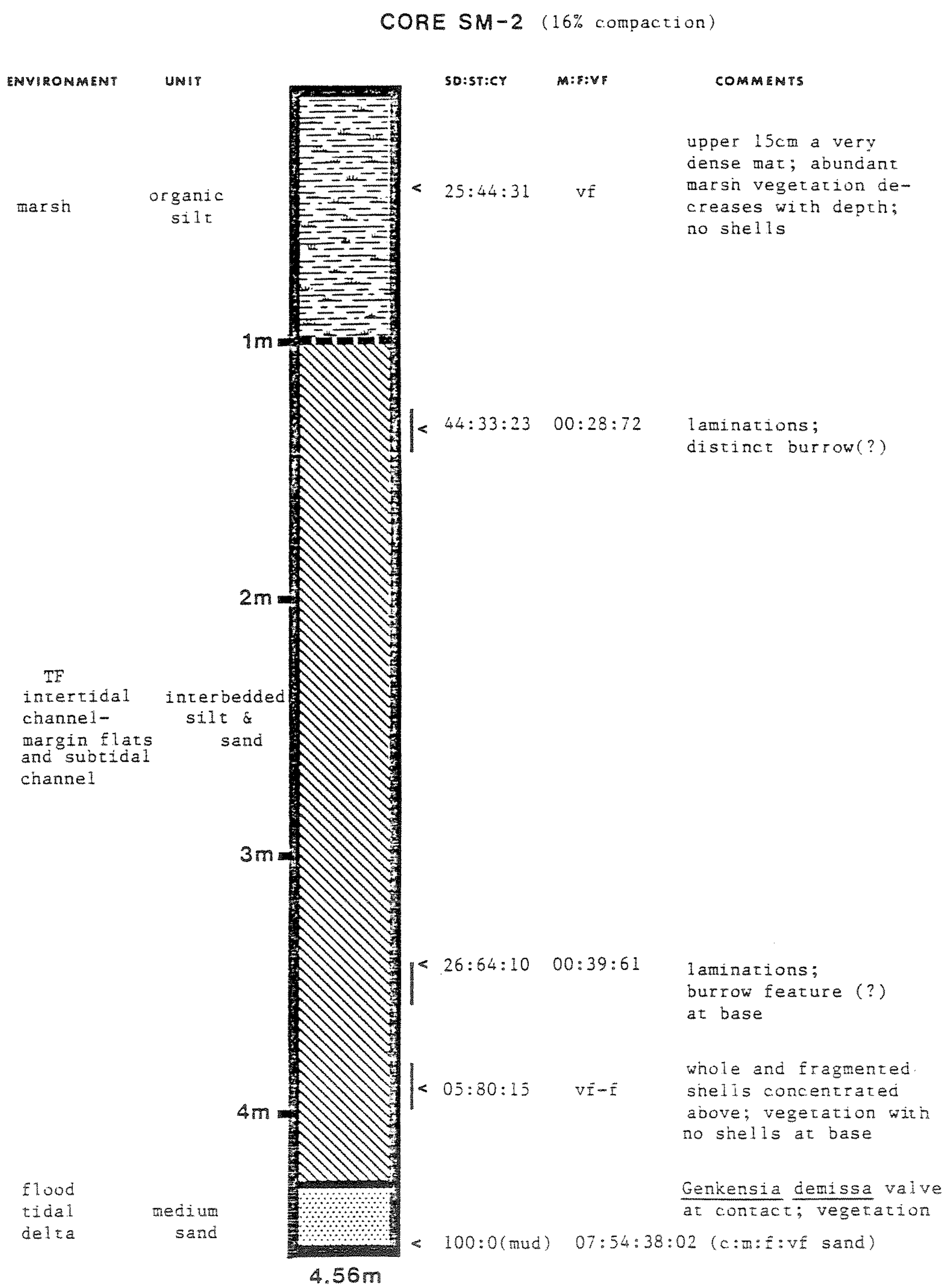
CORE SM-2 (16% compaction)
ENVIRONMENT
UNIT
SD:ST:CY
M:F:VF
COMMENTS
marsh
organic silt
< 25:44:31
vf
upper 15cm a very dense mat; abundant marsh vegetation decreases with depth; no shells
1m
< 44:33:23
00:28:72
laminations; distinct burrow(?)
2m
TF intertidal channel-margin flats and subtidal channel
interbedded silt & sand
3m
< 26:64:10
00:39:61
laminations; burrow feature (?) at base
< 05:80:15
vf-f
whole and fragmented shells concentrated above; vegetation with no shells at base
4m
flood tidal delta
medium sand
Genkensia demissa valve at contact; vegetation
< 100:0(mud)
07:54:38:02 (c:m:f:vf sand)
4.56m

FIGURE 29

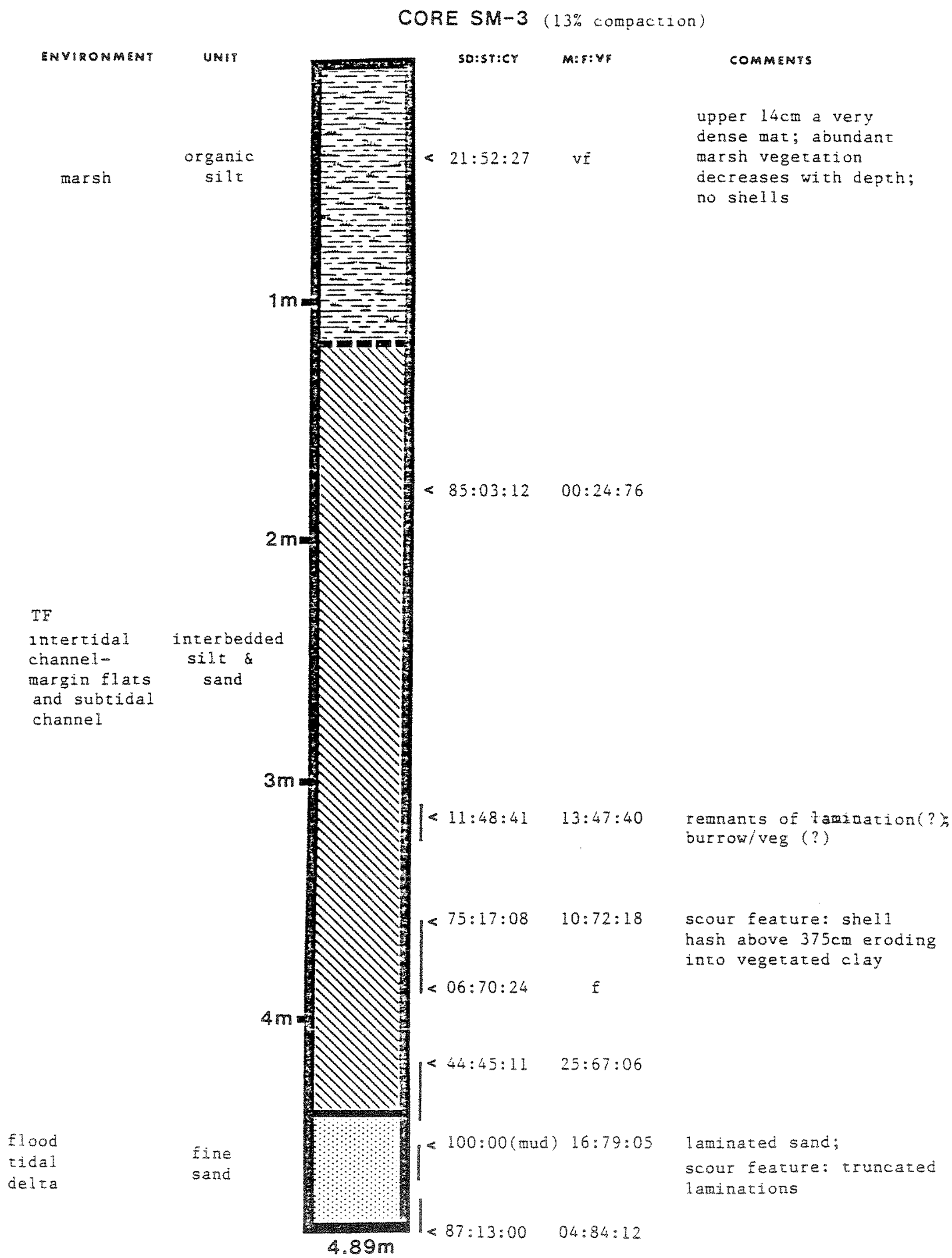
CORE SM-3 (13% compaction)
ENVIRONMENT
UNIT
SD:ST:CY
M:F:VF
COMMENTS
marsh
organic silt
< 21:52:27
vf
upper 14cm a very dense mat; abundant marsh vegetation decreases with depth; no shells
1m
< 85:03:12
00:24:76
2m
TF
intertidal channel-margin flats and subtidal channel
interbedded silt & sand
3m
< 11:48:41
13:47:40
remnants of lamination(?); burrow/veg (?)
< 75:17:08
10:72:18
scour feature: shell hash above 375cm eroding into vegetated clay
< 06:70:24
f
4m
< 44:45:11
25:67:06
flood tidal delta
fine sand
< 100:00(mud)
16:79:05
laminated sand;
scour feature: truncated laminations
< 87:13:00
04:84:12
4.89m

FIGURE 30

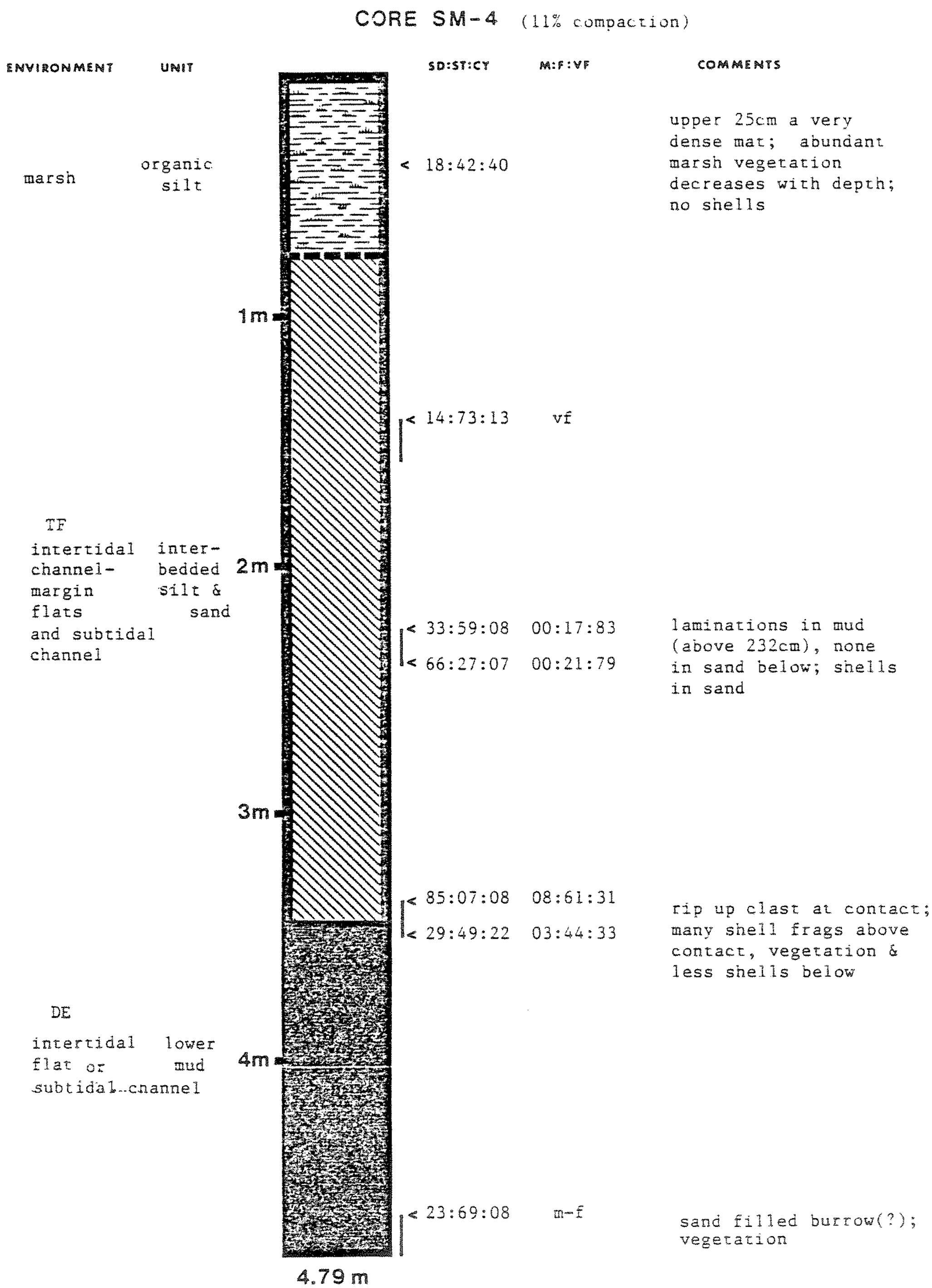
CORE SM-4 (11% compaction)
ENVIRONMENT
UNIT
SD:ST:CY
M:F:VF
COMMENTS
marsh
organic silt
< 18:42:40
upper 25cm a very dense mat; abundant marsh vegetation decreases with depth; no shells
1m
< 14:73:13
vf
TF
intertidal channel-margin flats and subtidal channel
inter-bedded silt & sand
2m
< 33:59:08
00:17:83
< 66:27:07
00:21:79
laminations in mud (above 232cm), none in sand below; shells in sand
3m
< 85:07:08
08:61:31
< 29:49:22
03:44:33
rip up clast at contact; many shell frags above contact, vegetation & less shells below
DE
intertidal flat or subtidal channel
lower mud
4m
< 23:69:08
m-f
sand filled burrow(?); vegetation
4.79 m

FIGURE 31

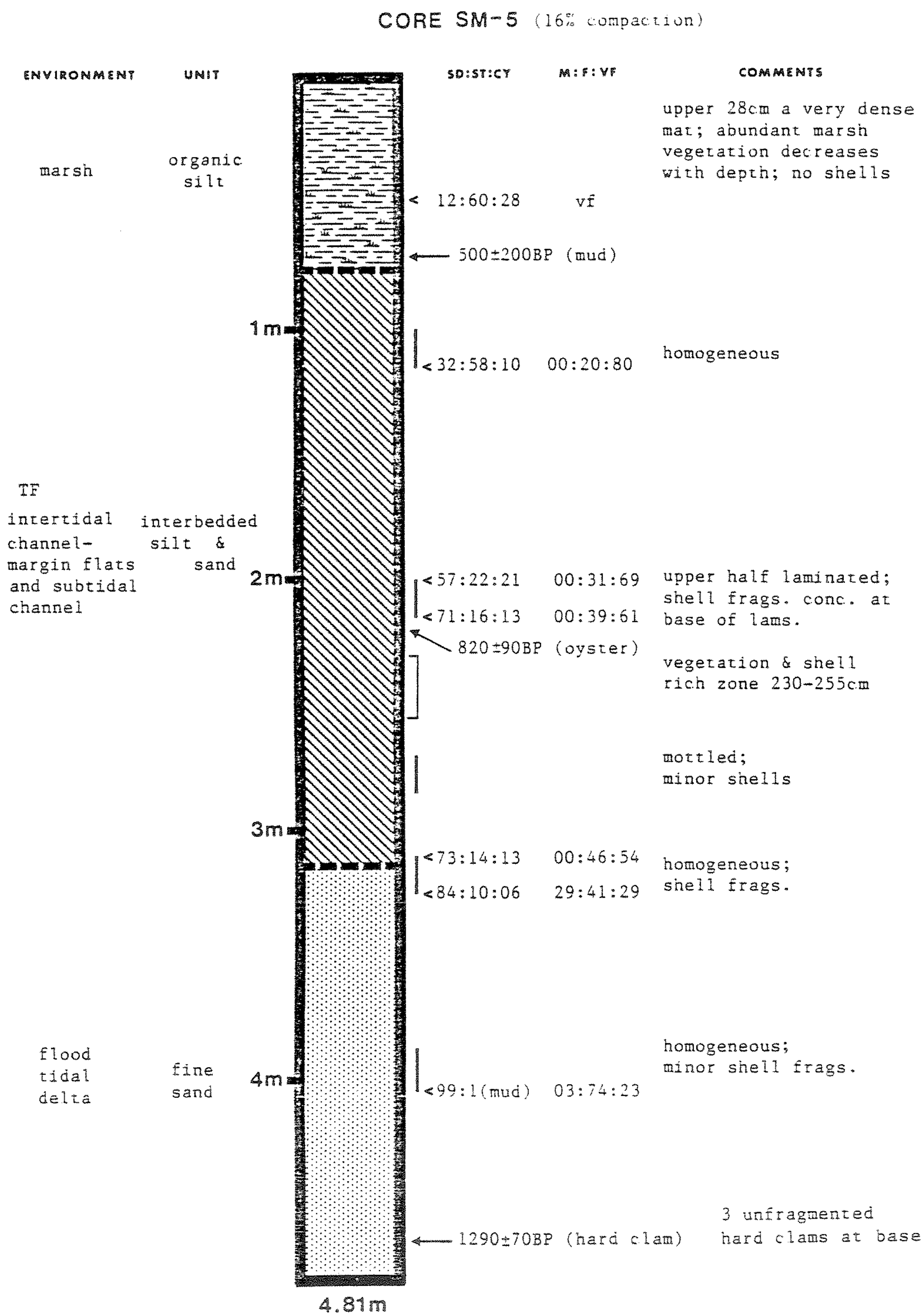
CORE SM-5 (16% compaction)
ENVIRONMENT
UNIT
SD:ST:CY
M:F:VF
COMMENTS
marsh
organic silt
upper 28cm a very dense mat; abundant marsh vegetation decreases with depth; no shells
< 12:60:28
vf
500±200BP (mud)
1m
< 32:58:10
00:20:80
homogeneous
TF
intertidal channel-margin flats and subtidal channel
interbedded silt & sand
2m
< 57:22:21
00:31:69
< 71:16:13
00:39:61
upper half laminated; shell frags. conc. at base of lams.
820±90BP (oyster)
vegetation & shell rich zone 230-255cm
mottled; minor shells
3m
< 73:14:13
00:46:54
< 84:10:06
29:41:29
homogeneous; shell frags.
flood tidal delta
fine sand
4m
< 99:1(mud)
03:74:23
homogeneous; minor shell frags.
1290±70BP (hard clam)
3 unfragmented hard clams at base
4.81m

FIGURE 32

Upper Organic Silt: The upper organic silt unit comprises the topmost portion of each core and varies 75-118 cm in thickness. It is capped with a very dense mat (14-28 cm thick) of modern marsh roots.

Vegetative remains are abundant, decreasing with depth. No shells are present. Silt predominates with a total mud content ranging 75-88%. There are no visible structures.

Sediment color varies brown to gray to black. A peat sample at the base of this unit in core SM-5 (at 71 cm depth) was radiocarbon dated at 500±200 BP. The contact with the underlying unit is gradational.

Interbedded Silt/Fine-to-Very Fine Sand: The interbedded silt/sand unit underlies the upper organic silt in each core and ranges 240-328 cm in thickness. It consists of interbedded silts and sands of a wide variety of sand:silt:clay ratios, with as much as 85% sand, 80% silt, or 41% clay. Sand fractions fine upwards from predominantly fine sand to very fine sand with more mud. The silts and sands occur with gradational or sharp contacts within the unit.

Vegetation and shell material are generally scattered to absent. There is, however, a vegetation- and shell-rich zone in core SM-5, and concentrations of shell fragments and whole gastropods are found in sands and at the base of scour features. Structures are laminations, mottling, scour features (e.g. rip up clasts), and possible burrows.

Sediment color is gray and very dark gray. An oyster shell (at 220 cm depth) in core SM-5 gave a radiocarbon date of 820±90 BP. The contact with the underlying unit is sharp or gradational.

Medium-to-Fine Sand: The medium-to-fine sand unit occurs at the base of three of the four cores (SM-2, -3, -5) and is most prominent in core SM-5 where it comprises the bottom 166 cm. It consists of medium or fine sand with as much as 16% mud. The proportion of medium sand of the sand fraction increases at the upper contact.

The unit is barren of vegetative remains with the exception of core SM-2. Aside from trace amounts of sand-sized shell fragments, the sole occurrences of shell material are the unfragmented, articulate and disarticulate, hard clams found at the base of core SM-5. They show no evidence of transport. Structures are stratification, scour features (truncation of strata), and mottling.

The sands are light to very dark gray with brown ground water (?) staining. One clam valve (at 463 cm depth) was radiocarbon dated at 1290±70 BP.

Lower Mud: The lower mud unit occurs only in the core that does not contain the sand unit (SM-4). It underlies the interbedded silt/sand unit with a sharp contact and is predominantly silt.

Vegetation is scattered with some shell material present below the upper contact. The unit is gray-brown and the only visible structure is a sand filled burrow (?).

DISCUSSION

Morphometric Analyses

<u>Order</u> <u>and</u> $\underline{R_b}$: Fluvial drainage patterns are described and compared by placing stream reaches in a hierarchical system of orders. The few previous studies that have applied this methodology to tidal marshes include Myrick and Leopold (1963), Pestrong (1965), Pethick (1980), and Wadsworth (1980).

Order versus number of channel segments is plotted in Figure 5 for this study and those noted above. Despite the fact that these individual marshes are quite disparate (Table 12), they all display a logarithmic relationship following Horton's 'law' of channel numbers established for rivers. The relationships show a logarithmic decrease in the number of channels with an increase in order.

The similarity of these plots may partly be a reflection of the systematics of ordering itself. As Bowden and Wallis (1964) have pointed out, this relationship is an inevitable consequence of the Strahler system because, by definition, an increase in order arises from the joining of two segments. Shreve (1966) adds that an adherence to Horton's law is simply the statistical end of considering large numbers of randomly merging channels. However, the fact that these tidal marsh plots are similar

TABLE 12

PREVIOUS MORPHOMETRIC STUDIES

LOCATION	TYPE	TIDAL RANGE	REF
Potomac River, VA	drowned river estuary	micro	Myrick & Leopold (1963)
SF Bay, CA	fringing bay protected	meso	Pestrong (1965)
N. Norfolk, UK	unprotected coast	high meso- high macro	Pethick (1980)
Sapelo Isl. GA	back-barrier no open water	high meso	Wadsworth (1980)
Avalon/ Stone H., NJ	back-barrier open water	low meso	this study

to those of river studies by consistantly showing a log relationship would suggest a common control on the development of these channelized flow patterns that bridges differences between rivers and tidal systems. It is suggested that this may be unidirectional flow.

As shown in Table 4, the vast majority of the channels in this study are low in order. These channels comprise the DE networks. The log relationships, then, are primarily determined by the DE systems.

Fluvial branching, dendritic drainage patterns develop from unidirectional, downslope processes (Leopold et al., 1964). Unidirectional, downslope flow in the development of DE patterns would be ebb drainage off aggrading marsh islands. This will be discussed in more detail in a subsequent section.

Accordance to the law is affected little by which ordering system is used (Leopold et al., 1964). The ordering system chosen will, however, affect R_b, or the slope (Shreve, 1966).

Length and R_s: Horton's (1945) 'law' of channel lengths was formulated on the basis of his ordering system and mean channel lengths. Strahler's method of segmentation will lead to shorter high order channel lengths and thus, length versus order plots of a lesser slope. This tendency is demonstrated in the plots of Figure 6 where each is a Strahler plot with the exception of Myrick and Leopold (1963).

Broscoe (1959), as cited in Bowden and Wallis (1964), suggested using cumulative mean length instead of mean segment length. Bowden and Wallis (1964) found that using this technique would increase the slope of a Strahler plot such that it closely mirrored a Horton plot of the same drainage net (Figure 7). In addition, a scattered, non-linear Strahler plot would become linear.

Pestrong (1965) compares plots of his Strahler data with other studies that ordered after Horton. He made no attempt, however, to normalize the data. In addition, the works cited in Pestrong (1965) plotted mean lengths while Wadsworth (1980) plotted cumulative mean lengths.

Despite the variety of analytic techniques mentioned above, there remains an adherence to the log relation first described by Horton (1945) in river systems. Again, a similar control in the development of the tidal networks and rivers is suggested.

Properties of stream length as measured by R_s are also significant. Pestrong (1965) found that the sinuosities of marsh channels of San Francisco Bay generally increase with increasing order, but with wide scatter and low sinuosities for 4th- and 5th-order channels. R_s values drastically decrease as channels leave the marsh and enter unvegetated flats (Pestrong, 1972). This was attributed by Pestrong to the different factors controlling channel form in these two environments, _i.e._ vegetation in the marsh and hydraulic flow in the flats. Garofalo (1980) found sinuosity to vary among marsh channels in salt- and freshwater marshes as a function of vegetation and substrate type.

At Avalon/Stone Harbor, 5th-order channels display the lowest sinuosity (1.4) and middle order channels are most sinuous (Table 4). Fairly straight rills develop on unvegetated flats and connect the marsh with larger channels. These features and properties are related to mode of origin and substrate control and will be discussed in greater detail when considering the evolution of the drainage patterns we see today.

Junction Angles: The pattern of junction angles of fluvial channels is related to surface slope, lithology, and structure (Morisawa, 1968). Horton (1945) specifically showed junction angles to be determined by the relative slopes of entrant and receiving channels. When the gradients of a tributary and its parent stream are approximately equal, the junction angle between them should be acute. It should approach 90° as the tributary slope exceeds the parent slope.

Junction angles should increase as the difference in the order of the joining streams increases because channel gradients decrease with increasing stream order (Lubowe, 1964). Pestrong (1965) found this to hold for his 1st- and 2nd-order segments in the salt-marshes of San Francisco Bay. However, junction angles decrease for 3rd- and 4th-order segments. Pestrong suggested that these differences are tied to different processes operating in lower and higher order channels, i.e. 1st- and 2nd-order segments effectively experience unidirectional flow and thus behave like terrestrial streams, whereas 3rd- and 4th-order segments experience bidirectional flow.

The data collected for Avalon/Stone Harbor shows a decrease in junction angle with increasing difference in the orders of joining segments (Table 5). However, the lack of channel bed slope data precludes a comparison with Pestrong's observations cited above. The rills draining the marsh that are found on unvegetated flats connect with larger channels at approximately 90°. This has a significant impact on the drainage patterns that eventually develop on the marsh and will be discussed further when considering the evolution of marsh drainage patterns.

Drainage Area and Density: Fluvial drainage density reflects topographic, lithologic, pedologic, and vegetative controls (Gregory and Walling, 1973). Drainage densities in salt-marshes range 9-60 km/km^2 in Georgia (Ragotzkie, 1959), 42-149 km/km^2 in San Francisco Bay (Pestrong, 1965), and 7 (straight) or 12 (sinuous) km/km^2 in this study (Table 4). The wide ranges reported in Georgia and California are not explained in their respective studies. As substrate and vegetation influence drainage channel development, they are certainly important controls in the degree of channel development and variety of drainage densities encountered in different marshes. As will become evident later, the mode of origin of channels also influences the nature, degree, and pattern of channelization present.

Width:Depth Ratios: Refer to Hydraulic Geometry section.

Hydraulic Geometry: As hydraulic geometry defines the adjustment of channel shape to changing hydraulic regime, one would expect hydraulic geometry equations to reflect differences between fluvial and tidal flow conditions. Any variations in flow conditions within the tidal drainage net should also be manifest in the equations. Both these predictions have been borne out in this study.

Leopold and Maddock (1953) found at-a-station exponents to be very similar for rivers spanning a great variety of physiographic settings (b=0.26, f=0.40, m=0.34). Previous studies of tidal marshes calculate values distinct from rivers (Table 7). The tidal values are similar for each marsh despite being measured in channels of various dimensions in marshes of different types. The values measured at six cross-sections in this study, however, fall into three distinct groups (Table 7).

The larger channels have exponent values similar to those in other tidal marshes (Group 1). The small channels have values similar to fluvial averages (Group 3). Oarlock Creek, intermediate in size and linking the two groups in space, has transitional values (Group 2). A map view of these channels shows Group 1 to be comprised of TF channels and a larger DE trunk channel and Group 3 consists of smaller DE channels.

Group 1 channels with very high m-values accommodate increasing discharge by increasing flow velocity rather than through an adjustment of shape (width or depth). Group 3 channels, on the other hand, accommodate an increase in discharge largely through an adjustment in channel shape (width and depth). Depth increases at a greater rate than width, i.e. f>b. This is evident in the field as vertical channel walls.

With the exception of Myrick and Leopold (1963), the values reproduced here from previous works were determined at single locations within a complex drainage system. Myrick and Leopold report data from only one channel, but state that values from other cross-sections are the same. It is suggested in the present study that the grouping of channels at Avalon/Stone Harbor is a reflection of the spatial variation of flow conditions within the system. The lack of similar findings by Myrick and Leopold(1963) is a site specific phenomenon rather than a characteristic of tidal drainage systems in general.

A variety of flow conditions are operative simultaneously within the many channels of this marsh (Ashley and Zeff, 1986). To say that flow in tidal systems is simply bidirectional in contrast to unidirectional river flow is an over-simplification. All the channels under study at Avalon/Stone Harbor are, indeed, subjected to bidirectional flow each day. The nature of this flow, however, varies in strength and time. As such, the competence of the channels vary. Each of these parameters exert a control on the hydraulic geometry relationships.

River channel form is largely maintained by bankfull flow (times of maximum velocity and discharge) with a recurrence interval of 1-2 years (Leopold et al., 1964). Dead-end channels, with hydraulic geometries most like rivers, reached maximum velocities and discharges like rivers, near bankfull (just after flooding) (Table 13). Maximum mean velocities measured are only about 10 cm/sec during neap tides and maximum neap discharges were less than 1 m^3/sec.

In contrast, TF channels, with hydraulic geometries similar to other tidal marsh channels, experienced maximum mean velocities and discharges well below bankfull (Table 13), a common occurrence in tidal channels. In the largest through-flower, Ingram Thorofare, maximum mean velocities reached about 100 cm/sec during spring flood tide and the corresponding maximum discharge reached about 700 m^3/sec. Neap v_{max} = 64 cm/sec and neap Q_{max} = 500 m^3/sec.

Channel form is also associated with sediment load. A relatively narrow and deep channel (low w:d) favors suspended load transport while a relatively wide and shallow channel (high w:d) is most efficient for

TABLE 13

WATER LEVELS AT v_{max}

TYPE/ GROUP	CHANNEL	CONDITIONS	STAGE @ v_{max}	DATA BASE
TF/1	IT	various	below bankfull	time-velocity curves
TF/1	LR	various	below bankfull	time-velocity curves
DE/1	RC	various	below bankfull and flooded	time-velocity & hydraulic geometry
DE/2	OC	flood neap	flooded	hydraulic geometry
DE/3	RGN	flood neap	flooded	hydraulic geometry
DE/3	AQ	flood neap	flooded	hydraulic geometry

bedload transport (Chorley et al., 1984). As the sediment comprising the channel perimeter (bed and banks) represents the material transported through that channel, the perimeter grain-size will reflect the dominant mechanism of transport.

Schumm (1960) specifically illustrated how the shape of a river channel cross-section, as expressed by its w:d ratio, is related to the mud content of its perimeter. Channels with low mud perimeters have a greater w:d than those with more mud. The tidal channels of the Avalon/Stone Harbor marshes follow this trend (Table 6). There is a dramatic increase in the mud content of the channel perimeter of the smaller, DE channels with low w:d ratios. This reflects favored suspended load transport in these channels and will be discussed in the next section.

The high w:d of LR-B may be due to its double thalweg, a feature found only in other through-flowers. If the volume of flow was accommodated by a single thalweg, it would be deeper, thereby reducing the w:d ratio.

Very little is understood about the hydrodynamics of salt-marsh tidal channel flow. Aside from the works of Boon (1975), Schwing and Kjerfe (1980), Ward (1981), Ashley and Zeff (1985a and b, 1986, 1987a and b), and this study there has been little data concerning tidal channel hydrodynamics in mesotidal back-barrier salt-marshes. The drainage characteristics of this system, described by the preceding morphometric analyses and culminating in hydraulic geometry, sheds some of light on the movement of sediment through this marsh.

Modern Sediments

Based upon the data of Tables 8, 9, and 10 sediment properties can be seen to vary in two ways (Tables 14 and 15). There are: i) inter-channel trends from one channel to another and ii) intra-channel trends at individual channel cross-sections.

Grain-size: Inter-channel grain-size trends are a fining of each subenvironment as one proceeds from the largest TF channel to the smallest DE channel. This can be explained in terms of current strength and proximity to source.

Bedload sands and silts are supplied to this system through Townsends Inlet as manifested by flood tidal deltas. Proximity to this source area can be viewed to be expressed by a site's distance along the tortuous path from inlet to Ingram Thorofare into DE systems. Flow velocities decrease with distance from the inlet (Ashley and Zeff, 1986, 1987a), and hence, so does flow competency. Suspended fines are supplied, in part, through Townsends Inlet as well (Kelley, 1983). The resuspension of sediments and erosion of channel cut-bank margins also add to the supply.

Thalweg sediments fine from sands in the higher order, TF channels to silts in the lower order, DE channels. Sediments found here are those that are carried

TABLE 14

INTER–CHANNEL SEDIMENT TRENDS

size	type	grain–size	T.O.M.	sedimentary structures
large	TF	coarser	lower	physical
↓	↓	↓	↓	↓
small	DE	finer	higher	biological

TABLE 15

INTRA-CHANNEL SEDIMENT TRENDS

	grain-size	T.O.M.	sedimentary structures
	coarser	lower	
thalweg region	↓	↓	*depends on grain-size*
channel-margin flat	↓	↓	
unvegetated	↓	↓	
vegetated	↓	↓	
channel-margin marsh	↓	↓	
levee	↓	↓	—
back-levee	finer	higher	—

through the channel, deposited during slack tide, and not re-entrained by a subsequent current. As current velocities decrease with distance from the inlet the ability to entrain sediments also decreases. Coarser material is left as a lag deposit and sediments available for continued transport become finer grained.

Fining by this mechanism is accentuated by the increased significance of suspended load transport with distance from the inlet. As discussed earlier, the correlation of low w:d with high mud content of DE channel perimeters suggests that suspension transport predominates over bedload transport in these channels. Ashley and Zeff (1986, 1987a) have shown that the simultaneous variations of time-velocity asymmetries in different channels of this marsh control the transport routes of suspended sediments. They have found that Ingram Thorofare acts as a conduit transporting suspended fines directly to Great Sound lagoon where they are deposited. In contrast, the smaller channels (Long Reach and Redfield Creek) act as pathways through which fines shift in location from one part of the marsh to another.

At a cross-section, intra-channel grain-size trends are fining with distance away from the thalweg region (toward the marsh). Suspended sediments are carried onto the marsh with twice daily flooding. Velocities near times of maximum flooding are low, thus, flow velocities do not sharply decrease with flooding. Therefore, the consequent drastic decrease in grain-size with distance from the bank margin (levee to back-levee), or the well developed levee common in river deposits, does not occur. There is a low competency of flow at times of flooding and coarse grains will be deposited on the marsh only during storm conditions.

Stumpf (1983) found that sedimentation during normal tidal conditions in a Delaware marsh was not great enough to keep up with sea-level rise. Storm deposition was responsible for the sedimentation necessary to maintain the marsh.

Ashley and Zeff (1987a) determined that sedimentation through the Avalon/Stone Harbor marsh differed during fair-weather (normal) and storm conditions. They found that peak flow velocities and total suspended sediment loads increased during storms. While channel-to-channel TF and trunk DE channels carry more suspended sediments than inlet-to-bay TF channels under normal conditions, the bulk of suspended sediment transported during storms is through the inlet-to-bay TF channels.

The process of fining perpendicular to thalweg appears to be controlled more by the presence or absence of flats and vegetation than by flow velocities. Flats and vegetation act as filters of sediment reaching the marsh surface. Cross-section LR-A illustrates each aspect of this fining mechanism (Figure 17). Velocities over flats are lower than thalweg flows. The lower energy flat environment should contain finer grained deposits. The north flat in LR-A is slightly finer than the thalweg region, having proportionately more very fine sand. With bedload and suspended sediment transport across the flat, vegetation on the upper flat traps and removes the coarser elements leaving little sand available to the levee marsh. In contrast, the absence of a flat to the south results in the direct deposition of available sands onto the marsh. At RC-A, while there is no east unvegetated flat, a vegetated flat acts as the sand sink (Figure 21). On the west, however, an unvegetated flat is present and acts as a sand sink leaving a silt vegetated upper flat and a sand starved marsh.

Because sediments in transport become finer in the DE systems, this mechanism, although active, produces less dramatic results.

The back-levee marsh is the environment most distant from allochthonous sediment sources and is the muddiest. Sand reaches here only during storm events. The sand marsh bordering Ingram Thorofare and the flatless LR-A south, close to Ingram, are probably recent storm deposits.

Sedimentary Structures: Sedimentation within thalweg and flats should produce stratification. Its occurrence is linked to the degree to which it is not destroyed by bioturbation. This is a function of grain-size. Stratification is preserved in sand deposits of both thalwegs and flats (Figure 28 and Table 10). Mud deposits support a more active infauna (R. Grizzle, pers. comm.) and exhibit distinct burrows and mottled textures due to bioturbation (Figure 28).

Stratification is produced by two processes, the recognition of which should be useful in facies analysis. The bedforms produced in a channel like Ingram Thorofare will be preserved as cross-stratified sands. Destruction through bioturbation is unlikely due to the high current velocities reached here, greater than those permitting biogenic mottling in lower energy sandy thalwegs.

Lower energy sandy thalwegs do not produce bedforms and will therefore not produce cross-stratification. However, these thalwegs, and the sandy intertidal flats, can be recognized by parallel stratification caused by alternating sand deposition and suspended sediment settlement, as well as slump features.

Edwards and Frey (1977) used the term "chaotic bedding" to describe the contorted and load-casted laminae, slump/fault structures, and discontinuity surfaces unique to the channels and creek banks of Georgia salt-marshes. Intense bioerosion produces instability which promotes slumping as well as facilitates plucking and redeposition of clasts by tidal currents.

Similar features were noted by Pestrong (1972) in the San Francisco Bay marsh of his study. Parallel laminations were attributed to alternating flocculated and non-flocculated muds. Vegetation, burrowers, and differential compaction disrupt stratification in a "chaotic mud" zone in channels of the marsh and flats.

Stratification of the marsh is exposed at cut banks although it is not evident at the surface where grass roots are extremely dense. Similar stratification is found in Barnstable, MA marshes (Redfield, 1972) and is ascribed to seasonal variations in deposition whereas plant roots destroy any stratification in Georgia marshes (Edwards and Frey, 1977).

Organic Matter: Organic matter is supplied to the channels from the marsh surface itself and is subsequently transported to each environment. In addition, each environment receives organic matter through *in situ* biologic productivity. TOM content increases with increasing proportion of mud (Table 9) due to the increased bioproductivity of mud-rich deposits.

The organic matter content of suspended sediments has been used as a tool in tracing sediment transport through salt-marsh systems (Boon, 1973; Settlemyre and Gardner, 1975; Ward, 1981). Organic matter in deposited sediments is a function of *in situ* bioproductivity and contributions from settling of the suspended sediments of the overlying water column. As this study has found the distribution of TOM in sediments to correlate strongly with *in situ* productivity as reflected in grain-size, it was determined to be of little value to analyze TOM in core sediments when grain-size would provide the same information.

Foraminifera

The sole purpose of examining the foram content was to note any differences among environments that may be difficult to differentiate on purely physical sedimentary characteristics alone. No significance is placed on the number of specimens isolated and identified. What may be significant, however, is the restriction of calcareous *Elphidium* to the two lagoon sites.

Salt-marshes and associated bays/lagoons and channels have been the subject of several detailed foram studies (Phleger and Walton, 1950; Parker and Athern, 1959; Lee et al., 1969; Phleger, 1970; Kraft and Margules, 1971; Scott and Medioli, 1978, 1980). In these studies environments have been distinguished based upon foram content (*e.g.* high versus low marsh, flat/channels versus marsh). However, different degrees of correlation are found between foram distributions and sediment type or physical parameters. It is beyond the scope of this study to suggest any explanation for the presence of *Elphidium* in the lagoon and its absence elsewhere. It may, or may not, be useful and/or significant. However, if future investigations provide support for using *Elphidium* as an indicator of lagoon conditions, one must then address the question of preservation.

The problem of preservation bias of agglutinated forams over calcareous forms must be considered in light of pH conditions. Bradshaw (1968) measured pH conditions that are conducive to the dissolution of calcareous forams below the sediment/water interface of tidal channels, mud flats, and marsh surfaces in a salt-marsh environment. A carefully designed salt-marsh foram investigation including modern distribution patterns, post-depositional changes before and after burial, and preservation in Holocene cores would be very helpful to future coastal studies.

ORIGIN OF AVALON/STONE HARBOR DRAINAGE PATTERNS

Through-Flowing Channels

Flood tidal delta sand bodies accumulate landward of a tidal inlet in response to prevailing tidal current hydraulics and sediment supply. Delta sands largely remain subtidal with actively shifting margins and channels separating them. As portions of the deltaic complex aggrade vertically to an intertidal elevation favorable to halophytic colonization, they will stabilize to islands fixed in position by the marsh grasses and rimmed by intertidal flats barren of vegetation (Figure 33).

It has previously been suggested that some back-barrier marshes developed when halophytes successfully colonized flood tidal delta sands in New Jersey (Lucke, 1934) and Virginia (Morton and Donaldson, 1973). Historical accounts, aerial photographs, and flight observations by the author verify that this process is

Figure 33. Progressive development of marsh islands from tidal delta sand shoals (after Lucke, 1934).

A) Subaqueous flood tidal delta sand shoals (a) landward of tidal inlet.

B) Delta sands of A) have aggraded to intertidal elevation (solid line) while new subtidal flood tidal delta lobes develop landward (b).

C) Halophytic colonization stabilize (a) to marsh islands, (b) are now intertidal, and new subtidal delta shoals have developed (c). Marsh islands and inter-island channels are bordered by intertidal flats.

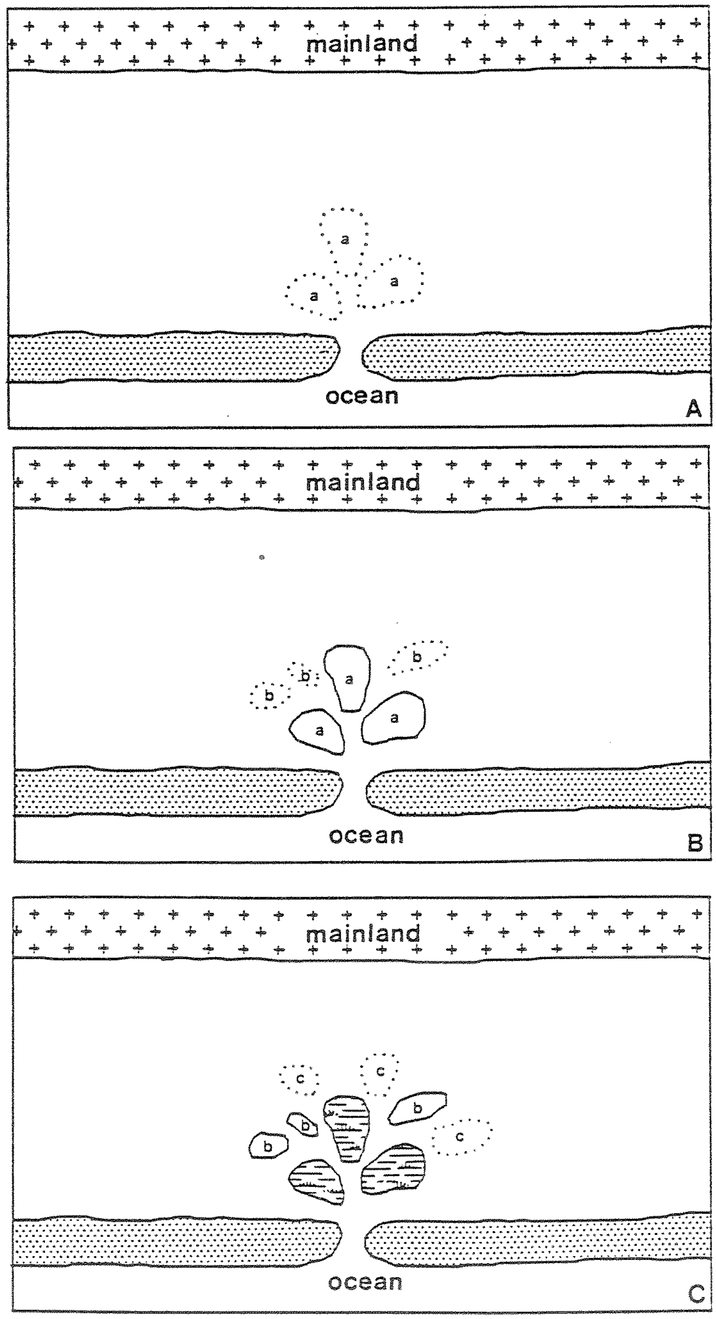
mainland
a
a
a
ocean
A
mainland
b
b
a
b
a
a
ocean
B
mainland
c
c
b
b
b
c
b
ocean
C

responsible for marsh islands behind Hereford and Townsends Inlets.

Aerial photographs from 1940 show unvegetated, subtidal sand shoals opposite Townsends Inlet that today support marsh vegetation (Figure 2).

As the intertidal flats of island perimeters expand and become vegetated, channels become narrower. Major portions of a broad, open, back-barrier lagoon with tidal delta sands fronting an inlet will transform into a back-barrier marsh consisting of marsh islands separated by TF channels fixed in position through time by vegetation and cohesive bank margins (Figure 34).

As marsh islands expand, the locations of tidal delta sand shoals shift landward to the interior lagoons where TF channels from the inlet empty. This can be seen at the point where Ingram Thorofare empties to Great Sound (Ashley and Grizzle, in prep.). Here, incipient marsh growth has begun amidst shifting subtidal sands and channels. Gull Island on the opposite side of Great Sound likely originated as a flood tidal delta sand body of Hereford Inlet (Figure 2). Cresse Thorofare and Gull Island Thorofare became fixed in their path when Gull Island was stabilized by marsh grasses. Today these channels are quite wide but will eventually narrow to the dimensions of other TF channels, a size that may be limited in this system by local hydraulic conditions.

Incomplete infilling will leave smaller, remnant

Figure 34. General model of development of TF channels by marsh island expansion.

A) Small marsh islands opposite inlet develop from flood tidal deltas (Fig. 33). Inter-island channels are wide. Back-barrier bay is broad and open.

B) Marsh islands grow and inter-island channels narrow as channel-margin flats expand and become vegetated. New tidal delta sand bodies (a) develop landward of inlet.

C) Back-barrier bay is becoming increasingly marsh filled and confined by island expansion. New tidal deltas build (b). Marsh islands are separated by TF channels. Seaward progradation of mainland marsh adds to bay confinement.

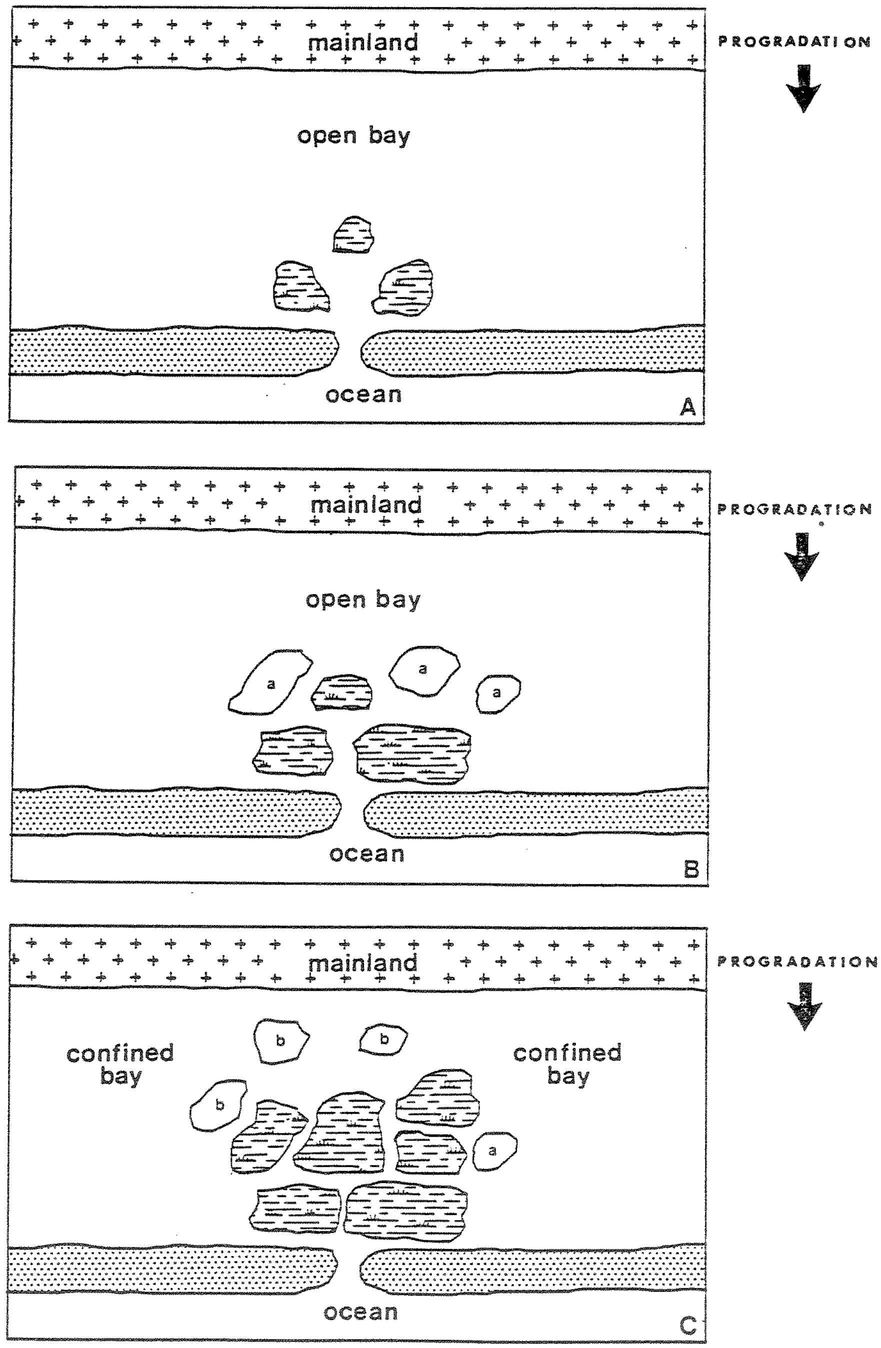
mainland
open bay
ocean
A
PROGRADATION
mainland
open bay
a
a
a
ocean
B
PROGRADATION
mainland
confined bay
confined bay
b
b
b
a
ocean
C
PROGRADATION

lagoons interspersed in an otherwise continuous marsh. The growth of fringing marshes seaward from the mainland is an additional process contributing to the infilling. This is the status of the marsh at Avalon/Stone Harbor and the remaining New Jersey coast south of Great Egg Harbor Inlet at present.

Dead-End Channels

The highly sinuous branching patterns of DE systems have an origin quite different from that of the TF channels.

Several general characteristics that distinguish DE systems from TF channels are: i) they consist of discrete networks feeding into TF channels or trunk DE channels, ii) the junctions of these networks with the TF and trunk channels are nearly 90° or have a distributary U-form, and iii) individual segments are extremely sinuous. Clues to their development can be found in the channels seen to dissect unvegetated portions of marsh islands today.

Highly sinuous branching patterns are found on the unvegetated portions of partly vegetated intertidal shoals and on salt pans (small circular areas on a fully developed marsh barren of vegetation). In addition, the exposure of channel-margin flats of very shallow channels during low tide reveal a very narrow and sinuous subtidal thalweg.

High sinuosity appears to develop on unvegetated substrates. The expansion of marsh vegetation to the bank margins of these sinuous channels are seen limiting migration and the further development of the meandering form.

Furthermore, rills serving to transfer water draining the marsh during the ebb to larger channels are found on unvegetated channel-margin flats. These rills are nearly perpendicular to the channels and may have a slightly meandering form. With time, rills should get more deeply incised. As flats become vegetated the channel forms will stabilize, the consequence being an approximately 90° confluence of a DE channel network with a through-flower.

U-form confluences are special cases likely arising from the deposition of sediments during ebb drainage as flow from smaller DE trunks empty into the larger, relatively less confined, TF channels in a manner similar to the formation of distributaries of river deltas.

Ashley and Zeff (1986) found DE channel velocities to peak early in the ebb cycle in contrast to TF channels which peak during the middle and late part of the ebb cycle. Temporal velocity variations are such that sediment laden DE trunk channels empty into quiet TF channel waters early in the ebb and may deposit their loads at the juncture. The deposition of sediments near such confluences can be seen today.

These observations, coupled with the adherence of channels to Horton's laws of drainage composition for rivers (as discussed earlier), leads this author to postulate that DE systems evolved from unidirectional, downslope (ebb) drainage patterns that developed on the unvegetated portions of stabilizing marsh islands (Figure 35). Channelization on unvegetated areas permitted migration and the development of meanders. As marsh grasses spread to the channel margins, meandering by lateral migration was inhibited. The dominant depositional mechanism became vertical aggradation by overbank deposition rather than lateral accretion in a manner similar to anastomosing rivers (Smith, 1976; Smith and Smith, 1980).

Thus, bank margins became fixed in position but thalwegs continued to migrate. They, too, stabilized and narrowed by infilling as flats accreted. The end result will be complete channel infilling and abandonment.

The geomorphic expression of channel abandonment would be meander scars, a feature very prominent in the marshes of South Carolina and Georgia (Ward and Domeracki, 1978). The marshes of southern New Jersey, however, have not produced scars to any appreciable extent indicating both rapid stabilization of channel form and incomplete channel infilling. Most reaches that are almost meander cut-offs are exclusively found in DE systems.

HOLOCENE SEDIMENTARY RECORD AT AVALON/STONE HARBOR

The four units recognized in the vibracores have been interpreted as follows: i) upper organic silt as marsh,

Figure 35. Development of DE systems from ebb drainage of marsh islands.

A) Drainage channels develop on sandy intertidal flood tidal deltas. Inter-island channel is wide.

B) As shoals vertically aggrade to an elevation favoring incipient salt-marsh vegetation it is accompanied by lateral island expansion and the narrowing of inter-island channel. Substrate is finer and downslope (ebb) drainage patterns have developed meanders and tributaries.

C) Today, marsh islands are stabilized by vegetation and meandering DE networks are locked into position forming perpendicular or distributary U-form junctions with the inter-island TF channel.

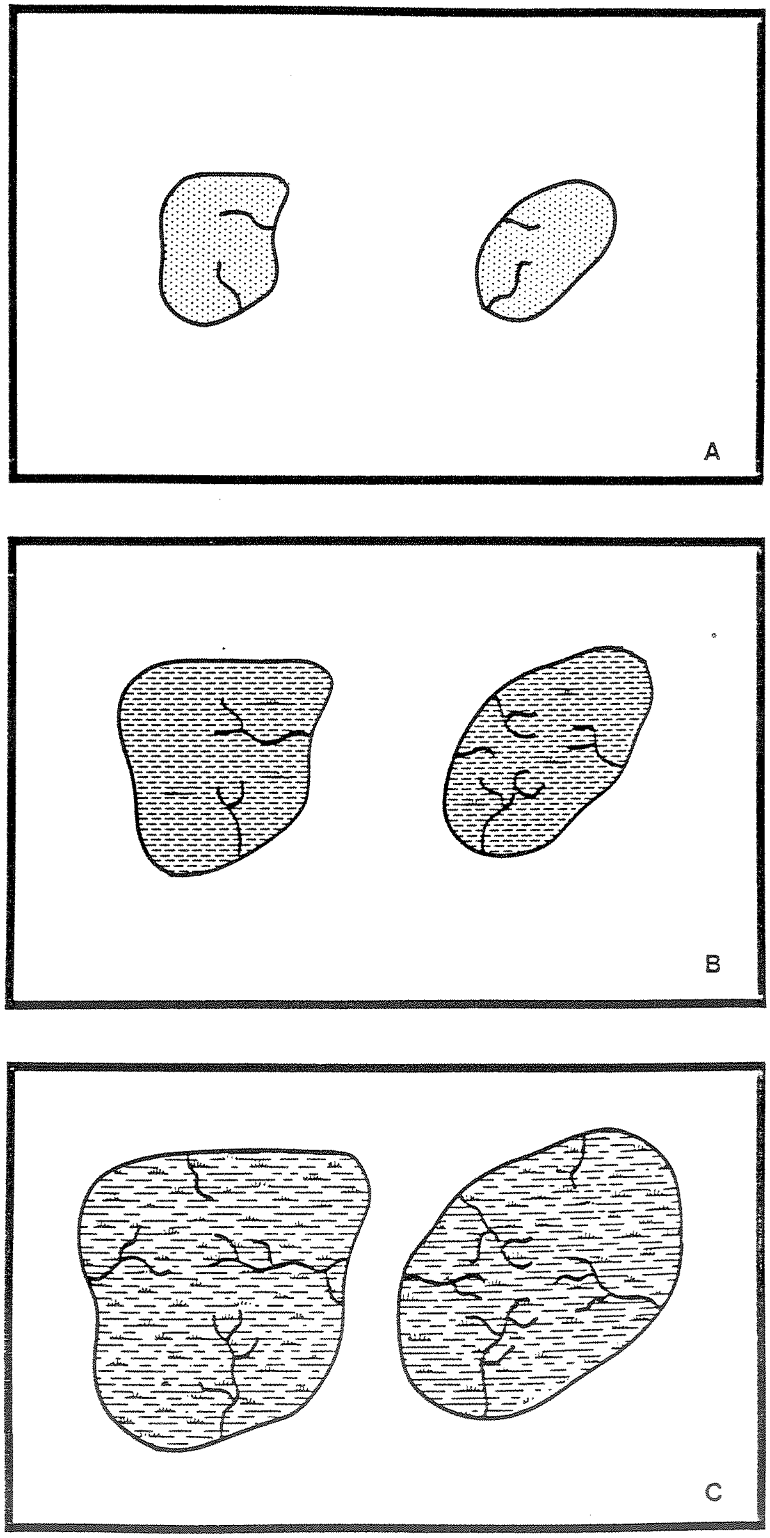
A
B
C

ii) interbedded silt/fine-to-very fine sand, marked by upward fining, as TF subtidal channel deposits grading up to intertidal channel-margin flats, iii) medium-to-fine sand as flood tidal delta, and iv) lower mud as DE subtidal channel or intertidal channel-margin flat (Figures 29-32).

The vibracore sites were positioned near three channels: Long Reach, Old Turtle Reach, and a DE system off of Old Turtle (Figure 3). These locations were chosen to maximize the likelihood of coring through the channel deposits recognized in modern sediments.

Long Reach is a TF channel and Old Turtle Reach is a through-flower in the process of closing in by marsh island expansion at its Great Sound end. Aerial photos of 1932 clearly show Old Turtle Reach to empty into Great Sound. By 1972 photos show marsh growth had already begun to close this end. Today the connection is maintained by a very narrow channel.

The processes proposed for the origin of TF and DE tidal channels are recorded in the Holocene sediments represented in the cores. In accordance with this theory, the marsh island bounded by through-flowing Long Reach and Old Turtle Reach originated as a tidal delta sand body. The DE system near the core sites developed after the shoals became intertidal and were stabilized by marsh vegetation.

It has been postulated that the modern barrier island chains of the east coast of the U. S. originated on the continental shelf during the lower stands of sea-level associated with late Wisconsin glaciation (40,000-20,000 years BP) and have migrated landward across the shelf as sea-level rose with glacial melting and crustal rebound (18,000-15,000 years BP) (Swift and Moslow, 1982; Leatherman, 1983; Rampino and Sanders, 1983; Panageotou and Leatherman, 1986). Halsey (1979), in the 'nexus' model, favors a more localized origin suggesting the redistribution of nearshore and eroded headlands sediment to present-day positions determined by the pre-Holocene topography.

Regardless of the precise mechanism for barrier island formation, Holocene barriers did form such that a back-barrier environment adjacent to the mainland was established. Idealized cross-sections at the coring area beginning with its back-barrier history are given in Figure 36.

At time 1 subtidal tidal delta sands have built up on the seaward side of the lagoon. Sediment size segregation of sediment entering the inlets may occur over the complex (Daboll, 1969). Shifting interlobe channels are represented by a coarse channel lag. By time 2 the shoals have built to the intertidal zone and intervening channels are more stable. Incipient halophyte colonization begins so that by time 3 marsh islands separated by TF channels are established. DE channel systems develop between times

Figure 36. Idealized Cross-Section of Coring Area.

Time 1. Subtidal delta sands with shifting interlobe channels.

Time 2. Sand shoals have built to intertidal level where incipient halophyte growth and the segregation of channel-margin flat and thalweg region deposits begins.

Time 3. Marsh islands are established. Considerable peat has accumulated along with TF channel facies as channels narrow.

Time 4. Modern marsh. Marsh islands are larger and TF channels narrower. Core representing SM-2, -3, and -5 is shown.

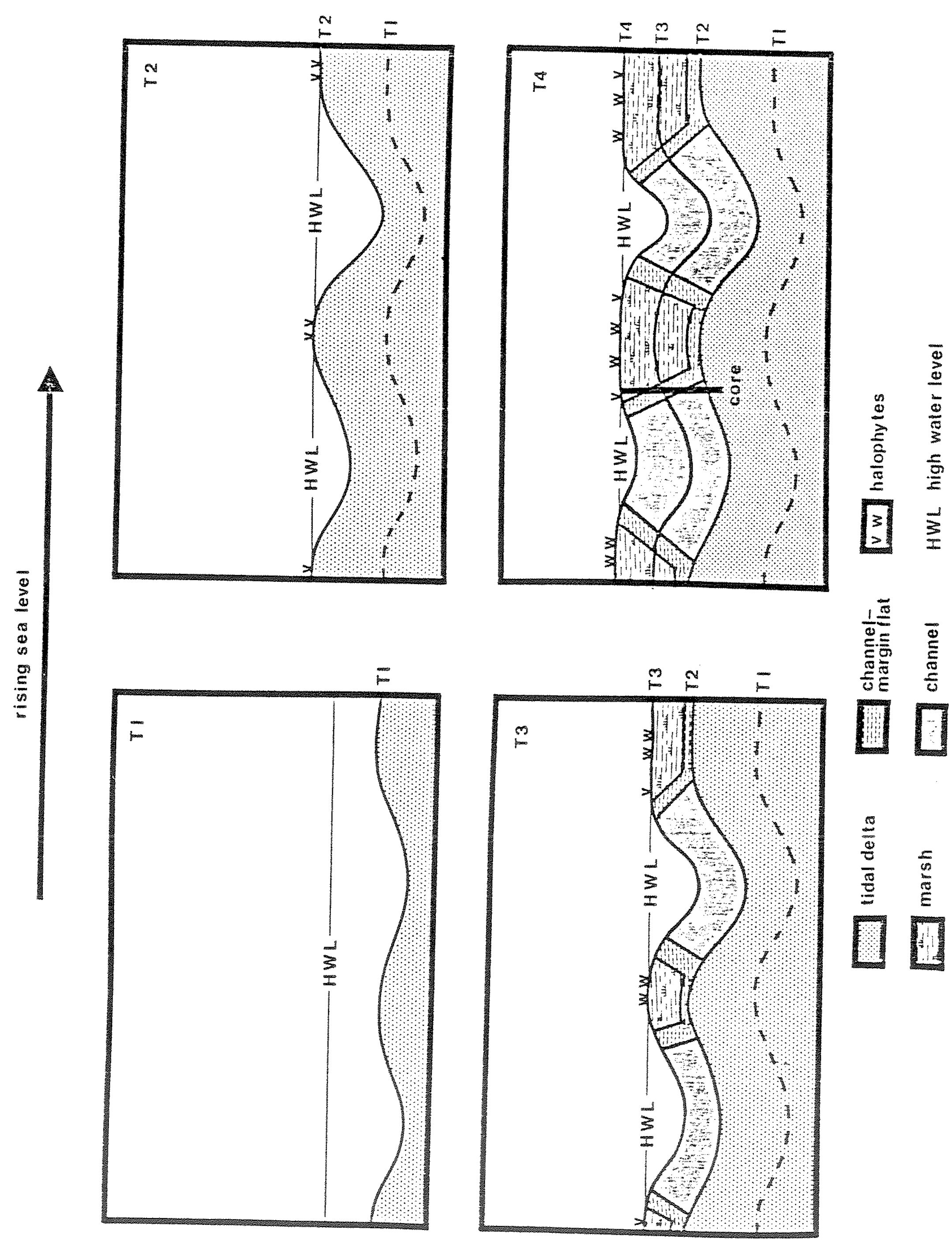

rising sea level
T1
HWL
T2
T3
T4
core
tidal delta
marsh
channel-margin flat
channel
halophytes
HWL high water level

2 and 3. Today, time 4, marsh islands are larger and TF channels narrower. Channel deposits fine up in the section as channels infill, become narrower, and v_{max} decreases. This sequence accretes under a continual rise in sea-level.

Cores SM-2, SM-3, SM-5 are similar and represent the section idealized in Figure 36. Tidal delta sands are overlain by TF channel deposits grading up to channel-margin intertidal flats, and all is capped by modern marsh. In core SM-4 the interbedded unit is underlain with the lower mud. The base of the interbedded unit (channel and channel-margin flat) is an erosional surface of shell hash and rip-up clasts (Figure 31). It is suggested that the lower mud unit represents the finer subtidal channel or intertidal channel-margin flat deposits of the nearby DE channel. This channel migrated and its channel deposits were eroded and overlain by the coarser TF channel deposits of Old Turtle Reach.

EVOLUTION OF THE SOUTHERN NEW JERSEY COASTLINE

Core transects of Daddario (1961), Force (1968), and Psuty (1986) near Great Bay (Figure 37) find a basal peat underlying lagoonal muds and modern salt-marsh deposits. Daddario and Force identified the peat as freshwater swamp and forest remains. The transects of Force and Psuty find the peat to pinch-out and the lagoon unit to grade laterally to a sand facies in the seaward direction.

Figure 37. Coring transects of Daddario (1961), Force (1968), and Psuty (1986) in the Great Bay area (after Psuty, 1986).

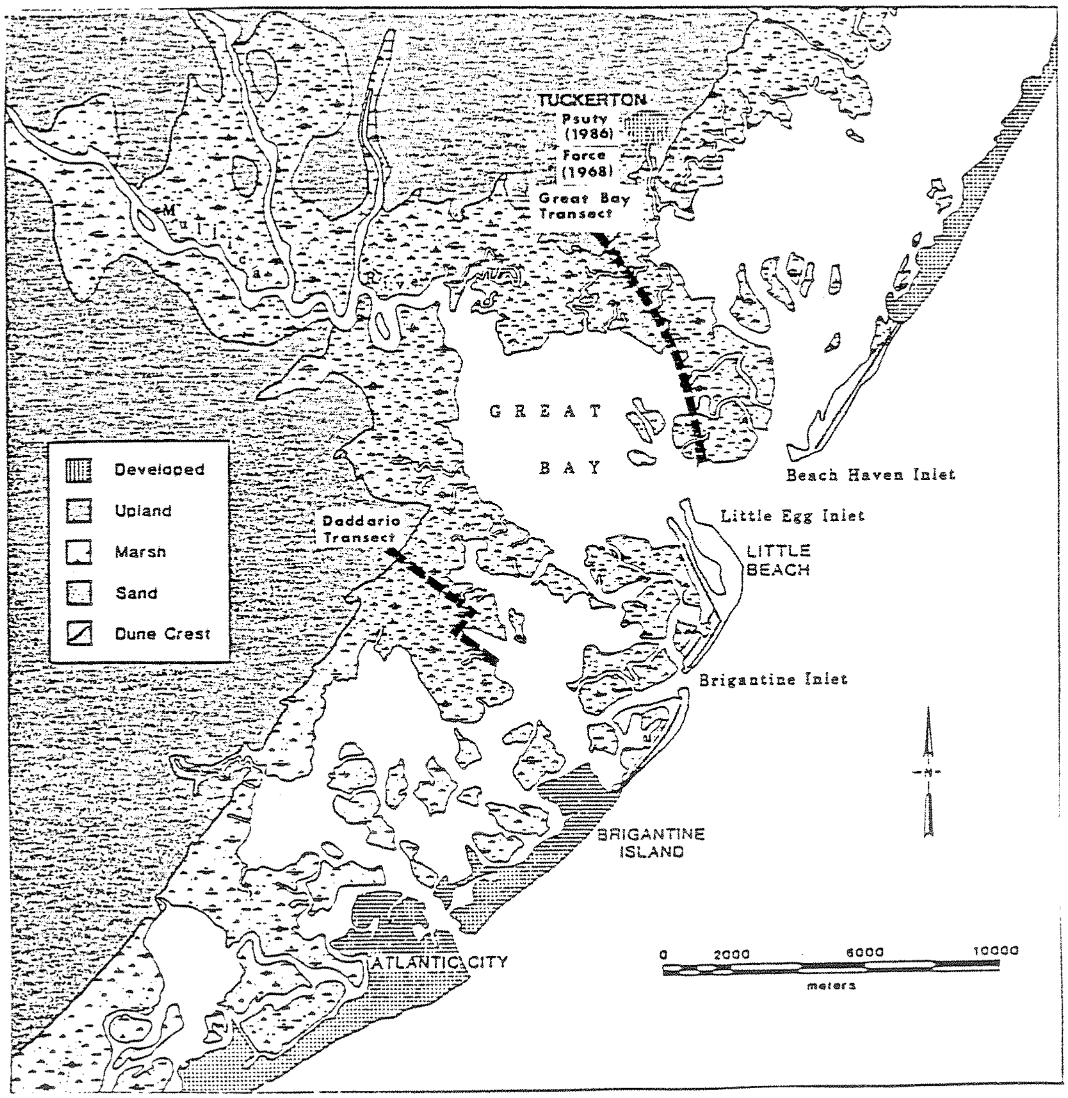
TUCKERTON
Psuty (1986)
Force (1968)
Great Bay Transect
G R E A T
B A Y
Beach Haven Inlet
Little Egg Inlet
LITTLE BEACH
Daddario Transect
Brigantine Inlet
BRIGANTINE ISLAND
ATLANTIC CITY
Developed
Upland
Marsh
Sand
Dune Crest
0 2000 6000 10000
meters
N

The barrier protected mainland of coastal New Jersey that supported freshwater wetlands and forests was gradually inundated with seawater as the Holocene transgression progressed. As marine waters encroached upon the mainland, freshwater wetlands were succeeded by brackish and salt water marshes that now fringed the landward margin of the back-barrier lagoon. This transition is preserved in the landward cores of Daddario (1961) and Force (1968) where freshwater peats grade vertically to salt-marsh peats. Along the seaward margin of the lagoon, salt-marsh islands evolved from tidal delta sands. The vertical transition of tidal delta sands to lagoon to modern salt-marsh at the seaward sides of back-barrier lagoons can be recognized in the core data of Force (1968), Ferland (1985), Psuty (1986), and this study.

Bay infilling only will occur if sedimentation culminating in the bayward expansion of both marsh types (landward fringing and seaward islands) exceeds the rate of sea-level rise. If both processes cannot keep pace with sea-level rise the lagoon will deepen and its landward margin migrate farther inland. The location of its seaward margin will depend upon the degree to which the bordering barrier islands migrate landward. Lagoon infilling, then, is a function of the balance between the rate of sea-level rise and sediment budget.

Carbon-14 data from coastal New Jersey indicate a marked decline in the rate of sea-level rise beginning 2000-2500 years BP from about 2-3 mm/yr to approximately 1 mm/yr (Ferland, 1985; Psuty, 1986). Prior to this time, a general mainland transgression had been marked with some episodes of bayward expansion of the landward fringing marshes that were followed by renewed wetlands retreat as sedimentation once again was unable to keep up with sea-level rise. Back-barrier peats as old as 6000-7000 years BP have been dated (Stuiver and Daddario, 1963; Psuty, 1986). Bay infilling leading to the growth of the modern salt-marsh appears to be a recent phenomenon initiated by the slowed pace of sea-level rise at 2000-2500 years BP.

The carbon-14 dates of the cores of this study indicate salt-marsh colonization was established at the seaward margin of the Avalon/Stone Harbor back-barrier lagoon within the last 700 years. This was likely initiated by a change in the sediment budget and the balance between sediment supply (relative increase) and rate of sea-level rise (relative decrease). The transition from tidal delta sand shoal to intertidal flat occurred at the coring site 800-1300 years BP. These dates are consistent with the contention of Psuty (1986) that bay infilling is a recent phenomenon.

SUMMARY

1. The tidal channels traversing the back-barrier salt-marshes of southern New Jersey can be classified as through-flowing (TF) or dead-ending (DE) based upon morphometric parameters (plan form, hydraulic geometry, w:d), hydraulic character (hydraulic geometry, v_{max}, Q_{max}), and sedimentary properties (grain-size, total organic matter, sedimentary structures).

2. TF channels are larger (approx. 100 m wide) and connect the ocean with bays or channels to each other and DE channels are smaller (<25 m wide), comprising branching networks that terminate on the marsh.

3. TF and the trunk DE channels have at-a-station hydraulic geometries similar to other tidal marsh channels (high m, low b and f values) and the smaller DE channels have hydraulic geometries similar to rivers (lower m, higher b and f values).

4. TF channels have high w:d ratios (34-129) and DE channels have low w:d ratios (5-21).

5. TF channels have higher flow velocities and discharges. The largest TF channels had a measured mean spring v_{max} = 100 cm/sec, a mean neap v_{max} = 64 cm/sec, a spring Q_{max} = 700 m^3/sec, and neap Q_{max} = 500 m^3/sec. The smallest DE channel had a mean neap v_{max} = 10 cm/sec and a neap Q_{max} < 1 m^3/sec.

6. TF channels have low mud perimeters (averaging 9%) and DE channels have high mud perimeters (averaging 79%).

7. Three distinct sedimentary environments are associated with the channels: i) a subtidal thalweg region, ii) an intertidal channel-margin flat (vegetated and unvegetated), and iii) a channel-margin marsh (levee and back-levee).

8. Inter-channel sedimentary trends, from large TF to small DE channels, are: i) fining of thalweg sediments from medium sand to silt, fining of channel-margin flats from very fine sand to silt, and fining of channel-margin marshes from very fine sand to silt and clay, ii) increasing total organic matter with increasing mud content, and iii) a change from predominantly physical to biological sedimentary structures.

9. Intra-channel trends at a cross-section are: i) the fining of sediments with distance away from the thalweg region and ii) increasing total organic matter content from the thalweg region to the marsh.

10. TF channels originated as flood tidal delta channels and DE networks developed from ebb drainage patterns of unvegetated portions of marsh islands that evolved from the tidal deltas.

11. The Holocene sedimentary record (since about 1300 years BP) of the seaward portion of the Avalon/Stone Harbor back-barrier marsh at sites near a TF channel is represented by tidal delta sands overlain by TF channel deposits grading up to channel-margin intertidal flats capped by the modern marsh. DE channel migration is

preserved by an erosional surface separating DE channel deposits below and TF channel deposits above.

The Holocene record of other areas of the marsh, e.g. those distant from a TF channel, would not contain TF tidal channel deposits. The sedimentary record at these locations would be represented by a basal tidal delta sand fining up to intertidal flats and capped by the modern marsh, perhaps punctuated by DE channel sequences.

12. Bay-infilling leading to the development of the modern salt-marsh was initiated by the reduced rate of sea-level rise at 2000-2500 years BP. The transition from tidal delta shoals to intertidal flat occurred 800-1300 years BP. Salt-marsh colonization of the seaward margin developed within the last 700 years and is continuing landward at present.

CONCLUSIONS

1. The hydraulic and sedimentary properties of tidal channels in a mesotidal back-barrier salt-marsh are variable.

2. The variable properties (w:d, hydraulic geometry, grain-size, organic matter content, sedimentary structures) are linked to processes which are similar to fluvial flow processes in some channels and unique to tidal flow processes in others.

3. The variability of sediment properties in modern back-barrier salt-marshes can be recognized in the

underlying Holocene back-barrier salt-marshes. Thus, properties of the modern marsh can be a useful tool in the facies analysis of ancient tidal marsh deposits.

4. The tidal channel drainage pattern in the marsh today is not a static configuration. Its role and spatial extent in the back-barrier region has changed through time concomitant with the initiation, growth, and expansion of the marsh.

Appendix 1. Three Basic programs used in morphometric analyses: TCLEN.BAS, AREA.BAS, JANG.BAS.

Listing of TCLEN.BAS

```
10 'CHANNEL LENGTH PROGRAM (revised 2-21-85: zeff)
20 ' CALCULATES CUMULATIVE CHANNEL SEGMENT LENGTHS
30 '
35 '
36 'SET PARAMETERS
37 '
40 CLS
52 TLEN=0:  'TRUE SEGMENT LENGTH
53 CUM=0:  'CUMULATIVE SEGMENT LENGTH
70 INPUT "ENTER MAP SCALE.................................";SC:  'INCHES
80 SC=2.54*SC:  'CONVERTS SCALE TO CM
85 PRINT ""
92 INPUT "ENTER DRAINAGE AREA..............................";AREA$
93 PRINT ""
101 INPUT "ENTER CHANNEL ORDER............................";ORDER
102 PRINT ""
103 '
145 '
146 'OPEN COMMUNICATIONS BUFFER FILE TO # 1
150 OPEN "COM2:9600,E,7,1" FOR INPUT AS #1:CLS
155 '
160 PRINT "LOCATE START POINT AND PRESS BUTTON 3"
165 PRINT ""
170 PRINT "INCREMENT A CHANNEL SEGMENT AND PRESS BUTTON 1"
171 PRINT "":PRINT "TO PAUSE FOR CONTINUE, PRESS BUTTON 2":PRINT ""
172 PRINT "TO END SESSION, PRESS BUTTON 4"
175 I$="":IJ$="":JI$=""
176 IF EOF(1) THEN 176
177  FOR I=1 TO 3:NEXT:IF EOF(1) THEN 295
178 I$=I$+INPUT$(LOC(1),#1)
179 ICR=0
180 ICR=INSTR(ICR+1,I$,CHR$(13))
181 IF ICR=0 THEN 185
182 IJ$=LEFT$(I$,ICR-1)
183 IK=LEN(I$)-ICR
184 JI$=RIGHT$(I$,IK):GOTO 187
185 J$=J$+I$:I$=""
186 GOTO 177
187 J$=J$+IJ$
188 FOR K=1 TO 3
189 IF LEFT$(J$,1)=" " THEN J$=RIGHT$(J$,LEN(J$)-1)
190 NEXT
191 II$=J$
192 PRINT II$
200 K = VAL(LEFT$(II$,1)):  'BUTTON
210 X=.001*VAL(MID$(II$,2,5))
220 Y=.001*VAL(RIGHT$(II$,5))
222 '
230 IF K = 4 THEN XC=X: YC=Y: PRINT "CENTERED, NOW INCREMENT":GOTO 260
240 IF K = 8 GOTO 905
250 IF K = 1 GOTO 260
251 IF K = 2 GOTO 295
255 '
256 'CALCULATE DIST WITH PYTHAG.
260 DIST = (X-XC)^2 + (Y-YC)^2
270 DIST = (DIST)^(.5)
```

Listing of TCLEN.BAS

```
280 TLEN = DIST*SC*.01
290 CUM = CUM + TLEN
295 II$="":J$="":IJ$="":I$=JI$:JI$="":XC=X:YC=Y
296 IF LOC(1)=0 THEN 300
297 IG$=INPUT$(LOC(1),#1)
300 GOTO 175
301 '
905 LPRINT AREA$;CHR$(10)
910 INPUT "ANALYSIS COMPLETE OR PARTIAL (C/P)................";Q$
911 IF Q$="C" OR Q$="c" THEN LPRINT "ANALYSIS COMPLETE":GOTO 940
912 IF Q$="P" OR Q$="p" THEN LPRINT "PARTIAL ANALYSIS":GOTO 940
940 LPRINT "SEGMENT LENGTH OF ORDER ";ORDER;"= ";CUM;" METERS"
950 LPRINT CHR$(10);CHR$(10)
1000 END
```

Listing of AREA.BAS

```
10 'AREA PROGRAM: zeff(revised 2-21-85)
20  'CALCULATES AREA WITHIN CLOSED PERIMETER
30   'SUMS AREAS OF TRIANGLES
31 '
32 '
33 CLS
40 AREA=0: TAREA=0
70 INPUT "ENTER MAP SCALE.........................";SC:   'INCHES
85 PRINT ""
90 INPUT "ENTER NAME OF AREA......................";AREA$
95 PRINT ""
100 '
101 'OPEN COMMUNICATIONS BUFFER FILE TO #1
102 OPEN "COM2:9600,E,7,1" FOR INPUT AS #1: CLS
103 '
104 PRINT "CHOOSE A CENTER AND PRESS BUTTON 3"
105 PRINT ""
106 PRINT "INCREMENT ALONG PERIMETER AND PRESS BUTTON 1"
107 PRINT ""
108 PRINT "IF DONE, PRESS BUTTON 4"
109 '
175 I$="":IJ$="":JI$=""
176 IF EOF(1) THEN 176
177  FOR I=1 TO 3:NEXT:IF EOF(1) THEN 295
178 I$=I$+INPUT$(LOC(1),#1)
179 ICR=0
180 ICR=INSTR(ICR+1,I$,CHR$(13))
181 IF ICR=0 THEN 185
182 IJ$=LEFT$(I$,ICR-1)
183 IK=LEN(I$)-ICR
184 JI$=RIGHT$(I$,IK):GOTO 187
185 J$=J$+I$:I$=""
186 GOTO 177
187 J$=J$+IJ$
188 FOR K=1 TO 3
189 IF LEFT$(J$,1)=" " THEN J$=RIGHT$(J$,LEN(J$)-1)
190 NEXT
191 II$=J$
192 PRINT II$
200 K = VAL(LEFT$(II$,1)):  'BUTTON
210 X=.001*VAL(MID$(II$,2,5))
220 Y=.001*VAL(RIGHT$(II$,5))
222 '
300 IF K=1 GOTO 600                          'INCREMENT PERIMETER
400 IF K=8 GOTO 1000                         'END
500 IF K=4 THEN OX=X:OY=Y                'START AND REMEMBER ORIGINAL CENTER
510 PRINT "CENTERED, NOW INCREMENT PERIMETER"
511 COUNT=1
512 II$="":J$="":IJ$="":I$=JI$:JI$=""
513 IF LOC(1)=0 THEN 515
514 IG$=INPUT$(LOC(1),#1)
515 '
516 GOTO 175
520 '
600 IF COUNT=2 GOTO 700
650 IF COUNT=1 THEN TX=X-OX:TY=Y-OY   'TRANSLATION
```

Listing of AREA.BAS

```
651 COUNT=2
653 II$="":J$="":IJ$="":I$=JI$:JI$="":OTX=TX:OTY=TY
655 IF LOC(1)=0 THEN 657
656 IG$=INPUT$(LOC(1),#1)
657 '
658 GOTO 175
659 '
700 A=X-OX:B=Y-OY
710 '
800 AREA=(ABS((TX*B)-(TY*A)))*.5
810 TAREA=TAREA+AREA
899 II$="":J$="":IJ$="":I$=JI$:JI$="":TX=A:TY=B
900 IF LOC(1)=0 THEN 902
901 IG$=INPUT$(LOC(1),#1)
902 '
910 GOTO 175
915 '
1000 AREA=(ABS((TX*OTY)-(TY*OTX)))*.5:                'SQ. INCHES
1001 TAREA=TAREA+AREA
1002 LPRINT ""
1007 LPRINT AREA$:LPRINT""
1008 LPRINT "TOTAL AREA BEFORE SCALING IN SQUARE INCHES= ";TAREA
1009 LPRINT "":LPRINT "SCALE= ";SC:RAREA=((TAREA)*(SC^2))*(6.4516E-04)
1010 LPRINT "":LPRINT "TOTAL AREA (SCALED) IN SQUARE METERS= ";RAREA;" (";RAREA*
(10^-6);"SQUARE KILOMETERS)"
1015 LPRINT ""
1040 END
```

Listing of JANG.BAS

```
10 'JANG PROGRAM: zeff(revised 7-23-85)
20  'CALCULATES ANGLE DEFINED BY THREE POINTS
30   ' TO BE USED FOR CALCULATING JUNCTION ANGLES
40 '
45 'LAW OF COSINES USED TO DETERMINE ANGLE(A) AFTER CALCULATING THE LENGTHS
50 '  a,b, and c OF DEFINED TRIANGLE
52 '
53 '
60 CLS:COUNT=0:PI=3.141593:DIM ANGLES(100):CUM=0:DIM VAR(100):VSUM=0
65 INPUT "ENTER DRAINAGE AREA.....................";AREA$
66 PRINT ""
70 INPUT "ENTER ORDER OF 'ENTERING' SEGMENT.......";TRIB:' TA,TB
75 PRINT ""
80 INPUT "ENTER ORDER OF 'RECEIVING' SEGMENT.......";REC:'TX,TY
90 '
95 OPEN "COM2:9600,E,7,1" FOR INPUT AS #1:CLS
100 '
105 PRINT "FIRST CHOOSE VERTEX AND PRESS BUTTON 1":PRINT ""
110 PRINT "THEN CHOOSE ENTERING POINT AND PRESS BUTTON 2":PRINT ""
115 PRINT "LASTLY, CHOOSE RECEIVING POINT AND PRESS BUTTON 3":PRINT ""
120 PRINT "IF DONE, PRESS BUTTON 4"
125 '
175 I$="":IJ$="":JI$=""
176 IF EOF(1) THEN 176
177  FOR I=1 TO 3:NEXT:IF EOF(1) THEN 295
178 I$=I$+INPUT$(LOC(1),#1)
179 ICR=0
180 ICR=INSTR(ICR+1,I$,CHR$(13))
181 IF ICR=0 THEN 185
182 IJ$=LEFT$(I$,ICR-1)
183 IK=LEN(I$)-ICR
184 JI$=RIGHT$(I$,IK):GOTO 187
185 J$=J$+I$:I$=""
186 GOTO 177
187 J$=J$+IJ$
188 FOR K=1 TO 3
189 IF LEFT$(J$,1)=" " THEN J$=RIGHT$(J$,LEN(J$)-1)
190 NEXT
191 II$=J$
192 PRINT II$
193 '
200 K = VAL(LEFT$(II$,1)):  'BUTTON
210 X=.001*VAL(MID$(II$,2,5))
220 Y=.001*VAL(RIGHT$(II$,5))
222 '
300 IF K=1 THEN VX=X: VY=Y: GOTO 600
350 IF K=2 THEN BX=X: BY=Y: GOTO 600
400 IF K=4 THEN CX=X: CY=Y: GOTO 700
450 IF K=8 GOTO 1000
500 '
600 II$="":J$="":IJ$="":I$=JI$:JI$=""
610 IF LOC(1)=0 THEN 620
615 IG$=INPUT$(LOC(1),#1)
620 '
625 GOTO 175
630 '
```

Listing of JANG.BAS

```
700 DVB=(BX-VX)^2 + (BY-VY)^2
705 DVB=(DVB)^(.5)
710 DVC=(CX-VX)^2 + (CY-VY)^2
715 DVC=(DVC)^(.5)
720 DBC=(BX-CX)^2 + (BY-CY)^2
725 DBC=(DBC)^(.5)
730 '
735 COSA=(DVC^2 + DVB^2 - DBC^2)/(2*DVC*DVB)
740 RTHETA=1.570796-ATN(COSA/SQR(1-COSA*COSA))
745 DTHETA=(RTHETA)*(180/PI)
858 '
900 CUM=CUM + DTHETA
905 COUNT=COUNT + 1
910 MEAN=CUM/COUNT
915 ANGLES(COUNT)=DTHETA
916 PRINT ANGLES(COUNT)
920 '
921 II$="":J$="":IJ$="":I$=JI$:JI$=""
922 IF LOC(1)=0 THEN 930
925 IG$=INPUT$(LOC(1),#1)
930 '
940 GOTO 175
950 '
1000 LPRINT "":LPRINT ""
1010 LPRINT AREA$:LPRINT ""
1020 LPRINT "ENTERING SEGMENT = ORDER ";TRIB
1030 LPRINT "RECEIVING SEGMENT = ORDER ";REC
1040 LPRINT "NUMBER OF JUNCTION ANGLES = ";COUNT
1045 LPRINT "MEAN ANGLE (DEGREES) = ";CINT(MEAN)
1046 FOR D=1 TO COUNT
1047   VAR(D)=(CINT(ANGLES(D))-CINT(MEAN))^2
1048   VSUM=VSUM+VAR(D)
1049   NEXT
1050 SD=(VSUM/(COUNT-1))^.5
1060 LPRINT "S.D.=";CINT(SD)
1080 LPRINT "ANGLES (DEGREES) ARE: "
1090 FOR D=1 TO COUNT
1100   LPRINT CINT(ANGLES(D))
1180   NEXT
1190 END
```

Appendix 2. Grain-size data of five samples (RU-83-IT-T1, -T3, -T4, -T5, -T6) analyzed with the sonic sifter (SS) and Ro-Tap (RT).

APPENDIX 2

wt% of total final weight

RU-83-IT-T1

1/4 PHI	SS-A		SS-B		SS-C		RT		
-1.00	<1		2		1		3		gravel
-0.75	<1	2	<1	3	<1	2	<1	4	
-0.50	<1		<1		<1		<1		
-0.25	<1		<1		<1		<1		
0.00	1		1		<1		2		vc sand
+0.25	2	30	2	31	2	27	2	25	
+0.50	4		5		3		5		
+0.75	7		8		6		7		
+1.00	17		16		16		11		c sand
+1.25	7	64	8	62	8	67	17	63	
+1.50	22		21		22		18		
+1.75	21		20		23		18		
+2.00	14		13		14		10		m sand
+2.25	1	3	1	3	1	2	2	3	
+2.50	<1		<1		<1		<1		
+2.75	<1		<1		<1		<1		
+3.00	<1		<1		<1		<1		f sand
+3.25	<1		<1		<1		<1		
↓ MUD	<1		<1		<1		<1		

APPENDIX 2

wt% of total final weight

RU-83-IT-T3

1/4 PHI	SS-A		SS-B		SS-C		RT		
-1.00	<1		-		<1		<1		gravel
-0.75	<1	2	<1	1	<1	2	<1	3	
-0.50	<1		<1		<1		<1		
-0.25	<1		<1		<1		<1		
0.00	1		<1		<1		1		vc sand
+0.25	2	33	2	35	2	34	3	32	
+0.50	5		4		4		6		
+0.75	8		8		8		9		
+1.00	19		20		19		13		c sand
+1.25	10	64	10	64	10	64	21	64	
+1.50	26		27		26		21		
+1.75	21		20		20		17		
+2.00	7		7		7		5		m sand
+2.25	<1	<1	<1	<1	<1	<1	<1	<1	
+2.50	<1		<1		<1		<1		
+2.75	<1		<1		<1		<1		
+3.00	<1		<1		<1		<1		f sand
+3.25	<1		<1		<1		<1		
↓ MUD	<1		<1		<1		<1		

APPENDIX 2

wt% of total final weight

RU-83-IT-T4

1/4 PHI	SS-A	SS-B	SS-C	SS-D	SS-E	SS-F	RT	
−1.00	<1	<1	<1	<1	<1	<1	<1	gravel
−0.75	<1	<1	--	<1	<1	--	<1	
−0.50	<1	<1	<1	<1	<1	<1	<1	
−0.25	<1	<1	<1	<1	<1	<1	<1	
0.00	<1	<1	<1	<1	<1	<1	1	
	<1	1	<1	<1	1	<1	2	vc sand
+0.25	<1	1	<1	<1	1	<1	1	
+0.50	3	3	3	2	3	2	4	
+0.75	5	6	6	6	6	5	7	
+1.00	18	18	19	17	18	16	14	
	27	28	28	26	28	25	27	c sand
+1.25	11	10	11	11	11	11	24	
+1.50	29	30	30	29	29	30	25	
+1.75	23	22	22	23	22	23	17	
+2.00	8	8	7	8	7	8	4	
	70	69	69	71	69	72	70	m sand
+2.25	<1	<1	<1	<1	<1	<1	<1	
+2.50	<1	<1	<1	<1	<1	<1	<1	
+2.75	<1	<1	<1	<1	<1	<1	<1	
+3.00	<1	<1	<1	<1	<1	<1	<1	
	2	1	1	2	1	2	1	f sand
+3.25	<1	<1	<1	<1	<1	<1	<1	
↓ MUD	<1	<1	<1	<1	<1	<1	<1	

APPENDIX 2

wt% of total final weight

RU-83-IT-T5

1/4 PHI	SS-A	SS-A subtotal	SS-B	SS-B subtotal	RT	RT subtotal	
-1.00	1		2		2		gravel
-0.75	<1		<1		<1		
-0.50	1	5	1	6	2	7	
-0.25	1		2		2		
0.00	2		2		3		vc sand
+0.25	3		3		4		
+0.50	6	43	6	41	8	39	
+0.75	11		10		11		
+1.00	23		22		16		c sand
+1.25	9		10		21		
+1.50	22	49	21	49	17	50	
+1.75	13		13		—		
+2.00	4		4		13		m sand
+2.25	<1		<1		<1		
+2.50	<1	1	<1	1	<1	<1	
+2.75	<1		<1		<1		
+3.00	<1		<1		<1		f sand
+3.25	<1		<1		<1		
↓ MUD	<1		<1		<1		

APPENDIX 2

wt% of total final weight

RU-83-IT-T6

1/4 PHI	SS-A	SS-A (sum)	SS-B	SS-B (sum)	RT	RT (sum)	
-1.00	<1		<1		<1		gravel
-0.75	<1	5	<1	5	<1	5	
-0.50	1		<1		<1		
-0.25	1		1		<1		
0.00	2		2		3		vc sand
+0.25	3	45	4	44	4	38	
+0.50	8		8		8		
+0.75	12		11		11		
+1.00	22		21		16		c sand
+1.25	9	49	9	50	20	56	
+1.50	21		20		18		
+1.75	14		15		13		
+2.00	5		5		4		m sand
+2.25	<1	<1	<1	1	<1	<1	
+2.50	<1		<1		<1		
+2.75	<1		<1		<1		
+3.00	<1		<1		<1		f sand
+3.25	<1		<1		<1		
↓ MUD	<1		<1		<1		

REFERENCES

Allen, E. A., 1977, Petrology and Stratigraphy of Holocene Coastal-Marsh Deposits Along the Western Shore of Delaware Bay: Sea Grant Tech. Rept. DEL-SG-20-77, Univ. of Delaware, Newark, DE, 287p.

Ashley, G. M. and Grizzle, R. E., 1987, Hydrodynamics and sedimentation in a tide-dominated back-barrier lagoon: GSA NE Mtg., Abs. with Prog., Vol. 19, No. 1, p. 3

______________ and ______________, in prep., Interactions between hydrodynamics, benthos, and sedimentation in a tide-dominated coastal lagoon: Mar. Geol.

______________ and Zeff, M. L., 1985a, Tidal channel hierarchy in a low-mesotidal salt marsh: flow and sediment characteristics: SEPM Mid-Year Mtg., Abs. with Prog., Vol. II, p. 7

______________ and ___________, 1985b, Flow characteristics and sediment flux in the Great Sound section of the Intracoastal Waterway: the role of tidal channels in sediment dispersal in a back-barrier salt marsh: NJ Sea Grant Annual Report 1983-1984, p. 24-25

______________ and ___________, 1986, The role of secondary tidal channels in sedimentation within the back-barrier environment, Intracoastal Waterway, NJ: NJ Sea Grant Annual Report 1984-1985, p. 28-29

______________ and ___________, 1987a, Flow characteristics and sediment flux in the Great Sound section of the Intracoastal Waterway (Avalon-Stone Harbor, NJ): NJ Sea Grant Annual Report 1985-1986, p. 31-32

______________ and ___________, 1987b, Tidal channel classification for a low-mesotidal salt marsh: GSA NE Mtg., Abs. with Prog., Vol. 19, No. 1, p. 3

Barwis, J. H., 1978, Sedimentology of some South Carolina tidal-creek point bars, and a comparison with their fluvial counterparts: in A. D. Miall (ed.), Fluvial Sedimentology, Can. Soc. Pet. Geol., Mem. 5, p. 129-160

Bayliss-Smith, T. P., R. Healey, R. Lailey, T. Spencer, and D. R. Stoddart, 1979, Tidal flows in salt marsh creeks: Estuarine and Coastal Marine Sci., 9:235-255

Boon, J. D.,III, 1973, Sediment transport processes in a salt marsh drainage system: unpubl. PhD dist., College of Wm. and Mary, Williamsburg, VA, 238p.

________________, 1975, Tidal discharge asymmetry in a salt marsh drainage system: Limn. Oceanogr., 20:71-80

Bowden, K. L. and Wallis, J. R., 1964, Effect of stream-ordering technique on Horton's laws of drainage composition: GSA Bulletin, 75:767-774

Bradshaw, J. S., 1968, Environmental parameters and marsh foraminifera: Limn. Oceanogr., 13:26-38

Broscoe, A. J., 1959, Quantitative analysis of longitudinal stream profiles of small watersheds: Columbia Univ. Dept. Geol. Tech. Rept. No. 18, 73p. cited in Bowden and Wallis (1964)

Byers, S. C., Mills, E. L., and Stewart, P. L., 1978, A comparison of methods of determining organic carbon in marine sediments, with suggestions for a standard method: Hydrobiologia, 58:43-47

Carson, B., A. J. Meglis, W. E. Griffiths, and K. F. Carney, 1987, Suspensate aggregation in the coastal lagoon complex at Stone Harbor, New Jersey: implications for detrital transport and deposition: GSA NE Mtg., Abs. w/ Prog., Vol. 19, No. 1, p. 8

Chapman, V. J., 1960, Salt Marshes and Salt Deserts of the World: Interscience Publishers, Inc., NY, 392p.

Chorley, R. J., Schumm, S. A., and Sugden, D. E., 1984, Geomorphology: Methuen and Co., NY, 605p.

DaBoll, J. M., 1969, Holocene sediments of the Parker River Estuary, Massachusetts: in Coastal Environments of Northeastern Massachusetts and New Hampshire, Field Guidebook, Geol. Dept., Univ. Mass., Amherst, MA, p. 337-355

Daddario, J. J., 1961, A lagoon deposit profile near Atlantic City, New Jersey: Bulletin N. J. Acad. Sci., 6:7-14

Dankers, N., M. Binsbergen, K. Zegers, R. Laane, and M. R. van der Loeff, 1984, Transportation of water, particulate and dissolved organic and inorganic matter between a salt marsh and the Ems-Dollard Estuary, the Netherlands: Estuarine Coastal and Shelf Sci., 19:143-165

Duc, A. W., 1981, Back-barrier Stratigraphy of Kiawah Island, South Carolina: unpubl. PhD dist., Univ. South Carolina, Columbia, SC, 253p.

Edwards, J. M. and Frey, R. W., 1977, Substrate characteristics within a Holocene salt marsh, Sapelo Island, Georgia: Senckenbergiana Marit., 9:215-259

Elliot, G. K., 1972, The Great Marsh, Lewes, Delaware: ONR Tech. Rept. No. 19, College of Marine Studies, Univ. of Delaware, Newark, DE, 139p.

Evans, G., 1965, Intertidal flat sediments and their environments of deposition in the Wash: Quart. J. Geol. Soc. Lond., 121:209-245

Ferland, M. A., 1985, The stratigraphy and evolution of the southern New Jersey backbarrier region: unpubl. MS thesis, Rutgers Univ., New Brunswick, NJ, 200p.

Fisher, J. J., 1967, Origin of barrier island chain shorelines: Middle Atlantic States (abs): GSA Sp. Paper 115:66-67

Folk, R. L., 1974, Petrology of Sedimentary Rocks: Hemphill Publ. Co., Austin, TX, 182p.

Force, E., 1968, Facies of Holocene sediments of the Tuckerton marshes, New Jersey: unpubl. MS thesis, Lehigh Univ., Bethlehem, PA, 51p.

Frey, R. W. and Howard, J. D., 1986, Mesotidal estuarine sequences: a perspective from the Georgia Bight: Jour. Sed. Pet., 56:911-924

Garofalo, D., 1980, The influence of wetland vegetation on tidal stream channel migration and morphology: Estuaries, 3:258-270

Gilbert, G. K., 1917, Hydraulic-mining debris in the Sierra Nevada: USGS Prof. Paper 105, 154p.

Gregory, K. J. and Walling, D. E., 1973, Drainage Basin Form and Process: John Wiley and Sons, NY, 458p.

Gross, M. G., 1971, Carbon determination: in R. E. Carver (ed.), Procedures in Sedimentary Petrology, Wiley-Interscience, NY, p. 573-596

Halsey, S. D., 1979, Nexus: new model of barrier island development: in S. P. Leatherman (ed.), Barrier Islands, Academic Press, NY, p. 185-210

Hayden, B. P. and Dolan, R., 1979, Barrier islands, lagoons, and marshes: Jour. Sed. Pet., 49:1061-1072

Healey, R. G., K. Pye, D. R. Stoddart, and T. P. Bayliss-Smith, 1981, Velocity variations in salt marsh creeks, Norfolk, England: Estuarine Coastal and Shelf Sci., 13:535-545

Hicks, S. D., DeBaugh, H. A., and Hickman, L. E., Jr., 1983, Sea Level Variations for the US, 1855-1980: US Dept. Commerce, NOAA, NOS, Rockville, MD, 170p.

Horton, R. E., 1945, Erosional developments of streams and their drainage basins: hydrophysical approach to quantitative morphology: GSA Bulletin, 56:275-370

Howard, J. D. and Frey, R. W., 1985, Physical and biogenic aspects of backbarrier sedimentary sequences, Georgia Coast, USA: Mar. Geol., 63:77-127

Jakobsen, B., 1962, The formation of ebb and flood channels in tidal channels described on the basis of morphological and hydrological observations (in Danish): Geografisk Tidsskrift, 61:119-141

Jarrett, J. T., 1976, Tidal prism-inlet area relationships: GITI Report #3: U. S. Army Coastal Engineering Research Center, Ft. Belvoir, VA, 32p.

Kayan, I. and Kraft, J. C., 1979, Holocene geomorphic evolution of a barrier-salt marsh system, sw Delaware Bay: Southeastern Geol., 20:79-100

Kelley, J. T., 1983, Composition and origin of the inorganic fraction of southern New Jersey coastal mud deposits: GSA Bulletin, 94:689-699

Kochel, R. C., Kahn, J. H., Dolan, R., Hayden, B. P., and May, P. F., 1985, US Mid-Atlantic barrier island geomorphology: Jour. Coastal Research, 1:1-9

Kodak Products for Industrial Radiography, 1984: Eastman Kodak Co., Rochester, NY, 32p.

Kraft, J. C. and Margules, G., 1971, Sediment patterns, physical characters of the water mass and foraminifera distribution in Indian River Bay, coastal Delaware: Southeastern Geol., 12:223-252

___________, Allen, E. A., Belknap, D. F., John, C. J., and Maurmeyer, E. M., 1979, Processes and morphologic evolution of an estuarine and coastal barrier system: in S. P. Leatherman (ed.), Barrier Islands, Academic Press, NY, p. 149-183

Kran, N., 1975, Tidal controls on suspended sediment in a coastal lagoon, Stone Harbor, New Jersey: Wetlands Institute Reprint Series, No. 2, Lehigh Univ., Bethlehem, PA, 46p.

Land, L. S. and Hoyt, J. H., 1966, Sedimentation in a meandering estuary: Sedimentology, 6:191-207

Leatherman, S. P., 1983, Barrier evolution in response to sea level rise: a discussion: Jour. Sed. Pet., 53:1026-1031

Lee, J. J., Muller, W. A., Stone, R. J., McEnery, M. E., and Zucker, W., 1969, Standing crop of foraminifera in sublittoral epiphytic communities of a Long Island salt marsh: Mar. Biol., 4:44-61

Leopold, L. B. and Maddock, T. M., 1953, The hydraulic geometry of stream channels and some physiographic implications: USGS Prof. Paper 252, 57p.

_______________, Wolman, M. G., and Miller, J. P., 1964, Fluvial Processes in Geomorphology: W. H. Freeman and Co., San Francisco, CA, 522p.

Letzsch, W. S. and Frey, R. W., 1980a, Deposition and erosion in a Holocene salt marsh, Sapelo Island, Georgia: Jour. Sed. Pet., 50:529-542

_______________ and __________, 1980b, Erosion of salt marsh tidal creek banks, Sapelo Island, Georgia: Senkenbergiana Marit., 12:201-212

Lubowe, J. K., 1964, Stream junction angles in the dendritic drainage pattern: Am. Jour. Sci., 262:325-339

Lucke, J. B., 1934, A theory of evolution of lagoon deposits on shorelines of emergence: Jour. Geol., 42:561-584

McManus, D. A., 1965, A study of maximum load for small-diameter sieves: Jour. Sed. Pet., 35:792-796

Meza, M. P. and Paola, C. R., 1977, Evidence for onshore deposition of Pleistocene continental shelf clays: Mar. Geol., 23:M27-M35

Morisawa, M., 1968, Streams - Their Dynamics and Morphology: McGraw-Hill Book Co., NY, 175p.

Morton, R. A. and Donaldson, A. C., 1973, Sediment distribution and evolution of tidal deltas along a tide-dominated shoreline, Wachapreague, Virginia: Sedimentary Geol., 10:285-299

Myrick, R. M. and Leopold, L. B., 1963, Hydraulic geometry of a small tidal estuary: USGS Prof. Paper 422-B, 18p.

Owens, J. P. and Sohl, N. F., 1969, Shelf and deltaic paleoenvironments in the Cretaceous-Tertiary formations of the New Jersey Coastal Plain: in Geology of Selected Areas in New Jersey and Eastern Pennsylvania and Guidebook of Excursions (S. Subitzsky, ed.), Rutgers Univ. Press, New Brunswick, NJ., p. 235-278

Panageotou, W. and Leatherman, S., 1986, Holocene-Pleistocene stratigraphy of the inner shelf off Fire Island, New York: implications for barrier-island migration: Jour. Sed. Pet., 56:528-537

Parker, F. L. and Athearn, W. D., 1959, Ecology of marsh foraminifera in Poponesset Bay, Massachusetts: Jour. Paleo., 33:333-343

Pestrong, R., 1965, The development of drainage patterns on tidal marshes: Stanford Univ. Publ., Geol. Sci., vol. X, no. 2, 87p.

______________, 1972, Tidal-flat sedimentation at Cooley Landing, southeast San Francisco Bay: Sedimentary Geol., 8:251-288

Pethick, J. S., 1980, Velocity surges and asymmetry in tidal channels: Estuarine and Coastal Mar. Sci., 11:331-345

Phleger, F. B., 1970, Foraminiferal populations and marine marsh processes: Limn. Oceanogr., 15:522-534

________________ and Walton, W., 1950, Ecology of marsh and bay foraminifera, Barnstable, Mass.: Am. Jour. Sci., 248:274-294

Psuty, N. P., 1986, Holocene sea level in New Jersey: Physical Geography, 7:156-167

Ragotzkie, R. A., 1959, Drainage patterns in salt marshes: in Proc. Salt Marsh Conf., Mar. Inst., Univ. Georgia, Sapelo Island, GA, p. 22-28

Rampino, M. R. and Sanders, J. E., 1983, Barrier island evolution in response to sea-level rise: a reply: Jour. Sed. Pet., 53:1031-1033

Redfield, A. C., 1972, Development of a New England salt marsh: Ecol. Mono., 42:201-237

Royer, D., 1980, The effects of sewage plant effluent on benthic macrofauna of a saltmarsh estuary: unpubl. PhD dist., Lehigh University, Bethlehem, PA, 104p.

Schumm, S. A., 1960, The shape of alluvial channels in relation to sediment type: USGS Prof. Paper 352-B, p. 17-30

Schwing, F. B. and Kjerfve, B., 1980, Longitudinal characterization of a tidal marsh creek separating two hydrographically distinct estuaries: Estuaries, 3:236-241

Scott, D. S. and Medioli, F. S., 1978, Vertical zonations of marsh formainifera as accurate indicators of former sea-levels: Nature, 272:528-531

____________ and ____________, 1980, Quantitative studies of marsh foraminiferal distributions in Nova Scotia: implications for sea-level studies: Cushman Fdn. for Foraminiferal Research, Sp. Pub. 17, 58p.

Settlemyre, J. L. and Gardner, L. R., 1977, Suspended sediment flux through a salt marsh drainage basin: Est. and Coas. Mar. Sci., 5:653-663

Shreve, R. L., 1966, Statistical law of stream numbers: Jour. Geol., 74:17-37

Smith, D. G., 1976, Effect of vegetation on lateral migration of anastomosed channels of a glacier meltwater river: GSA Bulletin, 87:857-860

____________ and Smith, N. D., 1980, Sedimentation in anastomosed river systems: examples from alluvial valleys near Banff, Alberta: Jour. Sed. Pet., 50:157-164

Strahler, A. N., 1952, Hypsometric (area-altitude) analysis of erosional topography: GSA Bulletin, 63:1117-1142

Stuiver, M. and Daddario, J. J., 1963, Submergence of the New Jersey coast: Science, 142:951

Stumpf, R. P., 1983, The process of sedimentation on the surface of a salt marsh: Est. Coas. Shelf Sci., 17:495-508

Swift, D. J. P. and Moslow, T. F., 1982, Holocene transgression in south central Long Island, New York: discussion: Jour. Sed. Pet., 52:1014-1019

Thorbjarnarson, K. W., Nittrouer, C. A., DeMaster, D. J., and McKinney, R. B., 1985, Sediment accumulation in a back-barrier lagoon, Great Sound, New Jersey: Jour. Sed. Pet., 55:856-863

Todd, R. and Low, D., 1981, Marine Flora and Fauna of the Northeastern US. Protozoa: Sarcodina: Benthic Foraminifera: NOAA Tech. Rept. NMFS Circular 439, 52p.

Tye, R. S., 1984, Geomorphic evolution and stratigraphy of Price and Capers Inlets, South Carolina: Sedimentology, 31:655-674

US Department of Commerce, 1986, Tide Tables. East Coast of North and South America: NOAA, NOS, Rockville, MD, 288p.

Wadsworth, J. R., 1980, Geomorphic characteristics of tidal drainage networks in the Duplin River system, Sapelo Island, Georgia: unpubl. PhD dist., Univ. Georgia, Athens, GA, 259p.

Ward, L. G., 1981, Suspended-material transport in marsh tidal channels, Kiawah Island, South Carolina: Mar. Geol., 40:139-154

__________ and Domeracki, D. D., 1978, The stratigraphic significance of back-barrier tidal channel migration (abs): GSA Abs. with Prog., vol. 10, no. 4, p. 201

Warme, J. E., 1971, Paleoecological aspects of a modern coastal lagoon: Univ. CA Publ. Geol. Sci. 87, Univ. CA Press, 181p.

Wolcott, R. T., 1978, Sieving precision: sonic sifter versus Ro-Tap: Jour. Sed. Pet., 48:661-664

VITA

Marjorie Lee Zeff

1953	Born October 1 in Brooklyn, New York
1970	Graduated from Elmont Memorial High School, Elmont, New York
1970-74	Attended University of Rochester, Rochester, New York. Majored in Geology.
1974	B.A. with Distinction, University of Rochester
1974-77	Attended Duke University, Durham, North Carolina
1977	M.S. in Geology, Duke University
1978-82	Research Assistant, Carnegie Institution of Washington, Washington, D.C.
1979	Zeff, M.L. and Perkins, R.D. Microbial alteration of Bahamian deep-sea carbonates. Sedimentology, 26:175-201
1981	Lee, T. and Zeff, M.L. A Mg survey for more FUN isotopic anomalies: Lunar and Planetary Sci. Conf. XII:604-606
1982-87	Graduate work, Teaching Assistant, Research Assistant, Department of Geological Sciences, Rutgers, The State University of New Jersey, New Brunswick, New Jersey
1983	Instructor, Department of Geological Sciences, Rutgers, New Brunswick, New Jersey
1987	Visiting Instructor, Department of Physics, Rutgers, Camden, New Jersey
1987	Ph.D. in Geological Sciences